CESRL REPORT NO. 79-1
AUGUST 1979

SHEAR BEHAVIOR OF REINFORCED CONCRETE MEMBERS UNDER BIDIRECTIONAL REVERSED LATERAL LOADING

By

K. MARUYAMA
and
J. O. JIRSA

Report on a Research Project
Sponsored by
National Science Foundation
Directorate for Applied Science and Research Applications
Division of Problem-Focused Research Applications
Grant No. ENV77-20816

DEPARTMENT OF CIVIL ENGINEERING / Structures Research Laboratory
THE UNIVERSITY OF TEXAS AT AUSTIN, TEXAS

50272-101

REPORT DOCUMENTATION PAGE	1. REPORT NO. NSF/RA-790270	2.	3. Recipient's Accession No. PB 80 140395
4. Title and Subtitle: Shear Behavior of Reinforced Concrete Members Under Bidirectional Reversed Lateral Loading			5. Report Date: August 1979
			6.
7. Author(s): K. Maruyama, J. O. Jirsa			8. Performing Organization Rept. No. CESRL Report No. 79-1
9. Performing Organization Name and Address: University of Texas at Austin, Department of Civil Engineering, Structures Research Laboratory, Austin, Texas 78712			10. Project/Task/Work Unit No.
			11. Contract(C) or Grant(G) No. (C) (G) ENV7720816
12. Sponsoring Organization Name and Address: Engineering and Applied Science (EAS), National Science Foundation, 1800 G Street, N.W., Washington, D.C. 20550			13. Type of Report & Period Covered
			14.

15. Supplementary Notes

16. Abstract (Limit: 200 words)

The influence of lateral load or deformation history on shear behavior was examined. Ten specimens were subjected to different loading histories. The dimensions and reinforcement of all test specimens were identical. Each load path or load sequence was imposed on the specimens using a specially fabricated servo-controlled loading system which applied lateral translations perpendicular to the longitudinal axis of the specimen. Rotation of the ends of the specimens was controlled to simulate a column between stiff floors. The influence on load and deformation history was examined by comparing performance in terms of shear strength deterioration, stiffness reduction, strain distribution in transverse reinforcement, and crack patterns. Based on test results, a conceptual model was developed for analyzing the shear behavior of members under multi-directional loading. The model was based on the concept of a damage index which was developed to help describe the shear failure mechanism. A sand-spring analogy was introduced as one component of the model. Details of the analytical procedure were based on measured response of the members. The model was used to estimate the shear response under various deformation histories and it is limited to members which have geometry similar to that of the members tested.

17. Document Analysis a. Descriptors

Earthquakes
Earthquake resistant structures
Dynamic structural analysis
Lateral pressure
Dynamic loads
Deformation
Shear properties
Reinforced concrete

b. Identifiers/Open-Ended Terms

Deformation history

c. COSATI Field/Group

18. Availability Statement: NTIS

19. Security Class (This Report)

20. Security Class (This Page)

21. No. of Pages

22. Price

SHEAR BEHAVIOR OF REINFORCED CONCRETE MEMBERS UNDER BIDIRECTIONAL REVERSED LATERAL LOADING

By

K. Maruyama

and

J. O. Jirsa

Report on a Research Project

Sponsored by

National Science Foundation
Directorate for Applied Science and Research Applications
Division of Problem-Focused Research Applications
Grant No. ENV77-20816

Civil Engineering Structures Research Laboratory
The University of Texas at Austin

August 1979

Any opinions, findings, and conclusions or recommendations expressed in this publication are those of the authors and do not necessarily reflect the views of the National Science Foundation.

A C K N O W L E D G M E N T S

The development of the bidirectional loading facility was supported by the Division of the Advanced Environmental Research and Technology of the National Science Foundation's Research Applied to National Needs Program under Grant No. ENV75-00;92. With this support a floor-wall reaction system was constructed. A system for applying bidirectional lateral load using a servo-controlled hydraulic actuator was developed. The loading and data acquisition are computer-controlled.

Under Grant No. ENV75-00192, testing of short columns was initiated. Funding for a comprehensive test program on columns failing in shear was received (Grant No. ENV77-20816) from the National Science Foundation's Directorate for Applied Science and Research Applications, Division of Problem-Focused Research. The grant provides funding for extensive experimental work, data reduction and evaluation aimed towards establishing behavioral models, and development of design recommendations for frame structures subjected to bidirectional deformations.

The project staff has had the guidance and input of an Advisory Panel consisting of the following:

Professor V. V. Bertero, University of California, Berkeley
Dr. W. G. Corley, Portland Cement Association, Skokie, Illinois
Mr. James Lefter, Veterans Administration, Washington, D.C.
Mr. C. W. Pinkham, S. B. Barnes & Associates, Los Angeles, California
Mr. Loring A. Wyllie, Jr., H. J. Degenkolb & Associates, San Francisco, California

The assistance of the Advisory Panel and the National Science Foundation Program Manager, Dr. John B. Scalzi, is gratefully acknowledged.

The project was conducted at the Civil Engineering Structures Research Laboratory at the Balcones Research Center of The University of Texas at Austin. The Laboratory is under the direction of Dr. John E. Breen. Many thanks are extended to Mr. Horacio Ramirez, who was the coworker for this project with the authors; Mr. George E. Moden, who made the necessary tools and equipment for construction of the loading frame; Mr. Dan Perez, for his help in building the hydraulic system; Mr. David Marschall, who had the responsibility for operating the electrical instruments and the computer-controlled system; Mr. Michael Lumsden, who drew figures for this project; and Mr. Kyle Woodward, who improved the software of the plotting system by computer. The authors wish to acknowledge the support of the other Laboratory staff, Messrs. Gorham Hinckley, Joe Longwell, Larry Johnson, and David Stolle, who assisted in the construction of facilities and in the testing.

Portions of this report were part of a Ph.D. dissertation by Kyuichi Maruyama presented to the Graduate School of The University of Texas at Austin. The dissertation was supervised by James O. Jirsa.

A B S T R A C T

Previous work on the behavior of reinforced concrete members has been concentrated on flexural and shear response of members subjected primarily to unidirectional loading. Some limited results are available for flexural response under bidirectional loading. To date there are no data regarding behavior governed by shear for members under bidirectional loading. Such data are needed for analysis or design of structures subjected to multidirectional loadings.

In this study the influence of lateral load or deformation history on shear behavior was examined. Ten specimens were subjected to different loading histories. The dimensions and reinforcement of all test specimens were identical. Each load path or load sequence was imposed on the specimens using a specially fabricated servo-controlled loading system which applied lateral translations perpendicular to the longitudinal axis of the specimen. Rotation of the ends of the specimens were controlled to simulate a column between stiff floors.

The influence of load and deformation history was examined by comparing performance in terms of shear strength deterioration, stiffness reduction, strain distribution in transverse reinforcement, and crack patterns. It was observed that the influence of previous deformation became significant when the level of previous deformation exceeded that which occurs at ultimate strength under monotonic loading. For loadings applied along a diagonal (corner to corner of column), the test results showed that as long as the resultant force and the resultant deflection were taken into account, the skewed direction of loading did not

significantly influence the shear behavior of square columns. For loading histories in which the column was displaced first in one direction and then in a perpendicular direction (square path) or if cyclic reversals of a deformation were applied to specimens which were held in a deformed state in the orthogonal direction, a severe reduction in strength and stiffness was observed. The square load path caused serious damage to the member at deflection levels which were not severe in other cases. From the tests it was concluded that loading or deformation history has a significant influence on the shear behavior of members. Both the level of deformation imposed and simultaneous variation of deformation in orthogonal directions were found to be important.

Based on the test results, a conceptual model was developed for analyzing the shear behavior of members under multi-directional loading. The model was based on the concept of a damage index which was developed to help describe the shear failure mechanism. A sand-spring analogy was introduced as one component of the model. Details of the analytical procedure were based on measured response of the members. The model was used to estimate the shear response under various deformation histories. The model is limited to members which have geometry similar to that of the members tested. Additional work is needed to extend the model to a wider range of loading and geometric parameters.

C O N T E N T S

L I S T O F T A B L E S

LIST OF FIGURES

CHAPTER 1

INTRODUCTION

1.1 General

The influence of bidirectional ground motion on the performance of structures has received increasing attention following recent major earthquakes, especially the Tokachi-Oki earthquake of 1968 and the San Fernando earthquake of 1971. Observations of structural damage in those earthquakes have led engineers to study the behavior of structures and structural members under multidirectional load reversals [1,2,3,4,5,6,7].

In seismic resistant design of frame structures, it has been assumed that the structure can be modeled as a planar frame and subjected to one component of the earthquake excitation. The lateral forces and the lateral resistance in each orthogonal direction are considered separately and independently. Such design procedures are utilized because

(1) It has been assumed that the maximum responses in each direction are unlikely to occur simultaneously and that the maximum 2D response will be only slightly greater than 1D response.

(2) There has been little documented evidence pointing to structural damage from two-dimensional (2D) involvement.

(3) 2D dynamic analyses of multistory multibay structures are complex and time-consuming.

(4) Very little information is available regarding structural behavior under 2D horizontal loadings on which to base models for use in analyses.

If the structural system includes stiff elements which limit deformation in one direction, a 1D analysis for each principal direction is likely to be quite accurate and entirely adequate for structural design purposes. However, if the structure is a frame in which the deformations in both directions may be significant, a 1D analysis may be inadequate.

1.2 Earthquake Damage

The San Fernando 1971 and Tokachi-Oki 1968 earthquakes provided full-scale tests of frame structures subjected to strong ground shaking in both horizontal directions. An analysis by Okada et al. [1] of the Hachinohe Library (Fig. 1.1) after the Tokachi-Oki earthquake indicated that the damage was greater than predicted by conventional 1D considerations. Following the San Fernando earthquake, the damage to the Olive View Hospital was studied extensively [2,3,4,5,6,7]. These studies showed that employing 1D procedures did not successfully explain the observed damage, even with the use of very high estimates of the intensity of ground motion.

The approach used by Okada, et al. [1] was to assume a model for structural response which was not dependent on the direction of motion. A single force-deformation relationship (Fig. 1.2) was assumed to describe the nonlinear response of the column in every direction. Using the Hachinohe record (maximum acceleration in both directions about 0.2g), and a structural representation of the one-story building as shown in Fig. 1.3, the maximum displacement of the columns (Fig. 1.3) was calculated, as was the displacement path of selected columns. The displacement path of the SW column is shown in Fig. 1.4. The columns along the west side of the building were the most heavily damaged and the observed damage was greater than predicted in the analysis. A similar approach

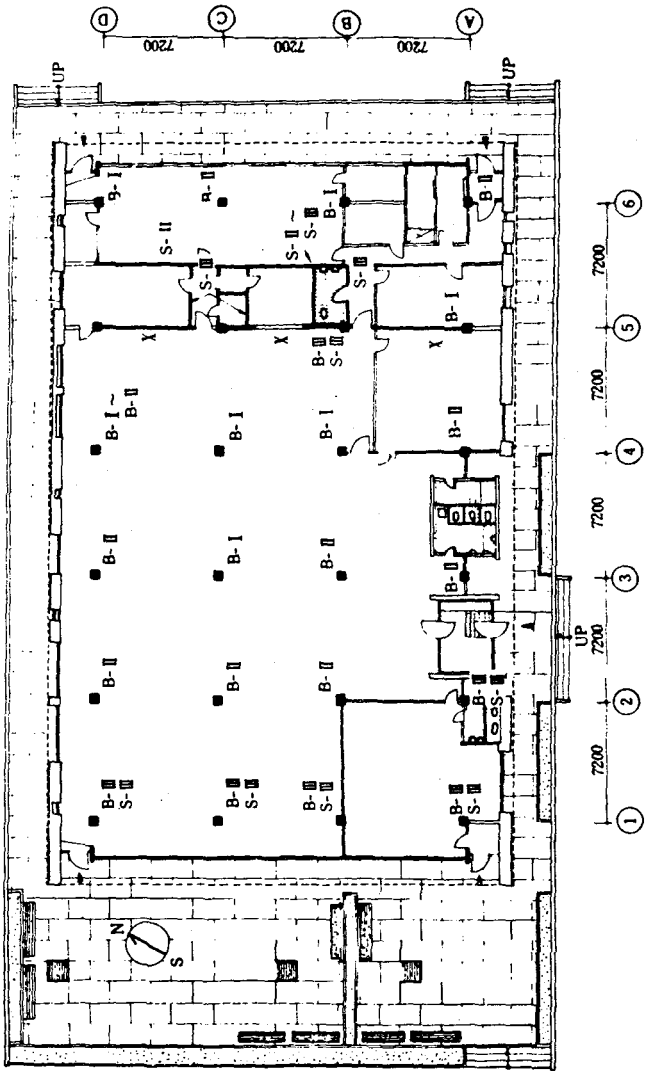

Fig. 1.1 Plan of Hachinohe Library [Ref. 1]

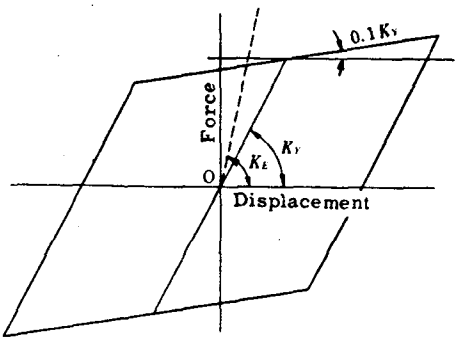

Fig. 1.2 Force-deformation relationship [Ref. 1]

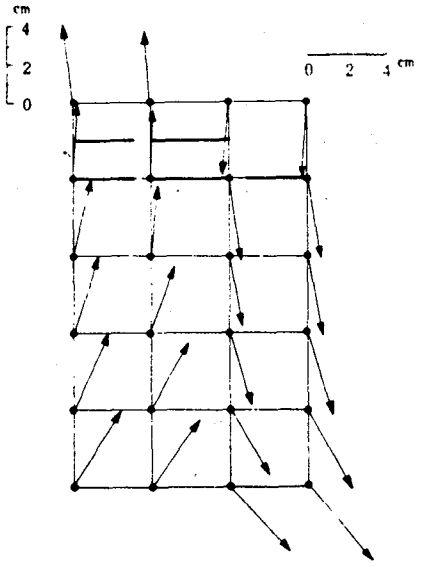

Fig. 1.3 Structural model (Hachinohe Library) and maximum calculated column displacement [Ref. 1]

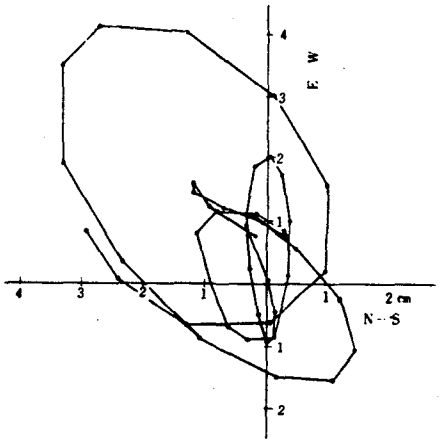

Fig. 1.4 Displacement path of SW corner column A1

was used by Mahin, et al. [6] to examine the structural behavior and damage due to the San Fernando earthquake. Almost the same observations as those made by Okada, et al. [1] were reported. The inability to predict the observed behavior using one-dimensional techniques or models based on planar responses of frames demonstrated the need for better 2D analyses and modeling techniques.

1.3 Two-Dimensional Analyses

In discussing the behavior of reinforced concrete members, two categories are taken into account according to failure patterns: flexural behavior and shear behavior.

Flexural Behavior. Several approaches have been suggested to better represent 2D flexural behavior. The first approach is to formulate a conceptual model for the section, member, or structure which describes phenomena observed in tests. The other approach is to consider the member to be made up of an assemblage of longitudinal elements (filaments) whose behavior is described by the uniaxial stress-strain characteristics of the steel and concrete materials.

(1) Conceptual Model. A bilinear conceptual model used by Okada, et al. [1] is shown in Fig. 1.2. Takizawa and Aoyama [8] used a trilinear model for uniaxial flexure in both principal directions, with both degrading and nondegrading hysteretic behavior, as shown in Fig. 1.5. Takizawa [9] has also used a quadrilinear model for uniaxial flexure. To extend the models to two-dimensional behavior, interaction equations between the two directions are developed and a plasticity approach is used to permit the interaction equations to shift in the moment space.

Figure 1.6 shows the measured and analytical force path for the square (or diamond) loading history which was studied by

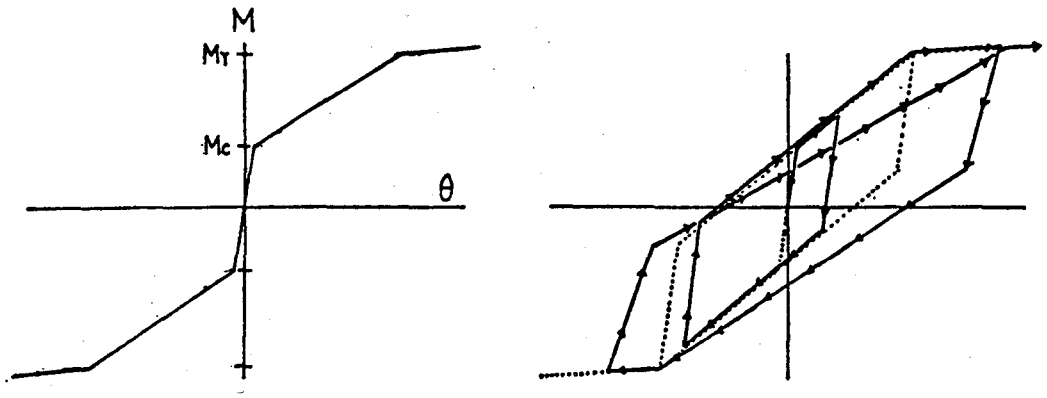

Fig. 1.5 Trilinear model [Ref. 8]

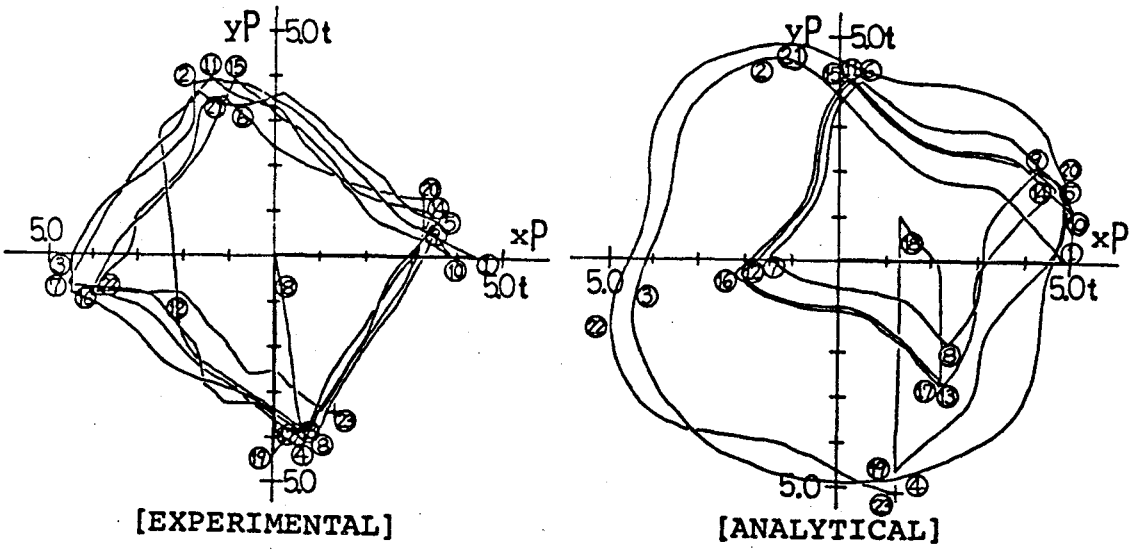

Fig. 1.6 Restoring force path

Takizawa and Aoyama [8]. At the largest deformation level, the measured forces were considerably less than predicted, but the procedure produces acceptable results.

(2) Element or Filament Model. The element or filament model can be used to develop moment-curvature relationships for a section and, by following the section response at selected sections along the axis of the member, the member response can be calculated.

A finite-filament model was used by Aktan, Pecknold, and Sozen [4] to study column flexural behavior. Relatively simple material stress-strain curves were used. The application of the finite-filament model to 2D response is shown in Fig. 1.7. It is interesting to note the comparison between calculated 1D and 2D response. Of particular interest is the change in moment under constant deformation in one direction while the deformation in the opposite direction is changing (note the drop in moment from 1A to 1B or 2B to 2D).

A similar approach has been used by Takiguchi, et al. [10,11,12] for short column specimens subjected to 2D moments. The cross section was divided into elements as shown in Fig. 1.8. The material stress-strain characteristics reflected observed hysteretic response (Fig. 1.9). Measured and computed response in two directions is shown in Fig. 1.10. Note that with a large constant moment (M_2) in one direction, the strength in the opposite direction deteriorates rapidly. However, with a low constant moment (M_2), the response under cyclic loading in the opposite direction is stable. In both cases the analytical procedure is quite accurate.

Okada, Seki, and Asai [13] used a finite element model of the cross section with the steel stress-strain relationship

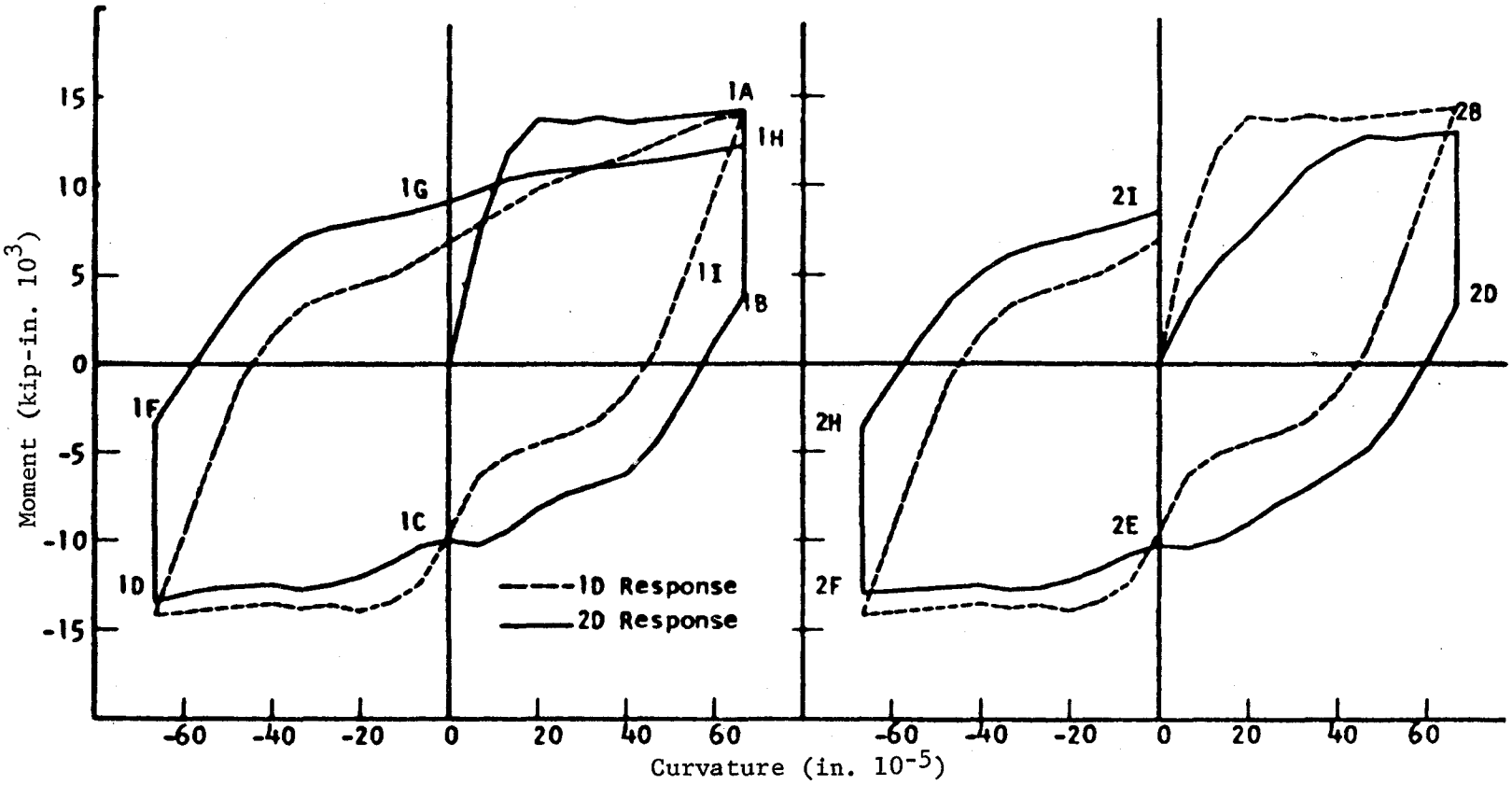

(a) First direction (b) Second direction

Fig. 1.7 One-dimensional and two-dimensional moment-curvature response [Ref. 4]

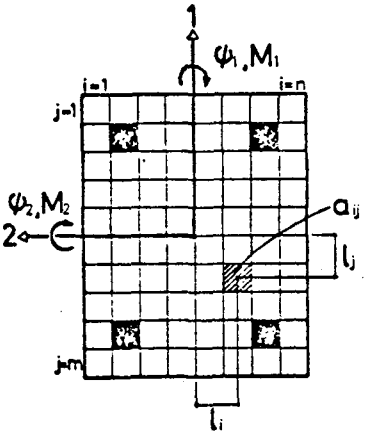

Fig. 1.8 Section elements [Ref. 12]

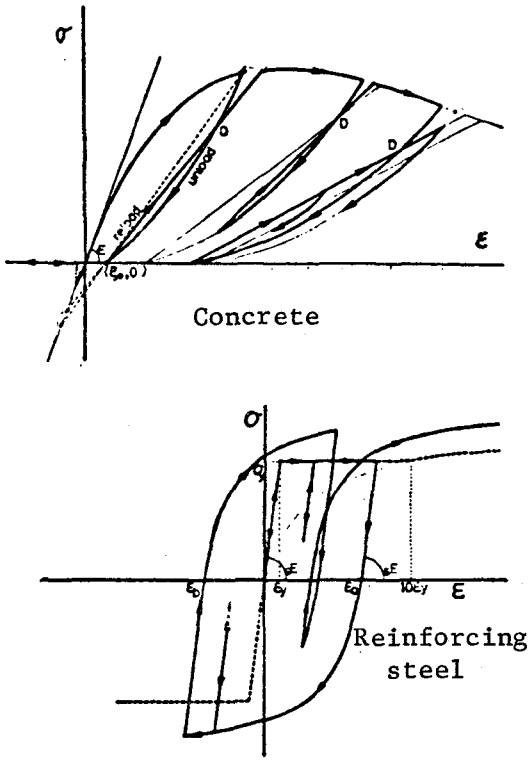

Fig. 1.9 Material response [Ref. 12]

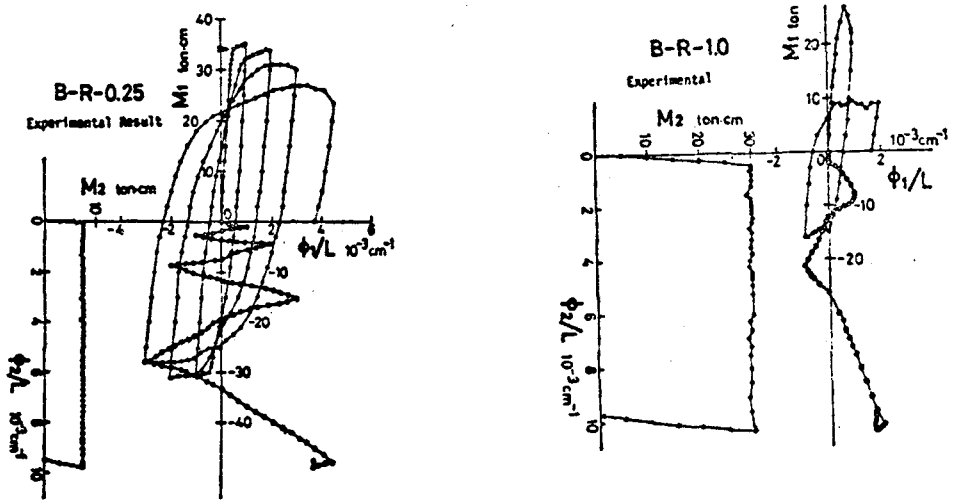

Fig. 1.10 Two-dimensional moment-curvature response [Ref. 12]

expressed by a Ramberg-Osgood function and the concrete material properties similar to those shown in Fig. 1.9. Different 2D loading histories [Fig. 1.11(a)] were applied to columns of identical geometry until flexural failure occurred. The measured and computed response is shown in Fig. 1.11(b) and (c). The measured response clearly indicates the deterioration of strength and deformability of the columns as the severity of the 2D loading increases. Once again, the element model simulates behavior reasonably well.

Shear Behavior. Studies considering shear behavior have been concerned only with uniaxial loading. ASCE-ACI Task Committee 426 reported the state-of-the-art regarding shear and diagonal tension of reinforced concrete members [14,15]. In that report the discussion dealt primarily with shear behavior of members subjected to static loading. The effect of type of loading was mentioned. The influence of repeated and dynamic loadings on ultimate shear strength has been studied. However, there are few studies regarding the influence of reversed loadings. The report by ASCE-ACI Committee 426 [14] commented that there still existed uncertainty regarding the effect of reversals of loading on ultimate shear strength.

The Building Research Institute of the Ministry of Construction in Japan [16] has conducted a very large and well-organized project concerned with the shear behavior of reinforced concrete columns under unilateral inelastic load reversals. This project was conducted over a five-year period (1973-1977) and about four hundred specimens were tested. Many parameters which were considered to influence the behavior of columns were examined [16]. The parameters used in that project were:

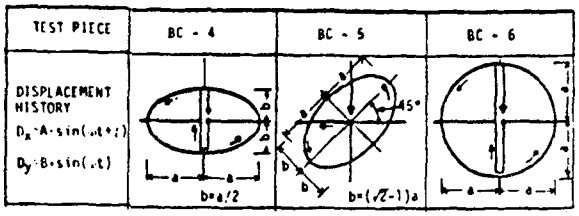

(a) Displacement history

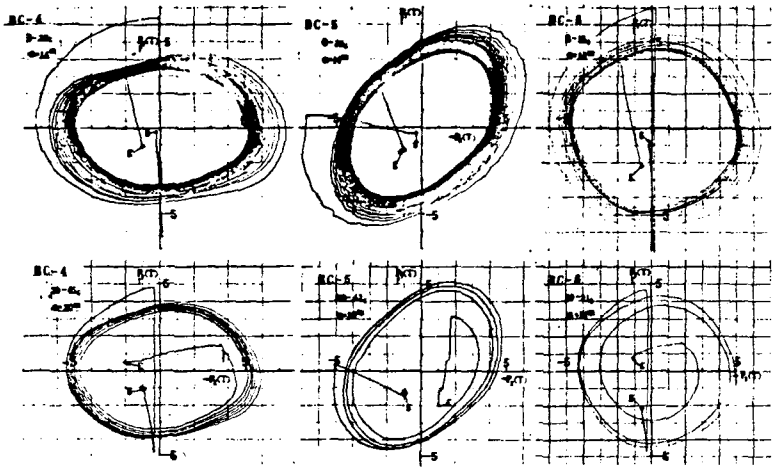

(b) Measured force orbits

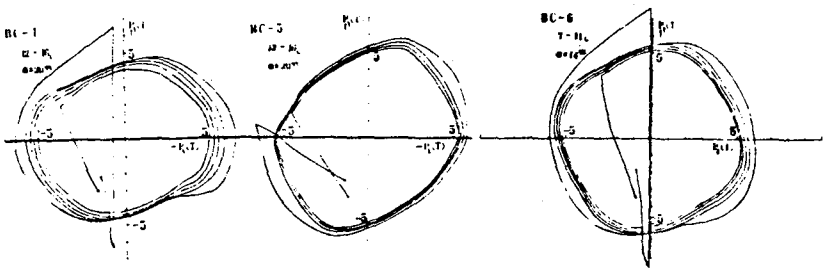

(c) Calculated force orbits

Fig. 1.11 Biaxial tests of columns [Ref. 13]

(1) Size of column - scale effect
(2) Longitudinal reinforcement ratio
(3) Transverse reinforcement ratio
(4) Type of transverse reinforcement: tie, spiral
(5) Column height
(6) Concrete strength
(7) Loading history
(8) Loading system--two different loading systems were used
(9) Column with walls
(10) Axial load

The parameters are so widely varied that the failure mode also varied from ductile flexural failure with large deformation to brittle shear failure or bond failure before flexural yielding. The type of failure was classified in four levels in terms of ductility (Table 1.1).

TABLE 1.1 CLASSIFIED DUCTILITY [Ref. 16]

Ductility	Characteristics
A	Very ductile columns which failed by shear or by buckling of compression bars at horizontal large deformation.
B	Ductile columns, where deterioration of shear capacity was small until $\mu = 4(\mu = \delta/\delta_y)$, but which failed by shear or by bond or by buckling of bar before $\mu = 6$.
C	Columns yielded by flexure at first, but deteriorated remarkably due to shear or bond failure or buckling of bars before they reached a large deflection.
D	Columns failed by shear or by bond before flexural yielding (other than A, B, and C).

This table indicates a possible standard for defining long columns failing in flexure and short columns failing in shear. Columns whose failure mode is classified in ductility A and B can be considered as long columns. The ductility levels C and D represent short columns.

Regarding the standard for defining short columns failing in shear, Yamada and Kawamura [17] proposed an equation for "a critical shear-story height ratio". The equation is given in terms of geometry and cross-sectional properties of the column, axial load, and material properties of concrete and steel. However, it does not include the influence of transverse reinforcement.

As stated before, many experimental and analytical studies have been conducted regarding ductile members (including long columns). Several models are successfully developed and are extended to apply to two-dimensional behavior.

On the contrary, for columns classified as ductility levels C and D in Table 1.1, there are very few experimental studies and those studies were conducted under unilateral reversed loading. There is no model developed for shear behavior under inelastic reversed loading.

Therefore, to better understand shear behavior of reinforced concrete members and to improve design, shear behavior under bidirectional lateral loading must be studied. Such studies can be used to develop models to predict the shear behavior of reinforced concrete members.

1.4 Scope of This Study

As discussed previously, there are many parameters governing the shear behavior of reinforced concrete members under bidirectional reversed lateral loading. It would be desirable to

study the influence of each parameter on shear behavior as was done in the studies of columns under unilateral inelastic load reversals in Japan [16]. As a minimum, sufficient testing is needed to determine if behavior under unilateral loading reflects behavior under bilateral loading.

At the Balcones Research Center of The University of Texas at Austin, research on the shear behavior of reinforced concrete frames is being conducted. Studies of columns and beam-column joints are underway. This report covers one phase of the column studies. Objectives of the column studies are:

(1) To study the influence of bidirectional lateral load history on shear behavior

(2) To develop models for shear behavior under bidirectional lateral loading

(3) To study the influence of axial loading combined with bidirectional lateral load history

(4) To study the transition between shear and flexural failures under bidirectional lateral load history by varying the transverse and longitudinal reinforcement, the shear span-to-depth ratio, and possibly cross section dimensions.

The study reported herein is concerned with objectives (1) and (2). The main parameter is the variation of load history; other parameters were fixed throughout. For example, axial load was held at zero and the same geometry and cross section properties were used for all test specimens.

The test specimen was designed to fail in shear so that the dimension and the cross section properties of the specimen were determined referring to other experimental results under unilateral load reversals [16] and the concept of "a critical

shear-story height ratio" proposed by Yamada and Kawamura [17].

1.5 Objectives of This Report

(1) To evaluate the importance of load history (bidirectional lateral load history) on the response of members in reinforced concrete structures. The prime variable to be considered is the sequence and path of application of lateral movement. No axial load was applied to the specimens.

(2) To develop models which can be used to predict the behavior of members subjected to large shear forces.

CHAPTER 2

TEST SPECIMEN

2.1 Design Requirements

The objective of the overall program was to examine the behavior of reinforced concrete columns failing in shear. Therefore, it was necessary to design a test specimen with a short stiff column which could be used in all phases of the study. In addition, the specimen was to be subjected to axial tensile or compressive loadings. Based on these requirements, the specimen selected was a short element framing into enlarged end blocks which could be attached to a load frame. The loading frame was designed to restrain rotation of the end blocks. As a result, the specimen could be considered to simulate a short column framing into a relatively stiff floor system. Based on a review of available test results, a shear span-to-depth ratio less than 2 was selected to ensure that shear governed the mode of failure.

The prototype column was designed as an 18 in. square section with a height of 4.5 ft. (1.4 m), meeting the requirements of ACI 318-77 [18]. Because the fabrication cost of the test frame required to test the large section was excessive, the test specimen was scaled to produce a column section which could be conveniently and economically tested and which would permit the use of available reinforcing bar sizes.

2.2 Specimen Details

Column Section. The test specimen is shown in Fig. 2.1. The specimen is a 2/3-scale model of the prototype column. The

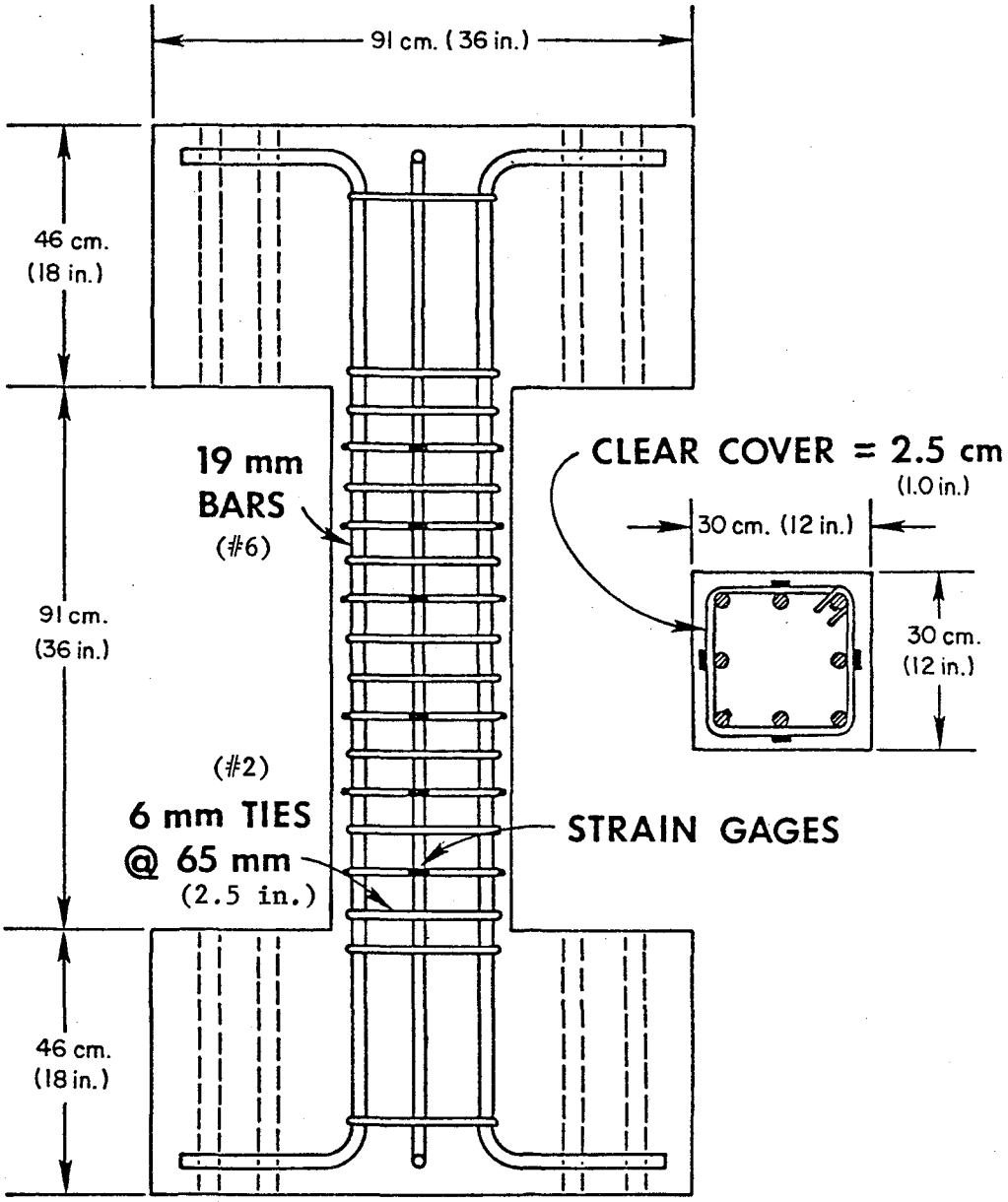

Fig. 2.1 Test specimen

prototype column has an 18 in. (46 cm) square section with eight #9 (28 mm) longitudinal bars (ρ_g = 0.025) and #3 bars for the transverse reinforcement. Cover in the prototype was 1-1/2 in. (3.8 cm). With the 2/3 scale factor, #6 (19 mm) longitudinal bars were used and cover was reduced to 1 in. (2.5 cm). The column height was reduced to 36 in. (0.9 m). For transverse reinforcement, special 6 mm (#2) deformed bars were obtained.

Transverse Reinforcement. The spacing of the transverse reinforcement was critical if a shear mode of failure was to be obtained. It was necessary to select a spacing which would typify a column section but would not have sufficient transverse reinforcement to preclude a shear failure. Using ACI 318-77, the required shear reinforcement can be determined using

$$A_v = (v_u - v_c)\, b_w s/f_y$$

With f_y = 60 ksi (414 MPa) and f'_c = 5 ksi (35 MPa), the calculated maximum moment with zero axial load of the column section is about 1000 in.-k (113 kN-M). To develop maximum moment at both ends of a column 36 in. long (91 mm), the shear force on the column section is about 56k (249 kN). Using ACI 318-77, Chapter 11, the required spacing of stirrup ties in the column is 1.7 in. (4.3 cm). It should be remembered that a maximum spacing of 1.7 in. is required if shear failure is to be avoided.

Appendix A (Seismic Design) of ACI 318-77 also specifies confinement reinforcement to be continued into the column from the ends. For columns with low axial load ($\leq$ 0.4 balance load), the column should be designed as a flexural member with the spacing not exceeding d/4 within a distance equal to four times the effective column depth from the end of the member (Secs. A.5.9 and A.6.3). If the axial load is greater than 0.4 balance load (Sec. A.6.4), confining reinforcement (Eq. A-4) is to be supplied

above and below connections over a minimum length from the face of the connection at least equal to the overall depth (larger dimension in a rectangular column), 18 in. or 1/6 the clear height of the column. The maximum spacing for the confining hoops is 4 in. (10 cm) or 2.7 in. (6.7 cm) in a 2/3-scale model. Using Sec. A.6.4, the required spacing is 2.4 in. (6 cm), and using Sec. A.6.3 (d/4), the spacing is 2.59 in. (6.6 cm).

Based on the requirements that the columns should fail in shear and also that the transverse reinforcement should be typical for a moment-resisting frame structure, the spacing of stirrup ties was set at 2.5 in. (6.5 cm).

Calculated Strength. As mentioned above, the ultimate moment of the test specimen is about 1000 in.-k (113 kN-M) without axial load. The lateral force which develops the ultimate moment is about 56k (249 kN) with a column height of 36 in. Although the ultimate moment capacity of the members can be calculated and estimated with accuracy, it is difficult to estimate the shear strength. ACI 318 recommends the shear strength be calculated as follows:

$$V_u = V_s + V_c$$

where V_u = ultimate shear strength
V_s = shear strength carried by transverse reinforcement
V_c = shear strength carried by concrete

$$V_s = \frac{A_v f_y d}{s} = \frac{0.1 \times 60 \times 10.4}{2.5} = 25k \text{ (111 kN)}$$

Shear strength carried by concrete is difficult to estimate. For design, ACI 318 (Chapter 11) specifies $V_c = 2\sqrt{f'_c}\, b_w d$ for members with large shear span-to-depth ratios subjected to

shear and flexure only. For members with short shear spans, ACI 318 permits shear stresses up to $6\sqrt{f'_c}$. Then,

$$V_c = 18k \text{ (80 kN)} \qquad 2\sqrt{f'_c}$$

$$V_c = 51k \text{ (227 kN)} \qquad 6\sqrt{f'_c}$$

$$V_u = V_s + V_c = 43 \sim 76k \text{ (191} \sim \text{338 kN)}$$

Mattock [15] presented test results relating the ultimate shear to the transverse reinforcement ratio and yield strength ($\rho_n f_y$). Judging from his test results, the ultimate shear capacity of the specimen in this study can be estimated as V_u = 72k (320 kN).

It should be noted that these calculated values are for the static strength. ACI-ASCE 426 [14] mentions the effect of type of loading. According to the report of Committee 426, the ultimate shear strength under repeated loadings is 50 ~ 70 percent of the static strength. However, for reversed loadings, the report says that uncertainty exists regarding the effect of reversals of loading on ultimate shear strength.

Therefore, it was expected that the specimens would fail in shear. In fact, all the specimens reported in this study failed in shear.

2.3 Specimen Fabrication

The dimensions of the end block were based on the requirements for attaching the specimen to the loading heads and for adequately anchoring the longitudinal column reinforcement. Details of the end block reinforcement and provisions for attachment to the loading frame are included in Refs. 23 and 24.

The specimens were cast in one operation. Special formwork details were developed to ensure proper concrete compaction in the column and the end blocks [23,24].

2.4 Materials

Concrete. Ready-mix concrete was obtained from a commercial supplier located near the laboratory. The mix proportions were as follows:

Concrete Mix Design (5000 psi, 35 MPa)

Proportions for 1 yd^3

Water	312 lb	w/c = 0.6 by weight
Cement	520 lb	
Fine aggregate	2200 lb	
Coarse aggregate (3/8 in.)	3240 lb	
Airsene (plasticizer)	25 oz	

The aggregate was Colorado River sand and gravel. Some of the water was withheld at the plant and adjusted at the laboratory to achieve the desired slump (6 in.). Twelve control cylinders were cast with each batch and cured with the specimens. Two specimens were cast in each operation. The forms were stripped two to three days after casting. Concrete strengths at the time of testing ranged from 4.4 to 6.0 ksi.

Reinforcement. No. 6 (19 mm) deformed bars were used for longitudinal reinforcement and Grade 60, #2 (6 mm) deformed bars for transverse reinforcement. The #2 deformed bars for all specimens were from the same shipment. The #6 deformed bars came from two different shipments. Coupons of the deformed bars were tested to obtain the modulus, yield, and ultimate for the steel. Stress-strain curves for the reinforcement are shown in Fig. 2.2.

The material properties in each specimen are summarized in Table 2.1.

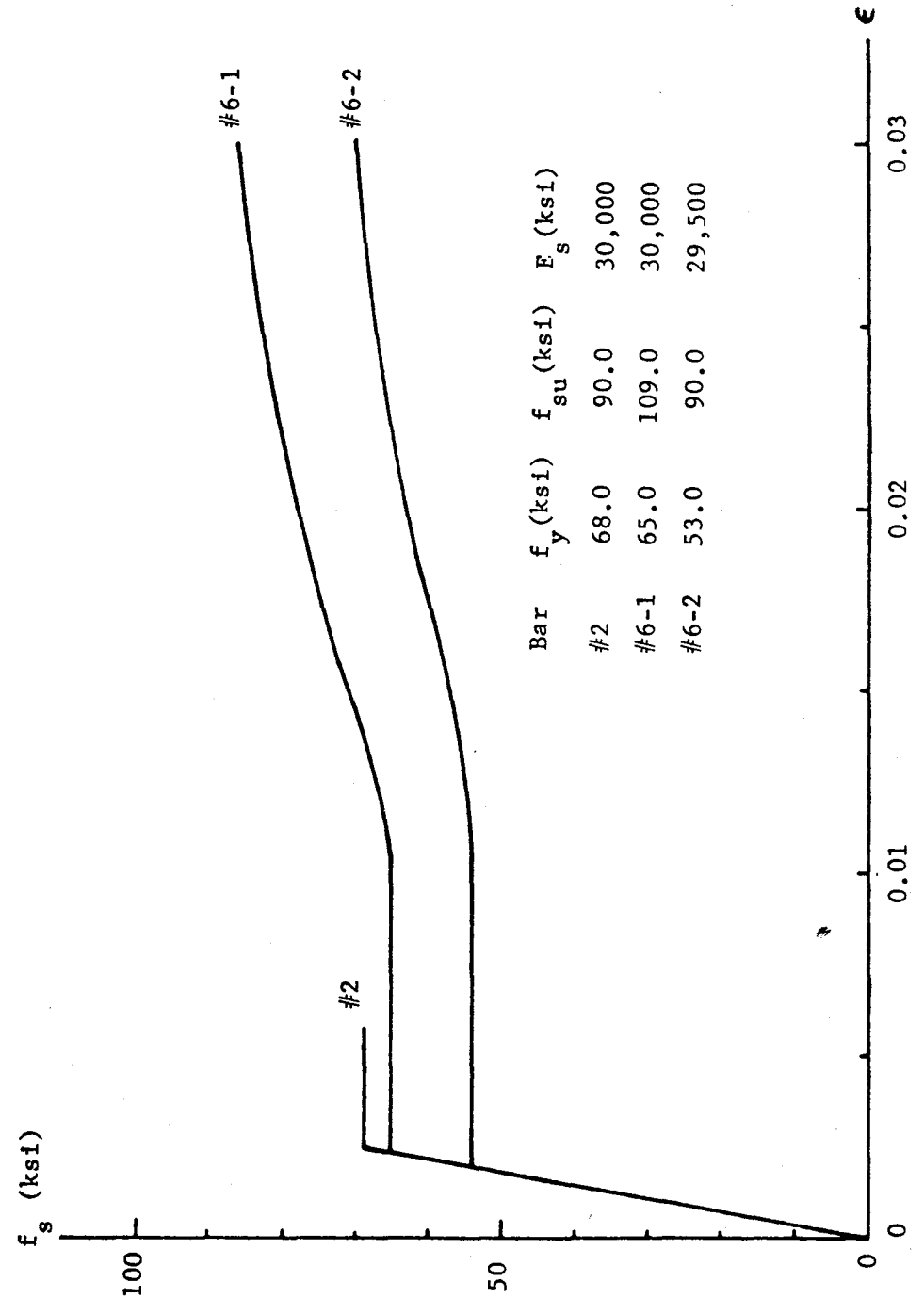

Fig. 2.2 Stress-strain curves for reinforcement

TABLE 2.1 MATERIAL PROPERTIES

Steel

	f_y (ksi)	f_{su} (ksi)	E_s (ksi)
#2	68.0	90.0	30,000
#6-1	53.0	90.0	29,500
#6-2	65.0	109.0	30,000

Concrete

Specimen	Concrete				Steel
	f'_c (psi)	Age (days)	Cast	Slump (in)	
00-V-0-I	5000	47	12/ 2 /77	5 1/4	#2, #6-2
00-V-2VP-I	4350	59	12/16/77	7	#2, #6-2
00-V-4VP-I	4350	55	12/16/77	7	#2, #6-2
00-V-V-A	6000	30	1/25/78	6	#2, #6-2
00-V-V-S	4950	28	3/31/78	8 1/2	#2, #6-1
00-V-V-SA	5050	35	3/31/78	8 1/2	#2, #6-1
00-V-2C-I	5500	35	4/14/78	6	#2, #6-1
00-V-4C-I	5000	56	12/ 2 /77	5 1/4	#2, #6-2
00-C-C-AH	5600	43	3/ 1 /78	7 1/2	#2, #6-2
00-C-C-AF	5250	28	4/14/78	6	#2, #6-1

CHAPTER 3

TEST PROCEDURE

3.1 Loading Histories

The objective of this study is to examine the influence of bidirectional lateral loading histories on reinforced concrete members.

Many variations of loading history can be considered. However, the importance of variation of loading history can be evaluated in two categories. One is the importance of loading sequence--the number of cycles of load imposed and the sequence and magnitude of applied load. The other is the importance of load path--the trace of deformation in the two-dimensional phase.

In this program the first category is labeled "sequential" and the other is labeled "simultaneous," because loads are applied in both directions at the same time in the second category.

The lateral loads are controlled by deflection, as shown in Fig. 3.1a (Basic Loading Pattern). The unit deflection Δ_i is defined as the deflection when the strain in the longitudinal bars shows first yield. The deformation applied is increased incrementally with three cycles at each level of deformation.

There are several papers in which the number of cycles of load are discussed. Higashi, et al. [20] reported that the largest change in response generally occurs between the first and second loading cycles at a given deflection level. Umemura, et al. [21] applied ten cycles of load to the specimen at each deflection level. The test results showed that the strength

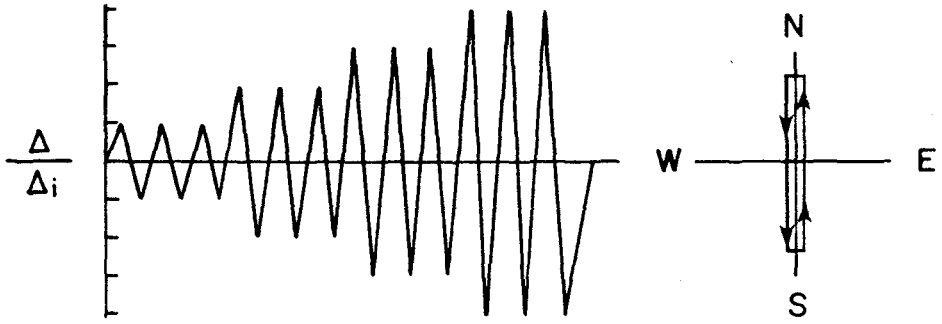

(a) OO-V-O-I (Basic Loading Pattern)

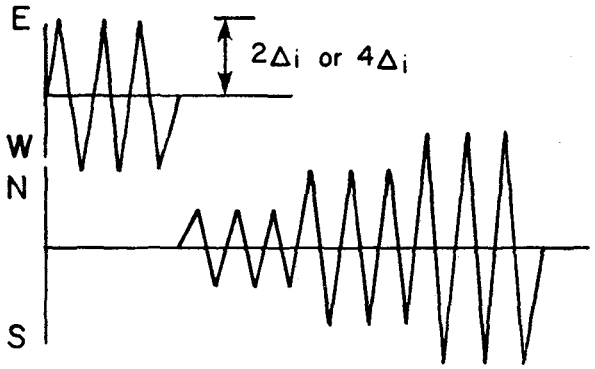

(b) OO-V-2VP-I

(c) OO-V-4VP-I

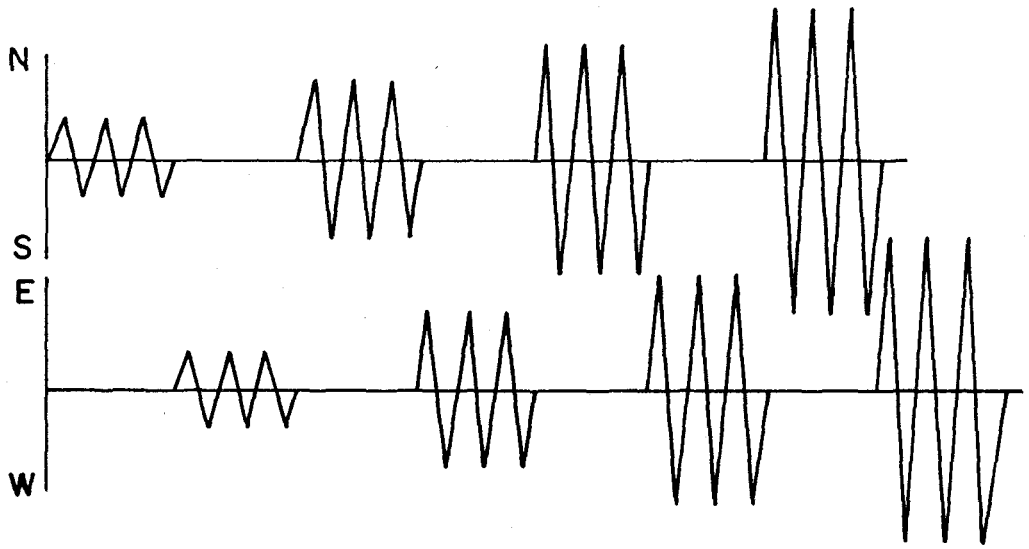

(d) OO-V-V-A

Fig. 3.1 Loading histories (Sequential)

reduction after three cycles of load was relatively very small compared with the reduction in the first three cycles of load. Moreover, Muto, et al. [22] made a simulation analysis of a high rise reinforced concrete building using the records of ground motion of two different earthquakes. According to the results, the number of the large peaks in the response spectrum is usually around three.

From these considerations the three cycles of load at each deflection level were selected as the basic loading pattern. The axial load is not taken into account in this study. The history of axial load can be another parameter. In all tests the axial load is held zero (except the relatively very small dead weight of loading head = 2 kips). Therefore, although the shape of the specimen looks like a column, the test results can be basically treated as the results of beams and also can serve as reference tests for columns under axial load.

The objective in the category of the sequential loading is to examine how the ultimate shear strength is influenced by previous loadings and how the strength deteriorates. The basic loading pattern (unilateral loading), shown in Fig. 3.1a, gives an indication of the influence of previous loading in the same direction on the shear strength. The next two cases, as shown in Fig. 3.1b and c,are to examine the influence of previous loading in an orthogonal direction. From the preliminary test, it was found that the unit deflection Δ_i was about 0.2 in. (5 mm) and the ultimate strength under monotonic loading was obtained at about 0.6 in. (15 mm) deflection, which corresponds to $3\Delta_i$. Therefore, two deflection levels, $2\Delta_i$ (before reaching ultimate strength) and $4\Delta_i$ (after reaching ultimate strength), were chosen for previous loading. The fourth case (Fig. 3.1d) is to examine the influence of previous loadings imposed alternately in both directions.

In the category of the simultaneous loading, the influence of load path on the shear behavior is of prime interest. The first two cases (Fig. 3.2 a and b) are to examine the influence of constant deflection in one direction. Two different deflection levels ($2\Delta_i$, $4\Delta_i$) are chosen for constant deflection. The other four cases in Fig. 3.2 (c, d, e, f) show different load paths; however, the extreme points in each case produce the same magnitude of deflection measured diagonally from the origin. From a comparison of these four cases, the influence of load path should become apparent.

[Category I: Sequential]

The notation used with the specimens is expressed as follows:

00-V-0-I

- I — Type of loading
- 0 — Loading in the E-W direction
- V — Loading in the N-S direction
- 00 — Axial load in kips

Axial load - all specimens have 00- because no axial load was applied in this study.

Loading in N-S or E-W direction -

- V deflection imposed is reversed with 3 cycles and increased incrementally.
- 2VP, 4VP previously imposed deflection with 3 cycle reversals at $2\Delta_i$ or $4\Delta_i$ deflection level
- 0 zero loading
- C constant deflection in given direction, e.g., 4C denotes a constant $4\Delta_i$ deflection

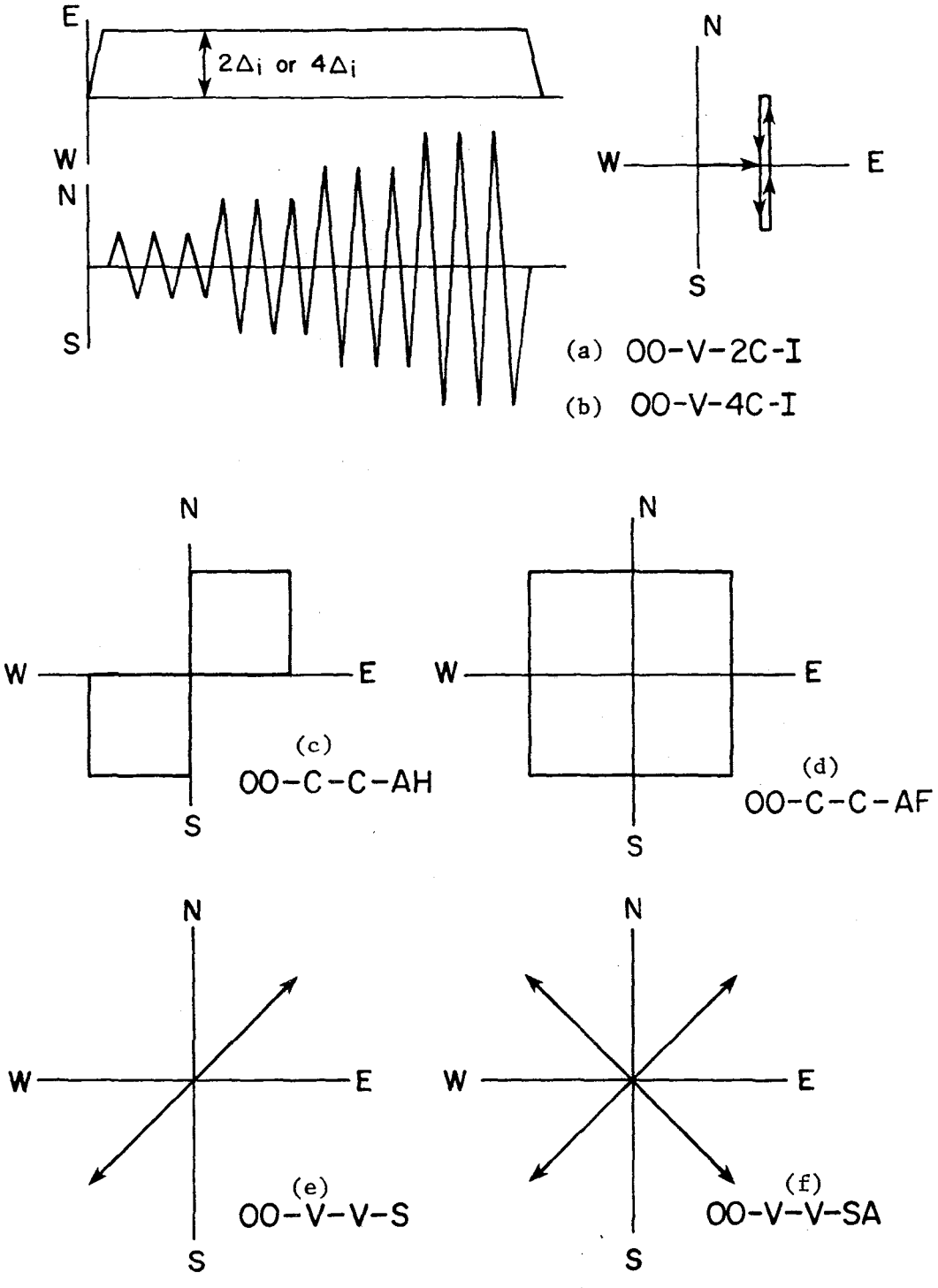

Fig. 3.2 Loading histories (Simultaneous)

Type of Loading

I loading in N-S direction and loading in E-W direction are independently imposed

A loading in N-S direction and loading in E-W direction are imposed alternately at each deflection level

AF loading along a square path as shown in Fig. 3.2d

AH loading along a "half" square load path as shown in Fig. 3.2c

S same deflections are imposed in both N-S and E-W direction simultaneously

SA same deflections are imposed in both N-S and E-W direction simultaneously and the combination of sign of loading in each direction changes after 3 cycles of load. For example

N-S	E-W	N-S	E-W
+ -	+ -	+ -	- +

The pattern of loading is applied alternately at each deflection level

OO-V-O-I As shown above and in Fig. 3.1a, this is the case of unilateral load reversals. The deformation applied in the N-S direction is increased incrementally with 3 cycles at each level of deformation. Zero deformation is maintained in the E-W direction. This type of loading is named the basic loading pattern. (Loading U in Ref. 24)

OO-V-2VP-I As shown in Fig. 3.1, initially 3 cycles at $2\Delta_i$ or
OO-V-4VP-I $4\Delta_i$ are applied in the E-W direction. After that, the basic loading pattern is imposed in the N-S direction with zero deformation in the E-W direction.

OO-V-V-A The deformation in the N-S and the E-W direction is imposed alternately at each deflection level. (Loading B in Ref. 24.)

The effect of the deflection level in previous loadings in an orthogonal direction is examined in 00-V-2VP and 00-V-4VP-I. This may represent the restoring force characteristics of columns after earthquakes. On the other hand, 00-V-V-A may represent the restoring force characteristics during earthquakes.

[Category II: Simultaneous]

00-V-2C-I
00-V-4C-I Initially $2\Delta_i$ or $4\Delta_i$ deformation is applied in the E direction and is held constant while the basic loading pattern is imposed in the N-S direction.

00-C-C-AF The deformation path is square, as shown in Fig. 3.2. The deflection level is Δ_i, $2\Delta_i$, $3\Delta_i$, and $4\Delta_i$ in all directions. Three cycles at each level are imposed. (Loading S in Ref. 24)

00-C-C-AH As shown in Fig. 3.2, this is the half circuit of 00-C-C-AF.

00-V-V-S The deformation is applied in the diagonal direction. This means that the basic loading pattern is imposed in both directions at the same time.

00-V-V-SA Alternate loading in both diagonal directions at each deflection level. (Loading D in Ref. 24)

The relationship between 00-V-V-S and 00-V-V-SA looks quite similar to that between 00-V-0-I and 00-V-V-A. Loading 00-V-V-S is the unilateral loading case if loading axes are transformed 45^{o}. In that case, the differences between 00-V-V-S and 00-V-0-I are only the cross section properties and the relative magnitude of deflection level.

The results from 00-C-C-AH and 00-V-V-S or 00-C-C-A and 00-V-V-SA can be compared to determine the importance of load path. Figure 3.3 show the possible load paths from one deflection

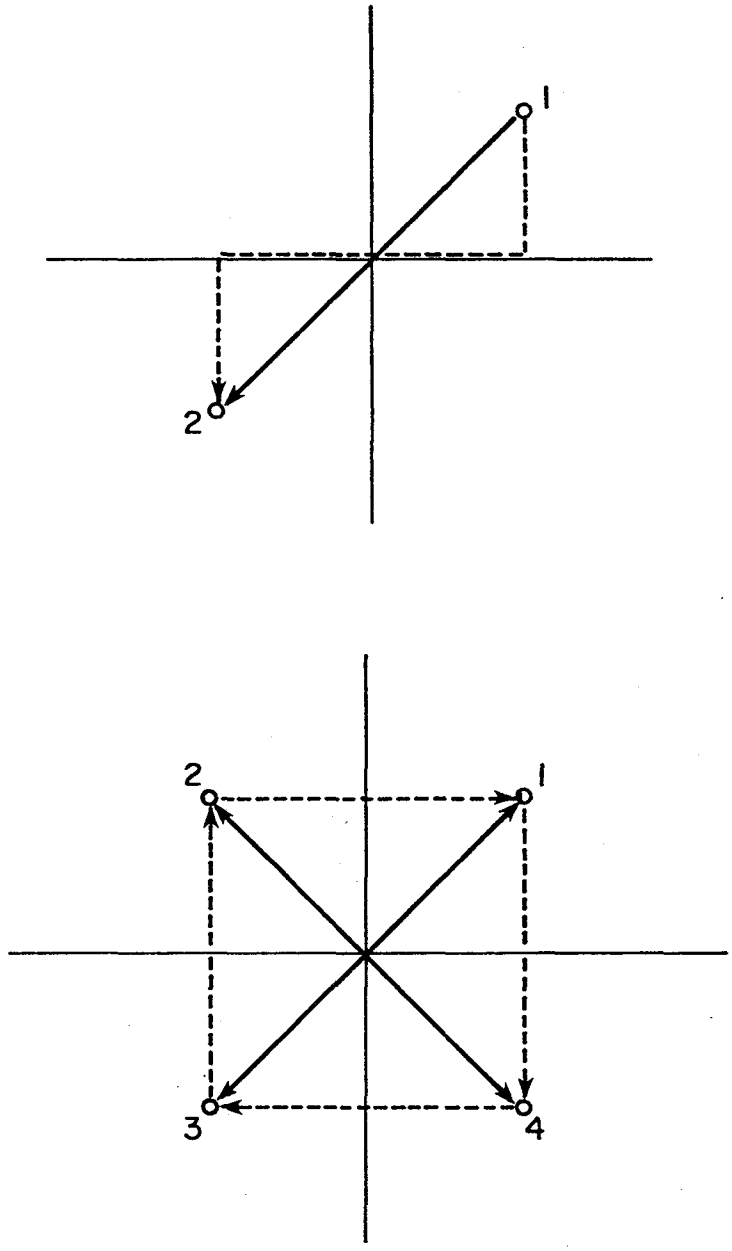

Fig. 3.3 Load paths

to a deflection elsewhere in the horizontal plane. The above four cases represent the typical load paths.

3.2 Loading System

Because of the complexity of the loading histories to be studied, it was necessary to develop a loading system which was capable of applying lateral loads independently in two directions and vertical loads with a range varying from tension through compression. The lateral loads had to be applied through fairly large deformations. To reduce the complexity of the loading frame, a structural floor-wall reaction system was designed and built in the Civil Engineering Structures Research Laboratory. The floor-wall system is described in detail in Ref. 19.

The test setup is shown in Fig. 3.4. Complete details of the design, construction, and operation of the loading system are contained in Refs. 23 and 24.

3.3 Instrumentation and Control

Loads, displacement, and strains were measured and recorded throughout the load history for each specimen. Selected load channels were monitored on X-Y plotters during testing for visual observation. Cracks were marked and photographed at selected stages in the load history.

Data were initially recorded on magnetic tape or on a disc unit. Following completion of the tests, data were processed on a minicomputer and line printer tabulations of basic information were obtained by load stage. The processed data were used to produce plots on a digital plotter which can provide figures in report quality format. Details of the data processing system are provided in Refs. 23 and 24.

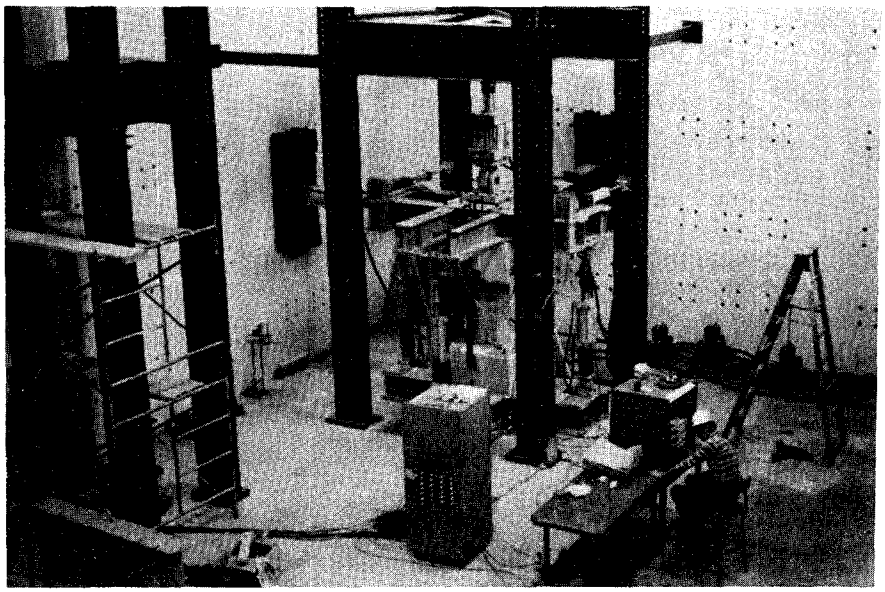

Fig. 3.4 Test setup

CHAPTER 4

OBSERVED BEHAVIOR AND RESULTS

4.1 General

As stated in Chapter 3, the loading history was deflection-controlled with a basic loading pattern of three cycles at each deformation level. First, the unit increment of deflection must be defined.

In the preliminary test, strain in the longitudinal bars was monitored and the initial deflection (= unit deflection) was defined as the deflection when the strain in longitudinal bars at the bottom of the column indicated a large increase with a small increase in load. In the first test, this deflection was about 0.2 in. (5 mm). In all other tests, 0.2 in. was taken as the unit increment of deflection (Δ_i).

The load was applied in the principal directions and the load-deflection curves were recorded in each principal direction. In this study, the terminology "the principal direction" is used to denote loading or deformation in the N-S or E-W direction. In all tests, the column behaved elastically up to the Δ_i (unit deflection) level. As will be shown, at the $2\Delta_i$ or higher deflection levels the peak shear strength reduced and the stiffness decreased. The load-deflection curve showed the so-called "pinched curve" or "inverted S shape" which is characteristic of shear behavior of columns. The typical "pinched curve" can be seen at the $3\Delta_i$ deflection level in the case of unilateral loading (Fig. 4.1b).

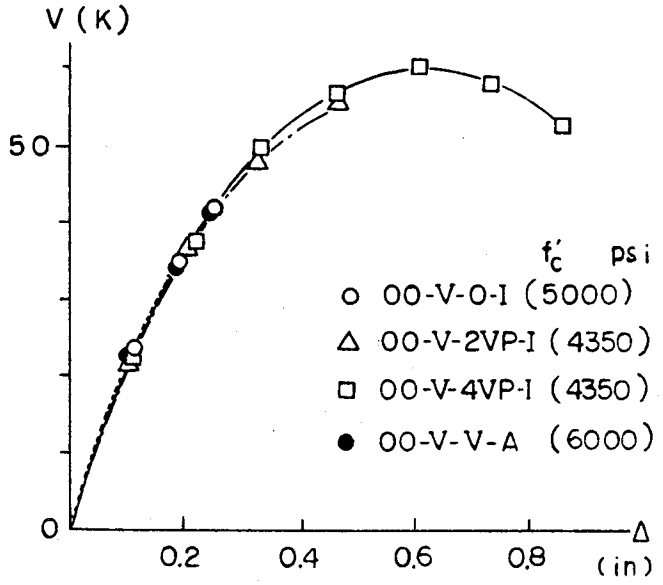

Fig. 4.1a Load-deflection relationships--monotonic loading

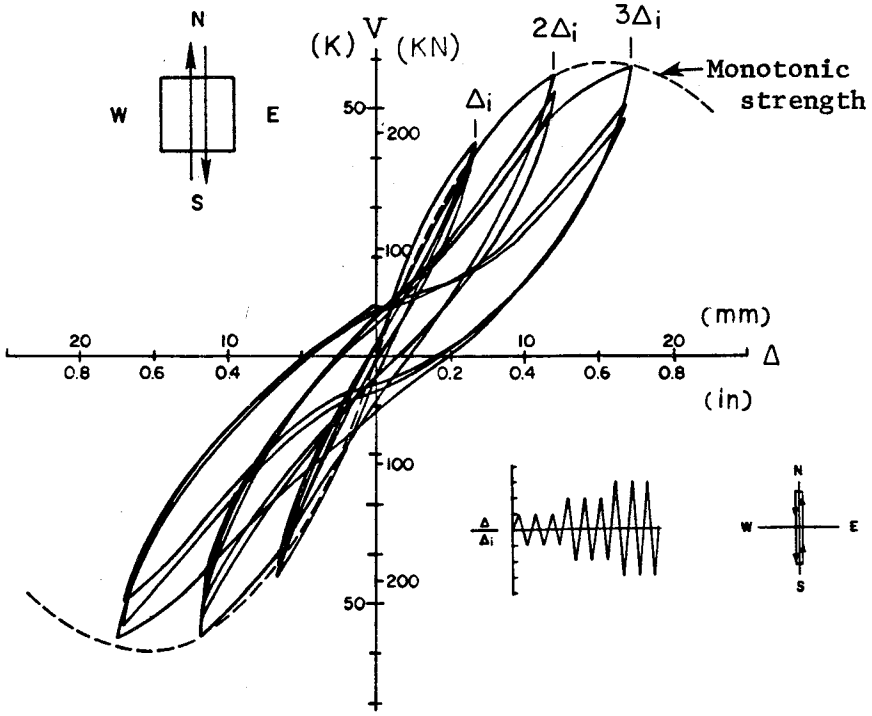

Fig. 4.1b Lateral load-deflection relationship--00-V-0-I

Strain gages were attached to the transverse reinforcement on all four sides. Based on the recorded strain in the transverse reinforcement, the strain distribution was obtained along the column height. Transverse reinforcement does not pick up much stress unless a crack in the concrete crosses the bar. Once the crack crosses the transverse reinforcement, the strain in that bar begins to increase rapidly. Therefore, the strain distribution in the transverse reinforcement may indicate how and where cracks initiate and propagate inside the core of the column. Strain measurements can also show the efficiency of the transverse reinforcement during reversed loading.

Cracks were marked on the surface of the specimen at every peak load stage. Generally, at the Δ_i level several shear cracks ran diagonally near both top and bottom ends of the column. With cycles of load or increase of deflection level, the cracks propagated and new cracks initiated. The shear cracks appeared to be symmetrically distributed about the middle of the column. The initiation of new cracks began at both end regions and moved toward the center. Finally, the entire region was covered with many cracks and a couple of large cracks went through the column. The typical crack patterns are shown in Fig. 4.34 and the appearance of the specimen at failure is shown in Figs. 4.44 and 4.45.

4.2 Load-Deflection Relationships

Load-deflection curves for the ten specimens subjected to different load histories are represented in Figs. 4.1 - 4.25. The case of 00-V-4VP-I shown in Fig. 4.4 provides the load-deflection curve under monotonic loading up to 0.8 in. deflection. In 00-V-4VP-I, three cycles of load with $4\Delta_i$ deflection

level were imposed on the column in the E-W direction. After that, the basic loading pattern was applied in the N-S direction. The monotonic curve is taken as the standard for comparing test results. As presented in Table 2.1, the concrete strength differed in each specimen. The ultimate shear strength may be influenced by the difference of the concrete strength. However, as far as the lower deflection levels are considered, the load-deflection curve in each specimen exhibited very little difference, especially from zero deflection up to Δ_i deflection, as shown in Fig. 4.1a. For this reason, the monotonic strength curve which is shown in each cyclic load-deflection curve as a dashed line is not modified by the concrete strength. However, in Chapter 5 the peak shear strength is normalized in terms of the concrete strength.

Detailed observation of the behavior of the specimens is presented below.

00-V-0-I (Basic Loading Pattern). This is the case of the unilateral loading with the basic loading pattern. As shown in Fig. 4.1, the reduction of shear strength at each peak deflection level (Δ_i, $2\Delta_i$, $3\Delta_i$ in Fig. 4.1b) is very small. Even with three cycles of Load at $3\Delta_i$ level, the shear strength does not decrease much. In comparison with the monotonic strength, the first peak strength at each deflection level looks almost the same as the monotonic strength. This phenomenon has been observed by others [16,21]. The envelope curve for cyclic loading is generally the monotonic curve. However, it should be noted that the maximum strength under monotonic loading appears at about 0.6 in. deflection. That value corresponds to $3\Delta_i$. In the unilateral loading case, cycles were not continued past $3\Delta_i$ because the deformation instrumentation was not adequate. In the region over the $3\Delta_i$ level deflection, the first cycle peak strength may not necessarily represent the monotonic strength.

Although the shear strength at the Δ_i level does not decrease with three cycles of load, the stiffness reduces slightly with cycling. The stiffness reduction is considerable between the second and third cycle at lower deflection levels.

The shape of the load-deflection curve at the second and third cycle is an inverted S. The residual deformation increases with increase in the peak deflection level. However, the residual deformation is almost constant under three cycles of load at a certain deflection level.

<u>00-V-2VP-I, 00-V-4VP-I (Previous Loading)</u>. These two cases examine the influence of previous loading in an orthogonal direction. The three load reversals (with a $2\Delta_i$ or $4\Delta_i$ level) were applied first in the E-W direction. After the initial E-W loading, the basic loading pattern was imposed in the N-S direction.

00-V-2VP-I. The load-deflection curves in both principal directions are shown in Figs. 4.2 and 4.3. The previous loading produces a slight reduction in stiffness and strength at Δ_i when compared with the results from 00-V-0-I. However, at the $3\Delta_i$ level the peak loads are about the same as those in the unilateral loading. The previous loading at the $2\Delta_i$ deflection level in an orthogonal direction has little influence on shear strength and the stiffness at deflections less than $2\Delta_i$ and none at levels greater than $2\Delta_i$.

00-V-4VP-I. As shown in Fig. 4.4, the peak shear strength and the stiffness reduced significantly within three cycles of previous loading at $4\Delta_i$. The specimen failed due to the first loading. The load-deflection curves in the N-S direction are very flat (see Fig. 4.5).

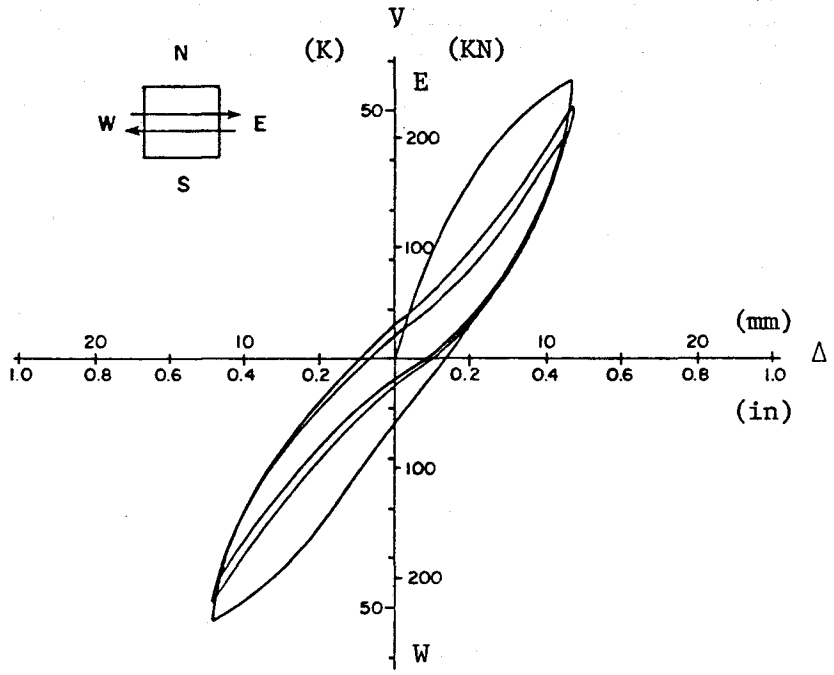

Fig. 4.2 Lateral load-deflection relationship--
00-V-2VP-I (E-W) initial cycles

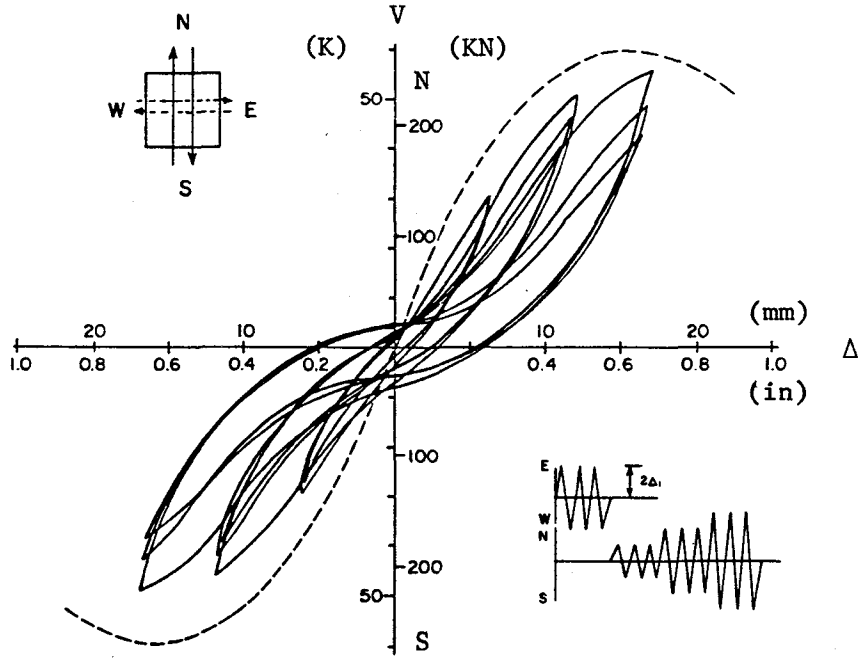

Fig. 4.3 Lateral load-deflection relationship--
00-V-2VP-I (N-S)

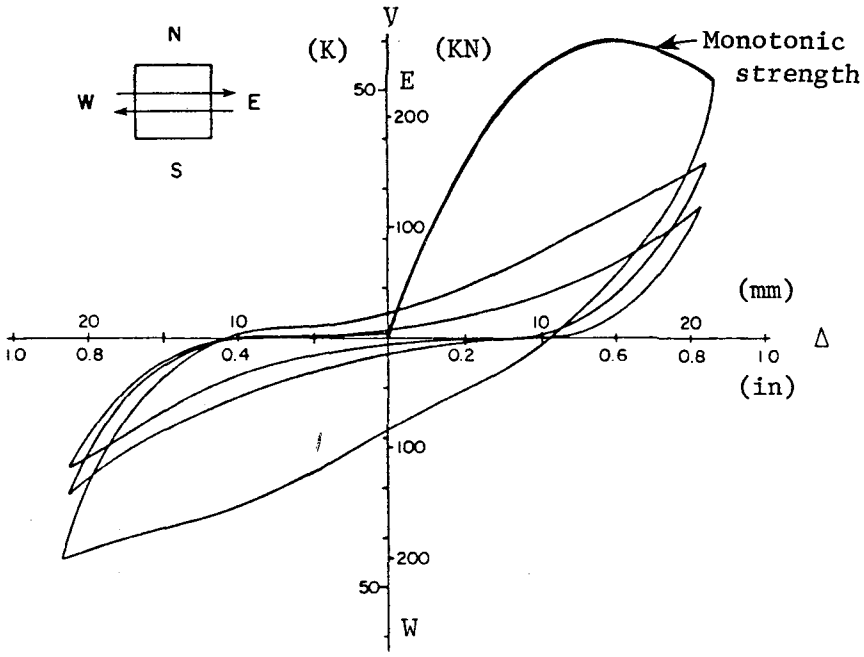

Fig. 4.4 Lateral load-deflection relationship--
00-V-4VP-I (E-W) initial cycles

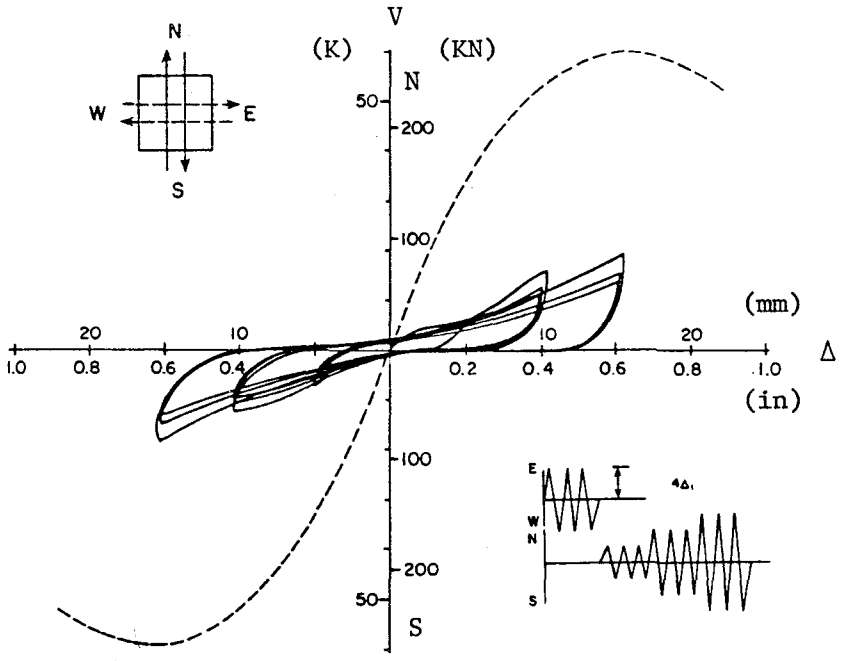

Fig. 4.5 Lateral load-deflection relationship --
00-V-4VP-I (N-S)

Note that the first cycle represents monotonic loading results.

00-V-V-A (Alternate Loading). Three load reversals were applied alternately in the principal direction at each deflection level. When the load-deflection curves in both directions are compared (Figs. 4.6 and 4.7), it can be seen that the two curves look almost identical except at the $4\Delta_i$ deflection level. In addition, at Δ_i and $2\Delta_i$ levels, the curves are quite similar to unilateral loading. The influence of the orthogonal previous loading is negligibly small at these levels. In other words, as long as the deflection level does not exceed $2\Delta_i$, the column holds it potential shear strength in each principal direction. The difference becomes clear at $3\Delta_i$ and above. Under the monotonic loading, the maximum load is obtained at about the $3\Delta_i$ deflection as in unilateral loading. However, in the alternate loading case, the first cycle peak load at the $3\Delta_i$ level is less than that at the $2\Delta_i$ level, although the difference is very small. The shear strength in the E-W direction decreases significantly at the $4\Delta_i$ level and is no longer similar to that in the N-S direction.

00-V-2C-I, 00-V-4C-I (Constant Deflection). These two loading patterns give an indication of the influence of constant deflection in one direction with cyclic loading in the orthogonal direction. Two constant deflection levels, $2\Delta_i$ and $4\Delta_i$, are considered.

At first the load was imposed in the E direction with a $2\Delta_i$ (or $4\Delta_i$) deflection. Then, with this deflection held constant, the load reversals were applied in the N-S direction. During load reversals in the N-S direction, the restoring force (the applied force needed to maintain a given deflection level) in the E direction was decreasing.

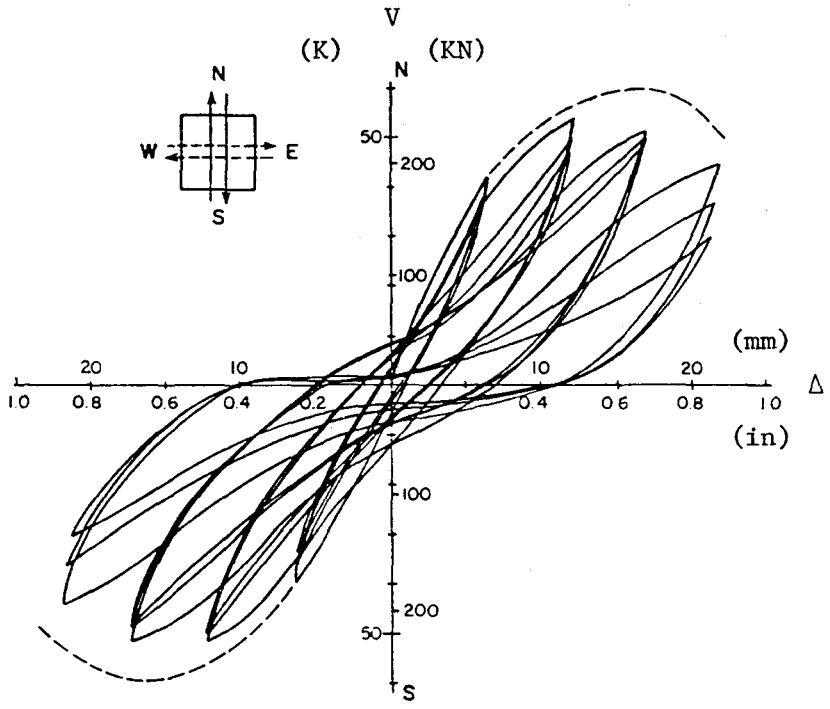

Fig. 4.6 Lateral load-deflection relationship--
00-V-V-A (N-S applied first)

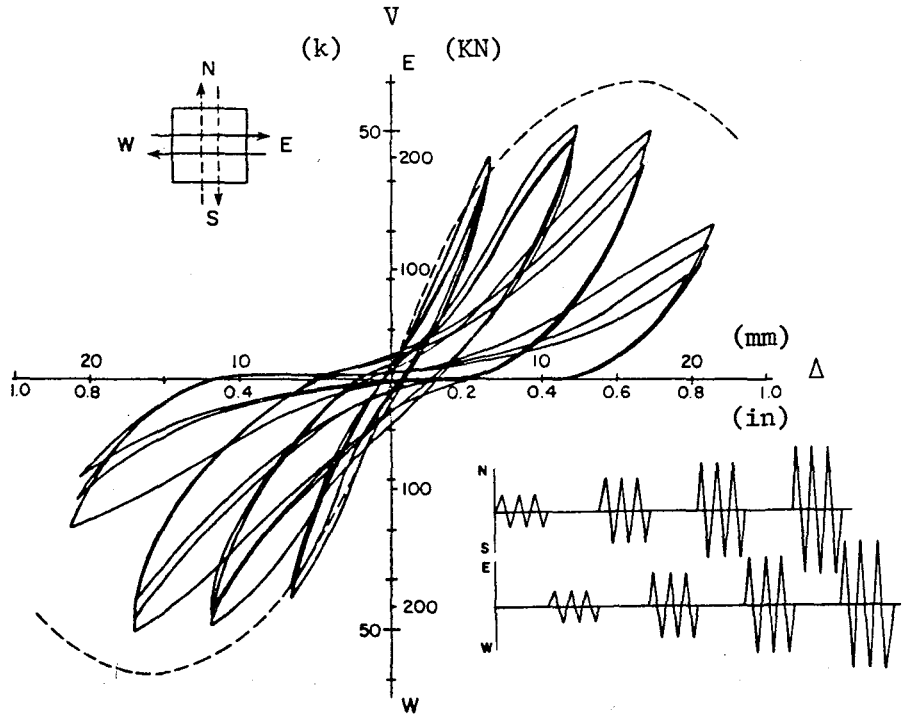

Fig. 4.7 Lateral load-deflection relationship--
00-V-V-A (E-W)

The decrease of load in the direction of the constant deflection is shown in Figs. 4.10 and 4.12, as well as the load deflection curves in Figs. 4.8 and 4.9. In order to see the influence of the constant deflection, the restoring force is shown in Figs. 4.11 and 4.13. The forces in each principal direction are plotted against one another.

In the case of $2\Delta_i$ constant deflection, the influence of the constant deflection is not significant at the Δ_i level in the N-S direction. The influence becomes serious at the $2\Delta_i$ level and above. The peak shear strength in the N-S direction is reduced significantly from the monotonic strength at the $3\Delta_i$ and $4\Delta_i$ level (see Fig. 4.8).

On the other hand, with a $4\Delta_i$ constant deflection in the E direction, a much more sever effect on the shear strength is observed. Even at the Δ_i level in the N-S direction, the peak shear strength in the N-S direction is reduced about 20 percent from the monotonic strength (Fig. 4.9).

As far as the reduction of the restoring force in the E direction is concerned, there is no major difference between the two cases (Figs. 4.11 and 4.13). The restoring force undergoes a large reduction with cycles at the Δ_i level.

<u>OO-V-V-S (Skewed Loading)</u>. The load path in this case is along the diagonal. The same magnitude and sign of force is given in the N-S and the E-W direction. The loading direction is NE-SW. The load-deflection curves are represented in Figs. 4.14 and 4.15 in terms of principal directional forces and deflections.

At the Δ_i level, as seen in the other cases, the shear strength reduction is almost negligible. However, after reaching the $2\Delta_i$ level, the strength deterioration becomes much more

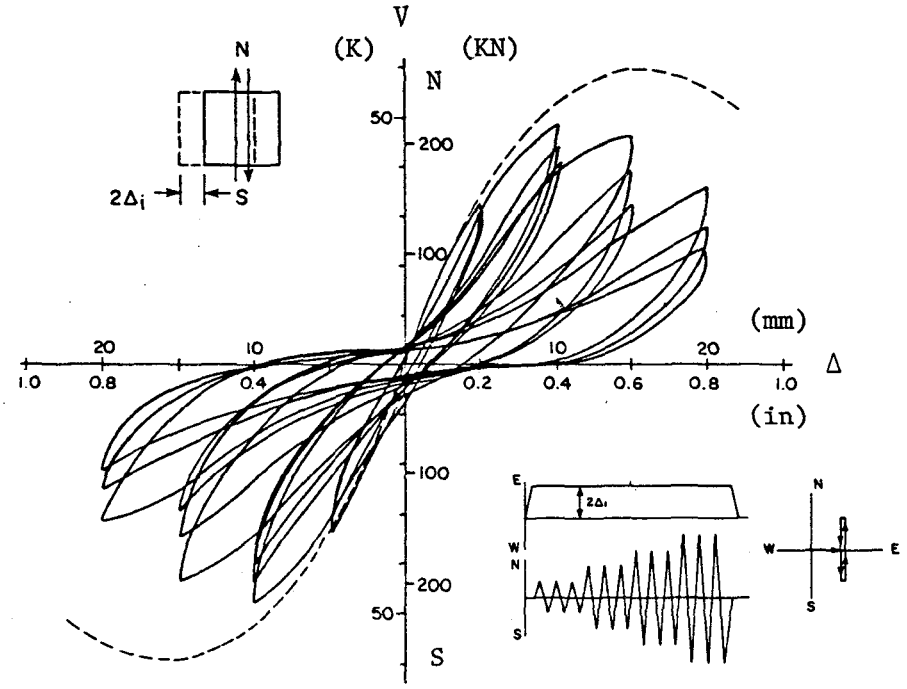

Fig. 4.8 Lateral load-deflection relationship--
00-V-2C-I (N-S)

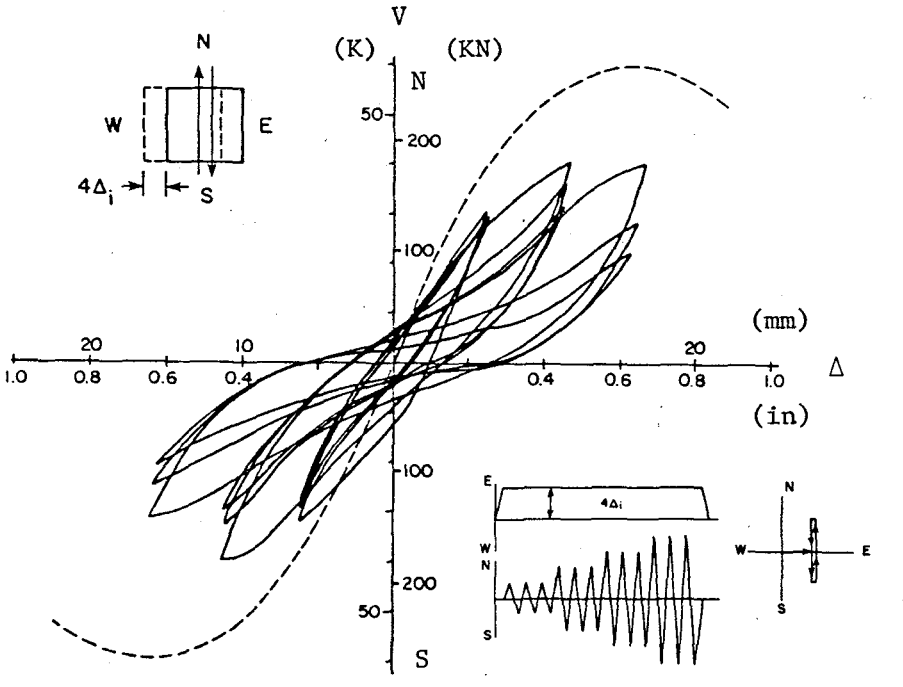

Fig. 4.9 Lateral load-deflection relationship--
00-V-4C-I (N-S)

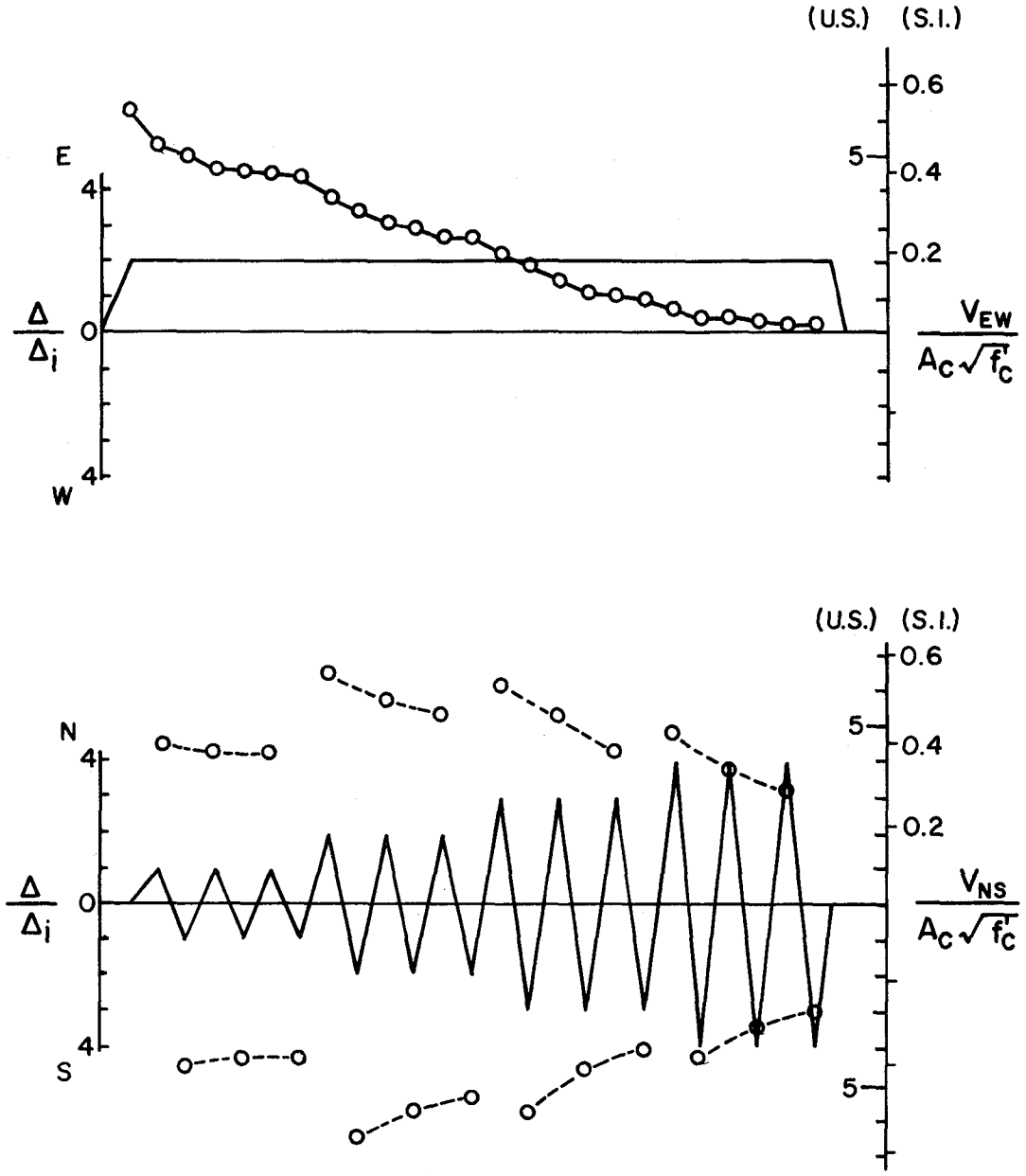

Fig. 4.10 Loading history and shear capacity--00-V-2C-I

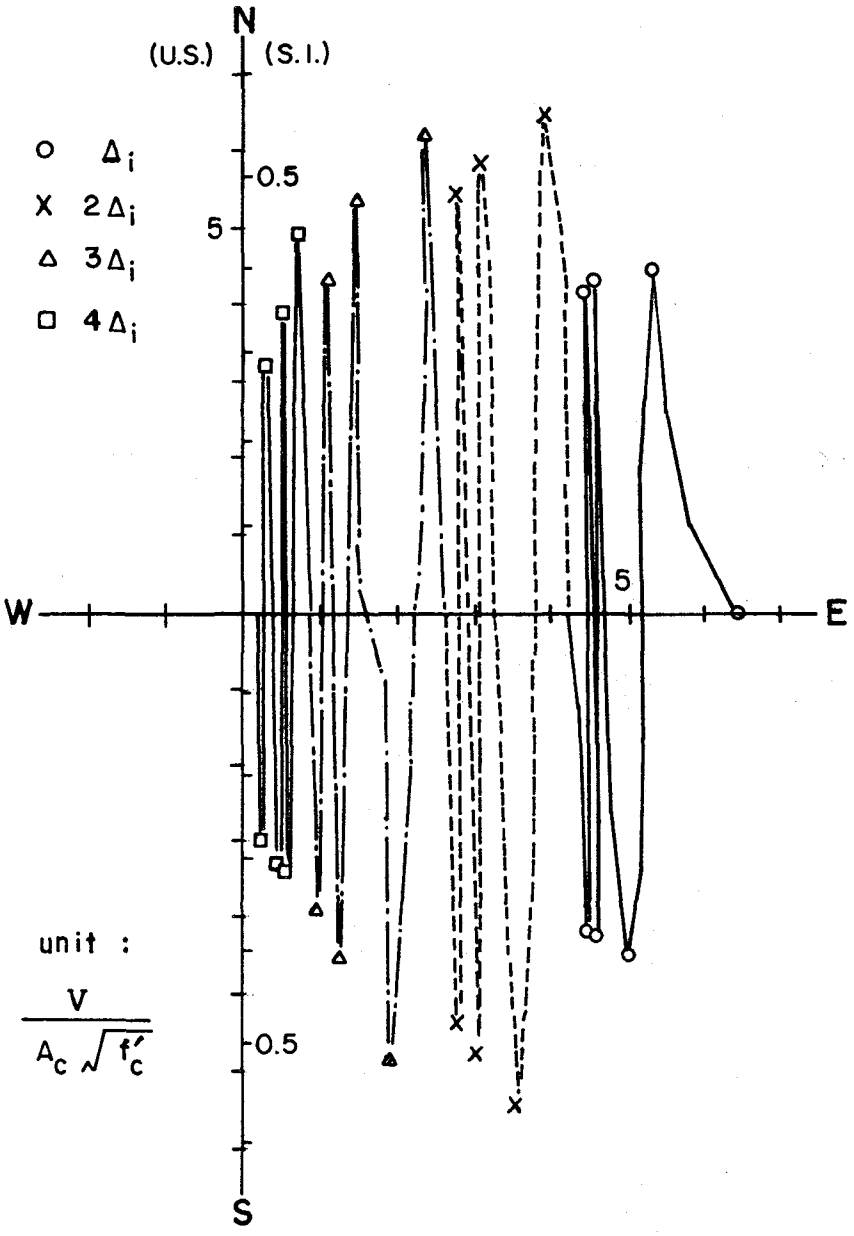

Fig. 4.11 Restoring force diagram--OO-V-2C-I

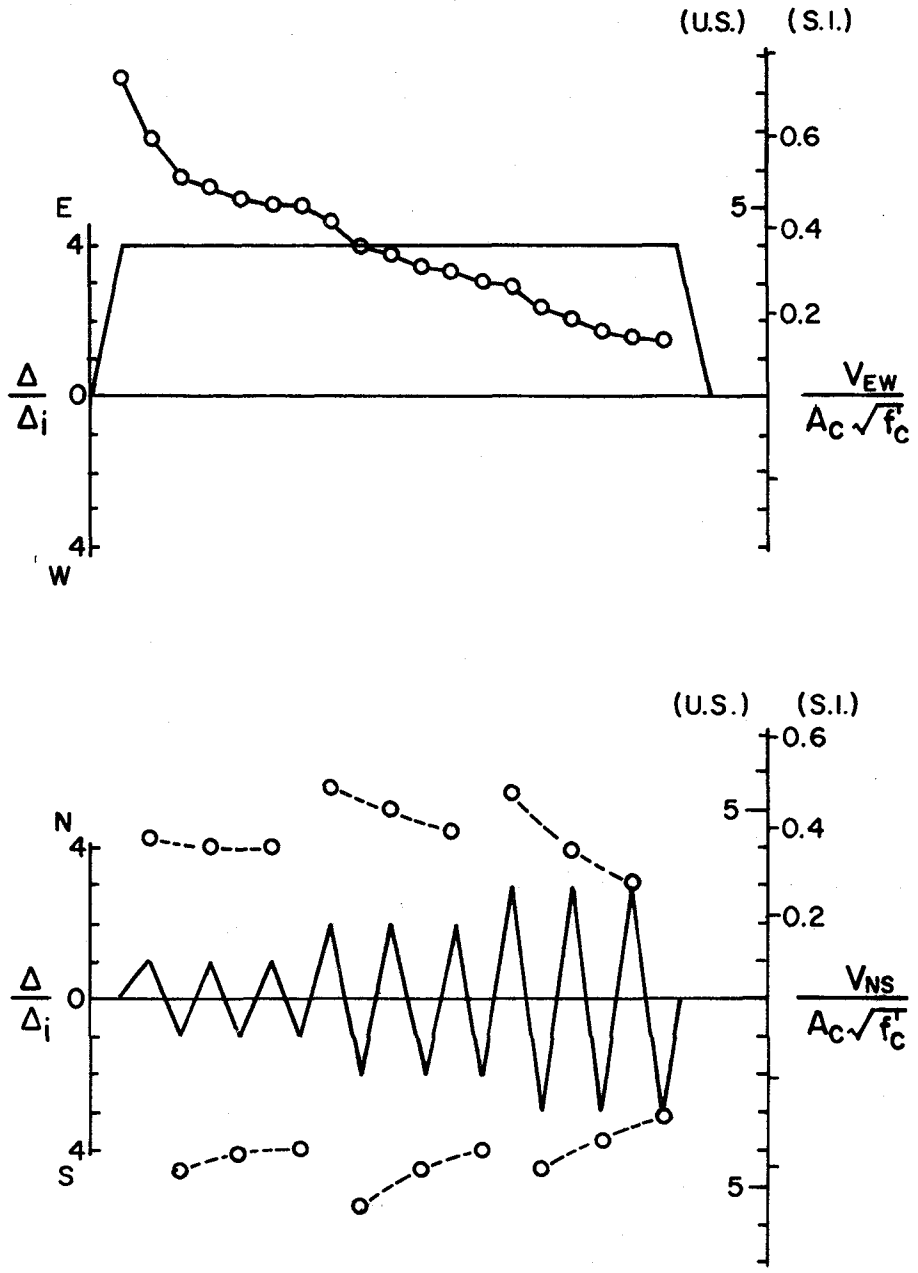

Fig. 4.12 Loading history and shear capacity--00-V-4C-I

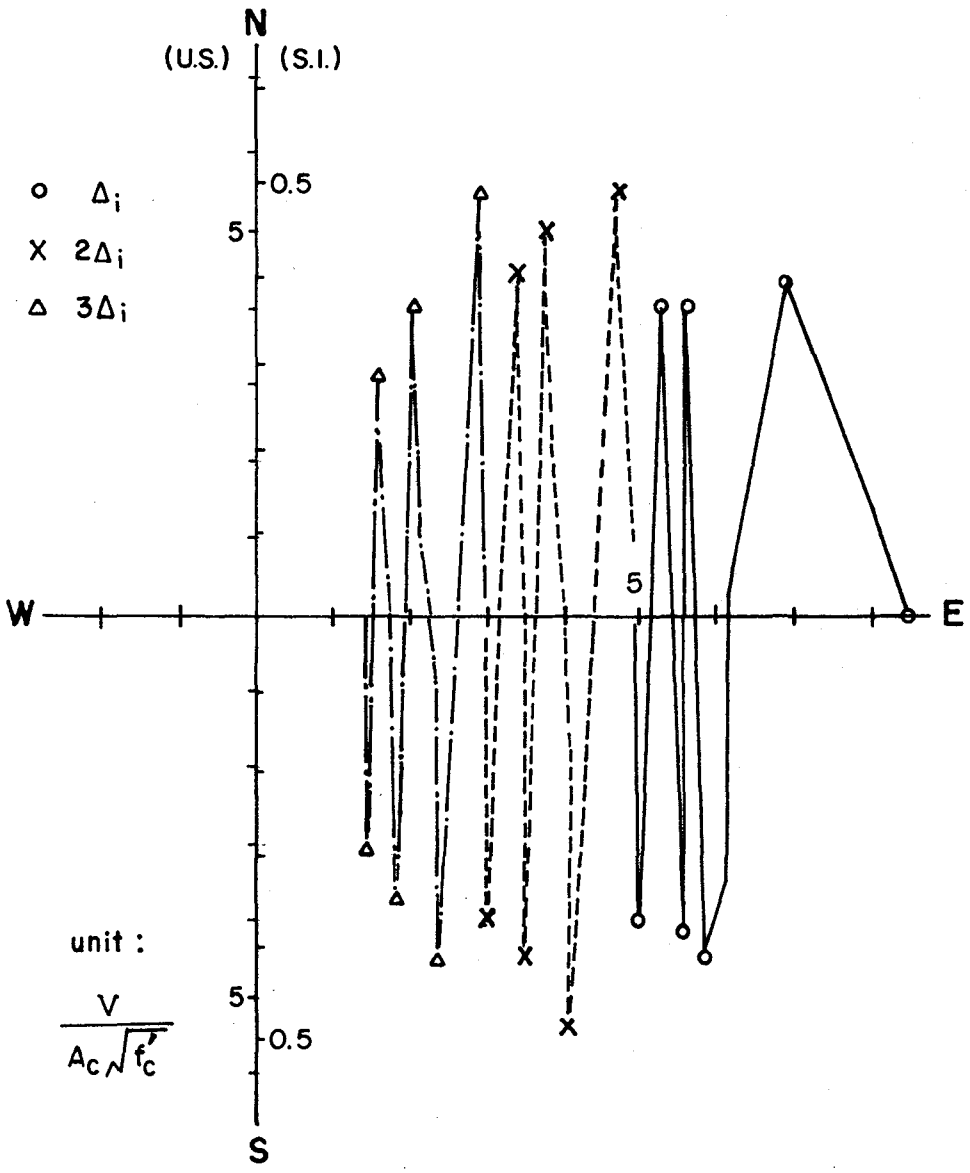

Fig. 4.13 Restoring force diagram--00-V-4C-I

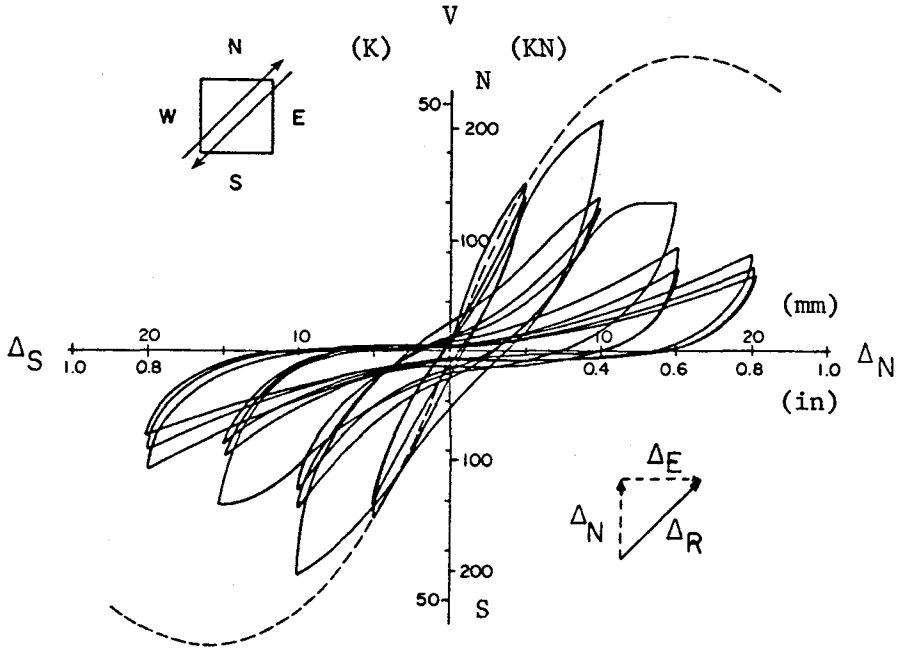

Fig. 4.14 Lateral load-deflection relationship--
00-V-V-S (N-S)

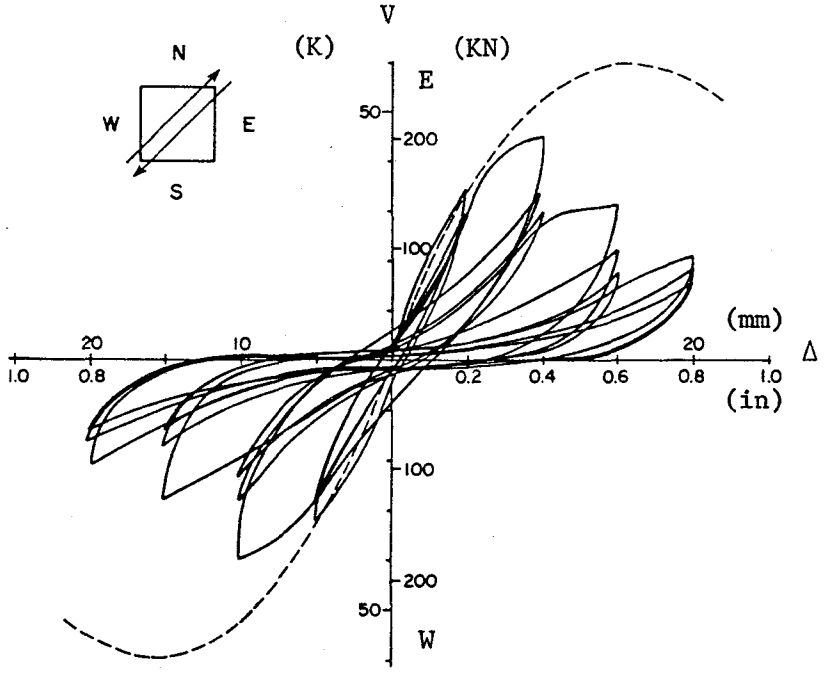

Fig. 4.15 Lateral load-deflection relationship --
00-V-V-S (E-W)

serious than for unilateral loading because the load applied in the other principal direction begins to affect the shear strength.

00-V-V-SA (Alternate Skewed Loading). In this case, the load path is along both diagonal directions, alternately. In the first three cycles of loading the magnitude and the sign of load in the N-S and in the E-W direction are the same. In the next three cycles at the same deflection level only the sign of load in the N-S direction is reversed.

The load-deflection relationships are represented in terms of principal directional forces and deflections. For NE-SW loading, curves are generated along both N-S and E-W axes, likewise, for NW-SE loading. Therefore, four figures are shown for load-deflection curves (Figs. 4.16 to 4.19).

As in other cases, the shear strength at Δ_i is quite stable and its value is almost the same as that under monotonic loading. After the $2\Delta_i$ level, the peak shear strength decreases in the same manner as the case of 00-V-V-S. The relationship between the case of 00-V-V-S and 00-V-V-SA seems to be quite similar to the relationship between the case of unilateral loading (00-V-0-I) and the case of alternate loading (00-V-V-A).

00-C-C-AF (Square Load Path). In this case, the load path is square and occupies all four quadrants. The load-deflection curves and the restoring force diagram are shown in Figs. 4.20 to 4.22.

At Δ_i, the shear strength is quite stable, as shown by the restoring force diagram (Fig. 4.22). However, severe shear strength deterioration is seen at the $2\Delta_i$ level. After three cycles of load at $2\Delta_i$, the shear capacity of the column is almost gone. The restoring diagram shows the shear strength reduction

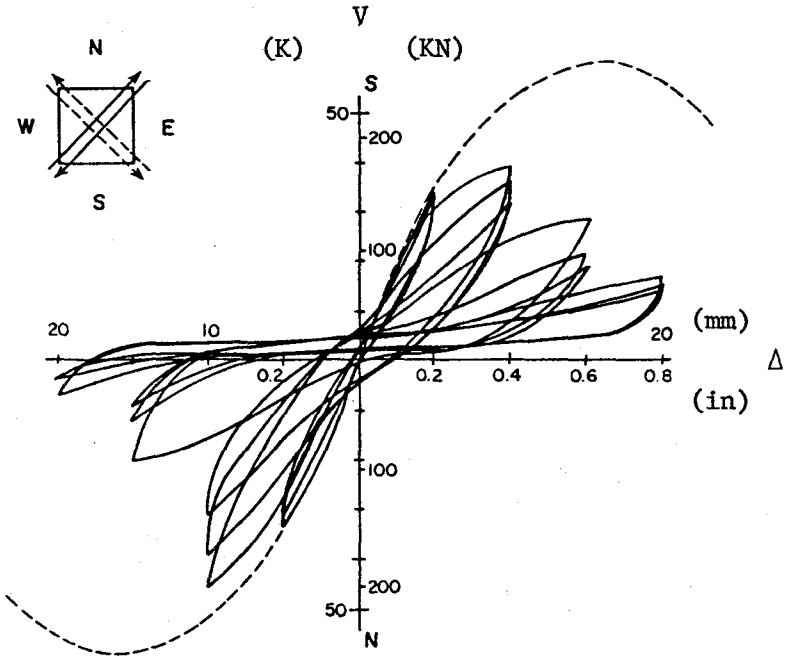

Fig. 4.16 Lateral load-deflection relationship--
00-V-V-SA (N-S)

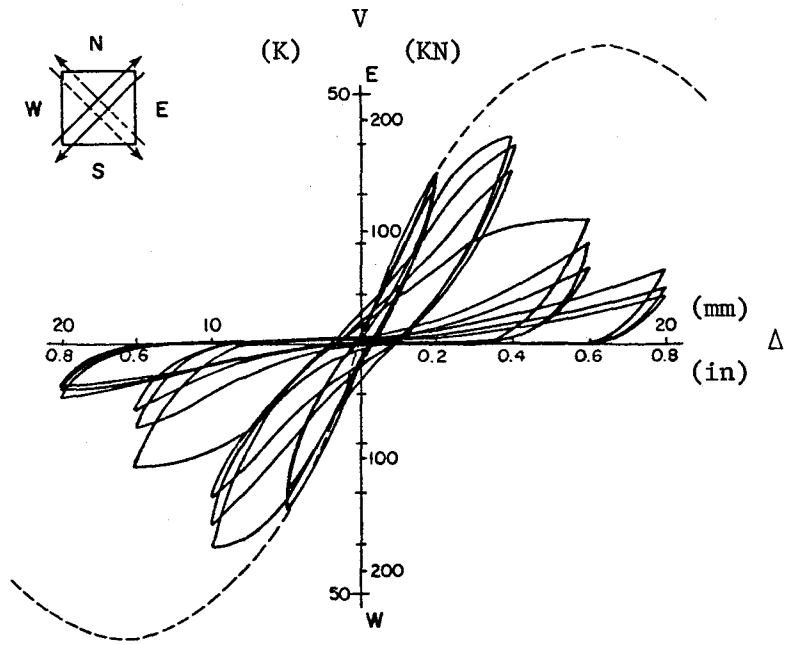

Fig. 4.17 Lateral load-deflection relationship--
00-V-V-SA (E-W)

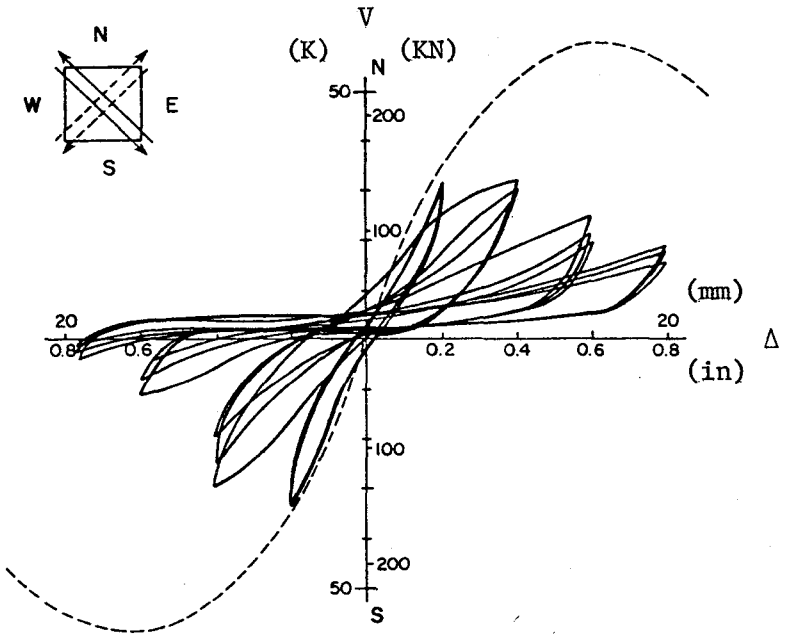

Fig. 4.18 Lateral load-deflection relationship--
00-V-V-SA (N-S)

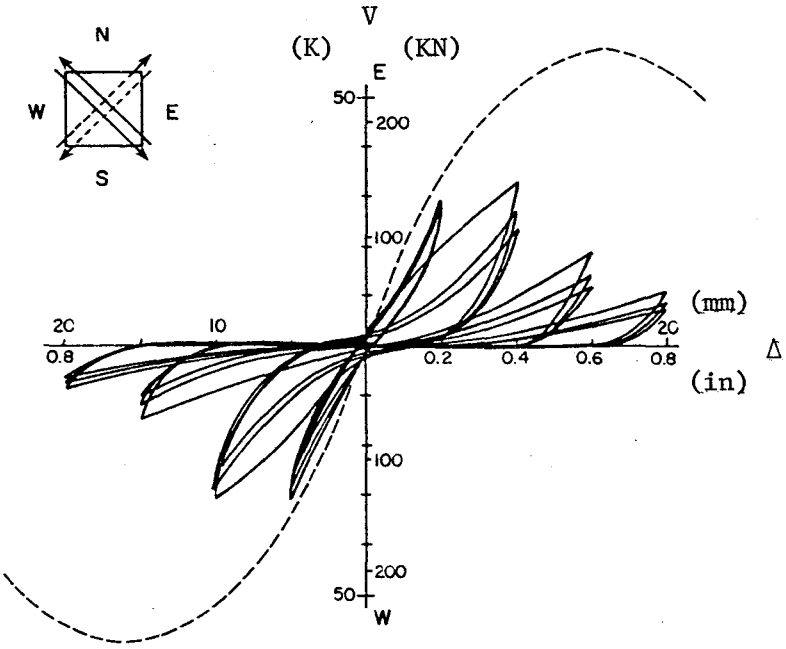

Fig. 4.19 Lateral load-deflection relationship --
00-V-V-SA (E-W)

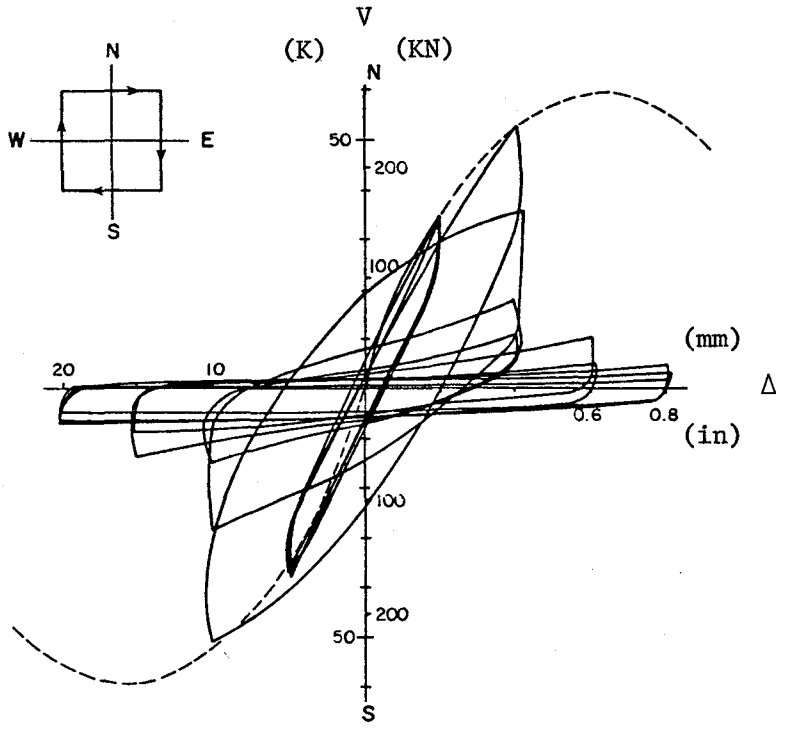

Fig. 4.20 Lateral load-deflection relationship--
00-C-C-AF (N-S)

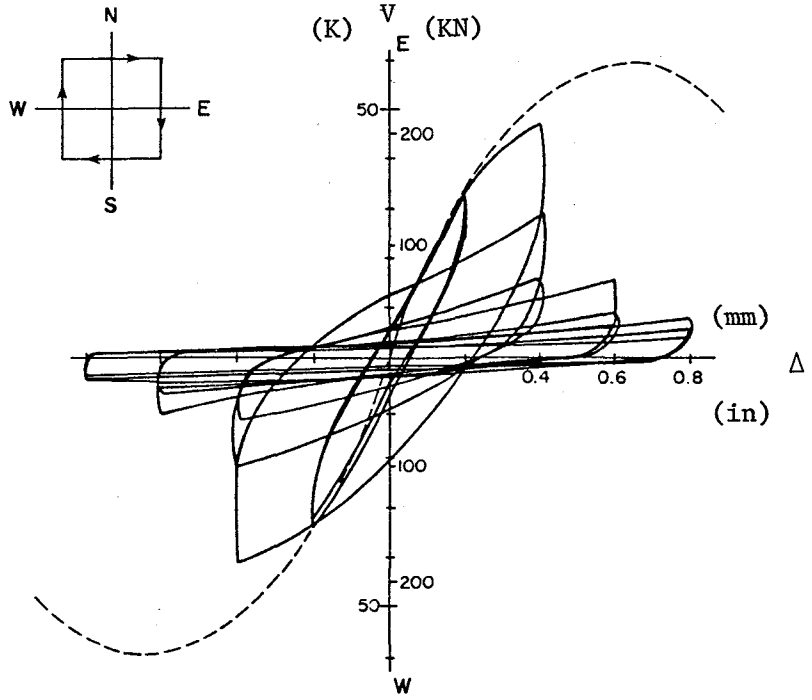

Fig. 4.21 Lateral load-deflection relationship --
00-C-C-AF (E-W)

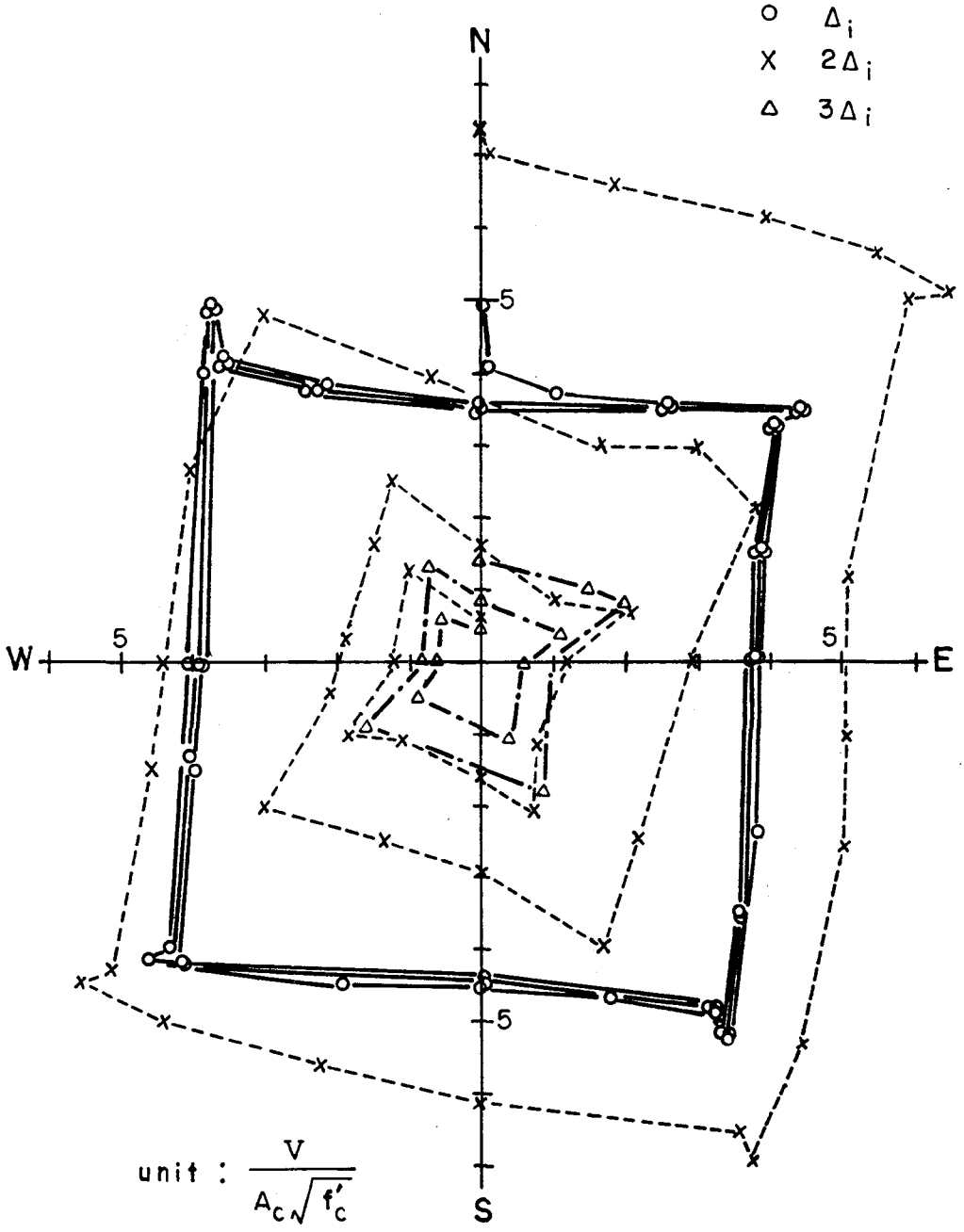

Fig. 4.22 Restoring force diagram--OO-C-C-AF

very clearly. For Fig. 4.22 the deflection path is always square at each deflection level. At the Δ_i level, the force path is very stable and almost square, corresponding to the deflection path. At the $2\Delta_i$ level, the deflection was applied first in the north direction. A larger force was required to move up to $2\Delta_i$ from Δ_i; however, as deflection was imposed along the $2\Delta_i$ square path, the force required to keep the deflection at $2\Delta_i$ was decreasing substantially. At the $3\Delta_i$ level, only a very small force was required to reach the $3\Delta_i$ deflection level.

In the square load path, the stiffness characteristics are different from other cases which show a pinched curve (so-called inverted S shape), but there is no pinching in this case. It seems that crushing of concrete or damage progresses with every loading cycle.

00-C-C-AH (Half Square Load Path). The load path is square only in the first and third quadrants. The load-deflection curves and the restoring force diagram are shown in Figs. 4.23 to 4.25.

The shear strength reduction can be seen even at the Δ_i level. Although the first cycle peak load at $2\Delta_i$ is not reduced very much from the monotonic strength, with additional cycles the reduction becomes significant.

When compared with the case of square load path (00-C-C-AF), the shear strength deterioration is less severe at the $3\Delta_i$ and $4\Delta_i$ level. The results in this case are similar to those in 00-V-V-S.

4.3 Strain Distribution in Transverse Reinforcement along Column Height

As shown in Fig. 2.1, strain gages were attached to the transverse reinforcement on all four legs at intervals along the

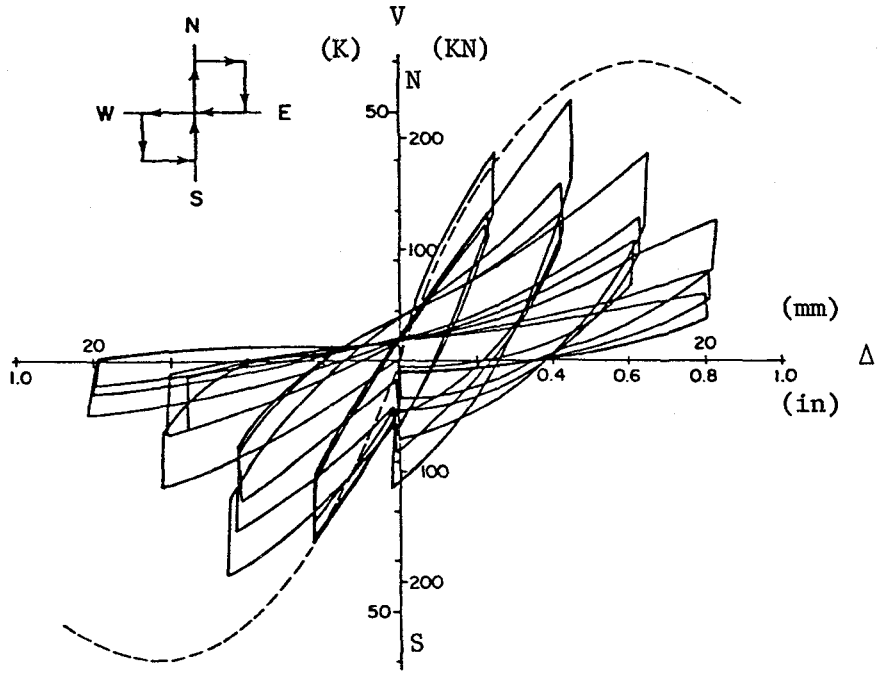

Fig. 4.23 Lateral load-deflection relationship--
OO-C-C-AF (N-S)

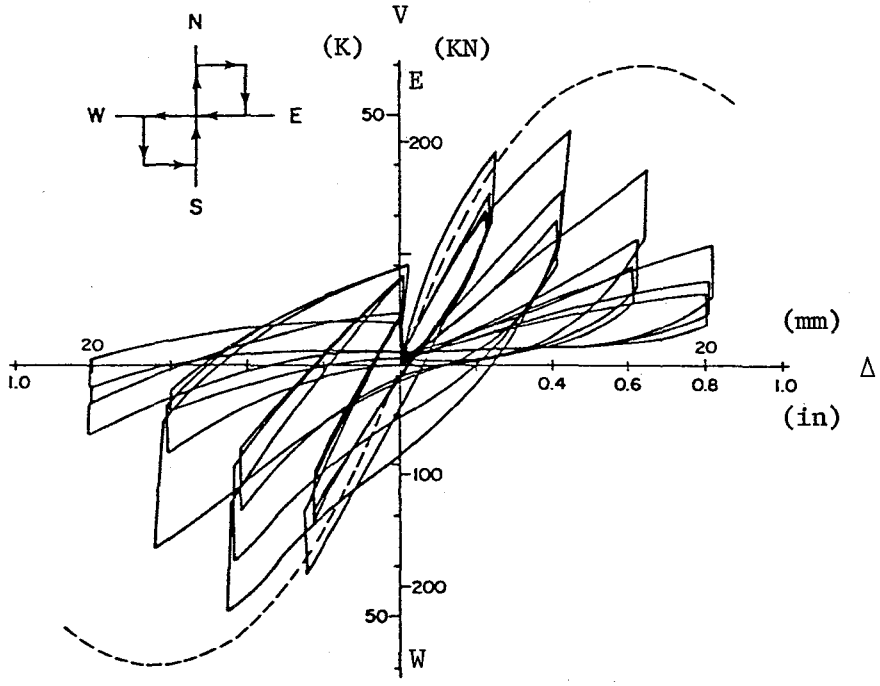

Fig. 4.24 Lateral load-deflection relationship--
OO-C-C-AF (E-W)

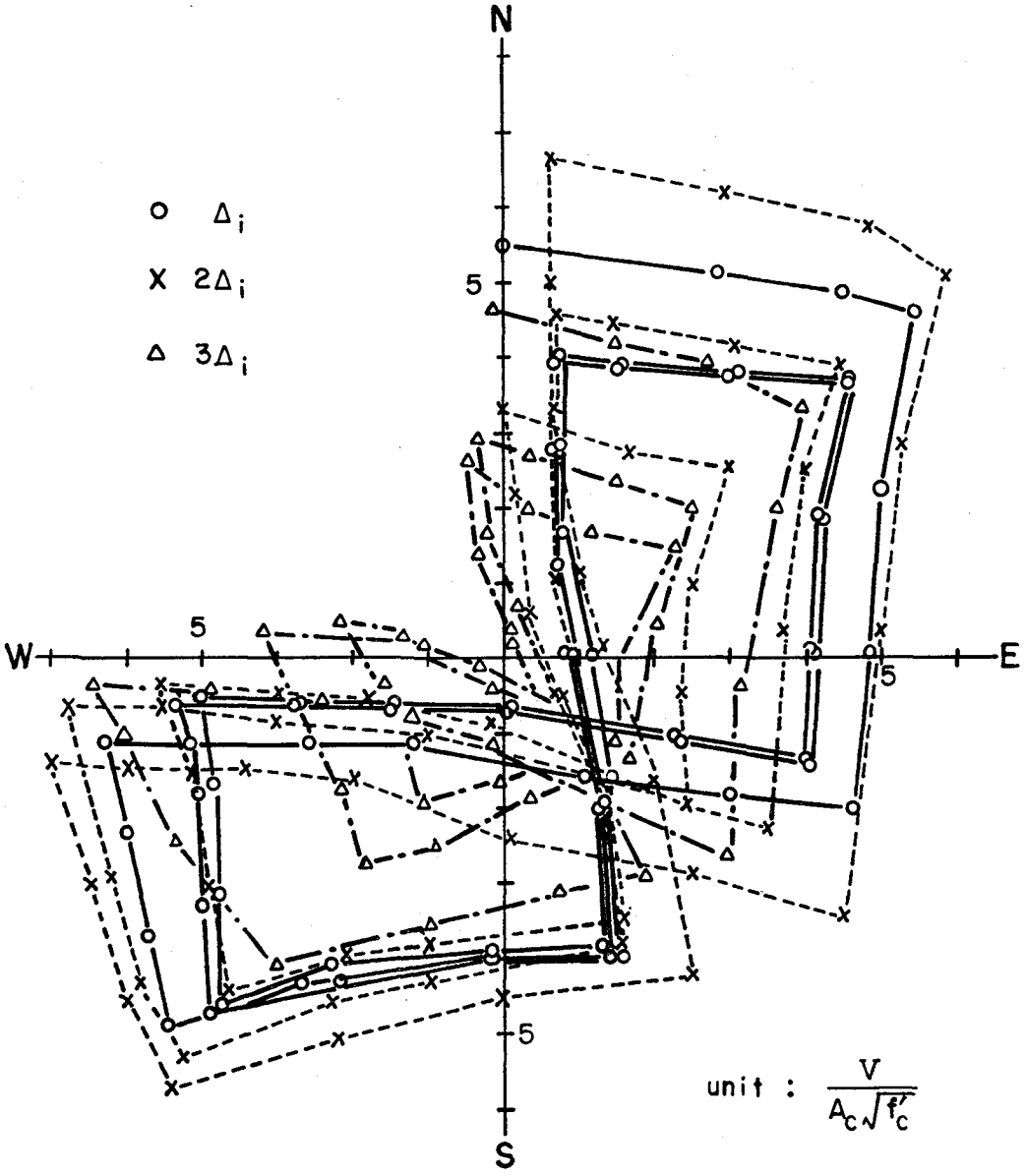

Fig. 4.25 Restoring force diagram -- OO-C-C-AH

column height. From the measured data, strain in the transverse reinforcement at selected stages was obtained and strain distributions along the column height were plotted.

The strain at each level was taken as the average strain in the two opposite legs of the tie. In the case of unilateral loading (OO-V-O-I), the strain distribution is obtained from the E-W legs because the loading was imposed in the N-S direction. Figure 4.26 shows the notation used. When the load is in the N-S direction, the E-W legs carry a portion of the shear force but the N-S legs do not. Figures 4.27 to 4.32 are plots of strains in the transverse reinforcement along the height of the column.

In the case of loading in the diagonal direction, the strain distribution in the N-S legs is quite similar to that in that E-W legs. Therefore, only the distribution for the N-S legs is plotted. The strain distribution in the other four cases is also from the N-S legs which provide resistance in the second loading direction (E-W loading).

In the two specimens with large initial deformation, OO-V-4VP-I (previous cycles to the $4\Delta_i$ level were imposed) and OO-V-4C-I (constant $4\Delta_i$ deformation in one direction), very few of the gages were operating after the first $4\Delta_i$ level loading. Two other cases (OO-V-V-A and OO-C-C-AH) are also not shown because te distribution in OO-V-V-SA is quite similar to that of OO-V-V-S as is OO-C-C-AH to that of OO-C-C-AF.

At the Δ_i level (Figs. 4.27 and 4.28), it is difficult to see differences in the six cases. This may imply that previous loading up to $2\Delta_i$ does not influence the strain distribution pattern in an orthogonal direction at the Δ_i level. It may also imply that at this deflection level, the forces or

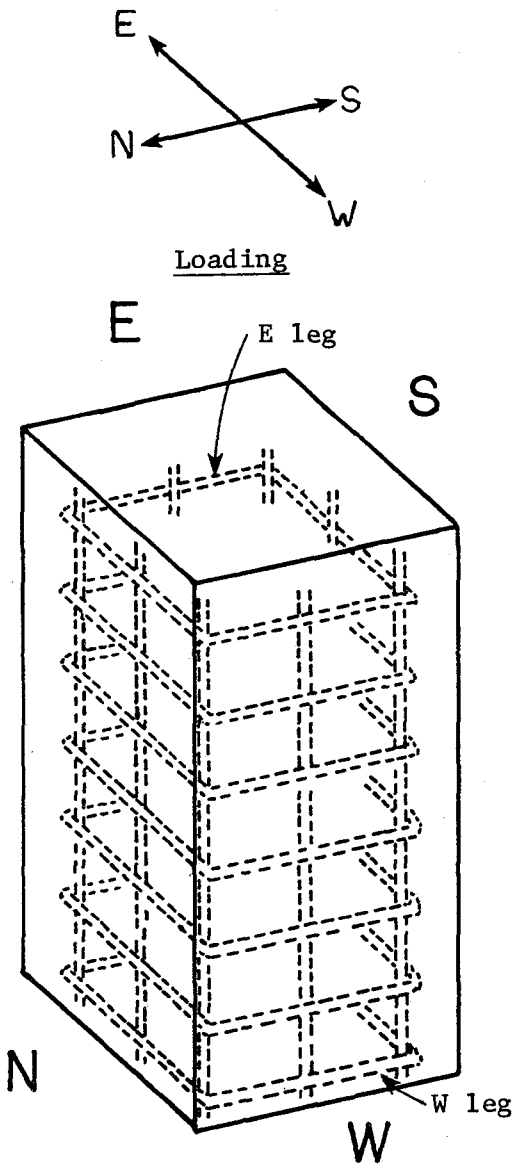

Fig. 4.26 Transverse reinforcing legs

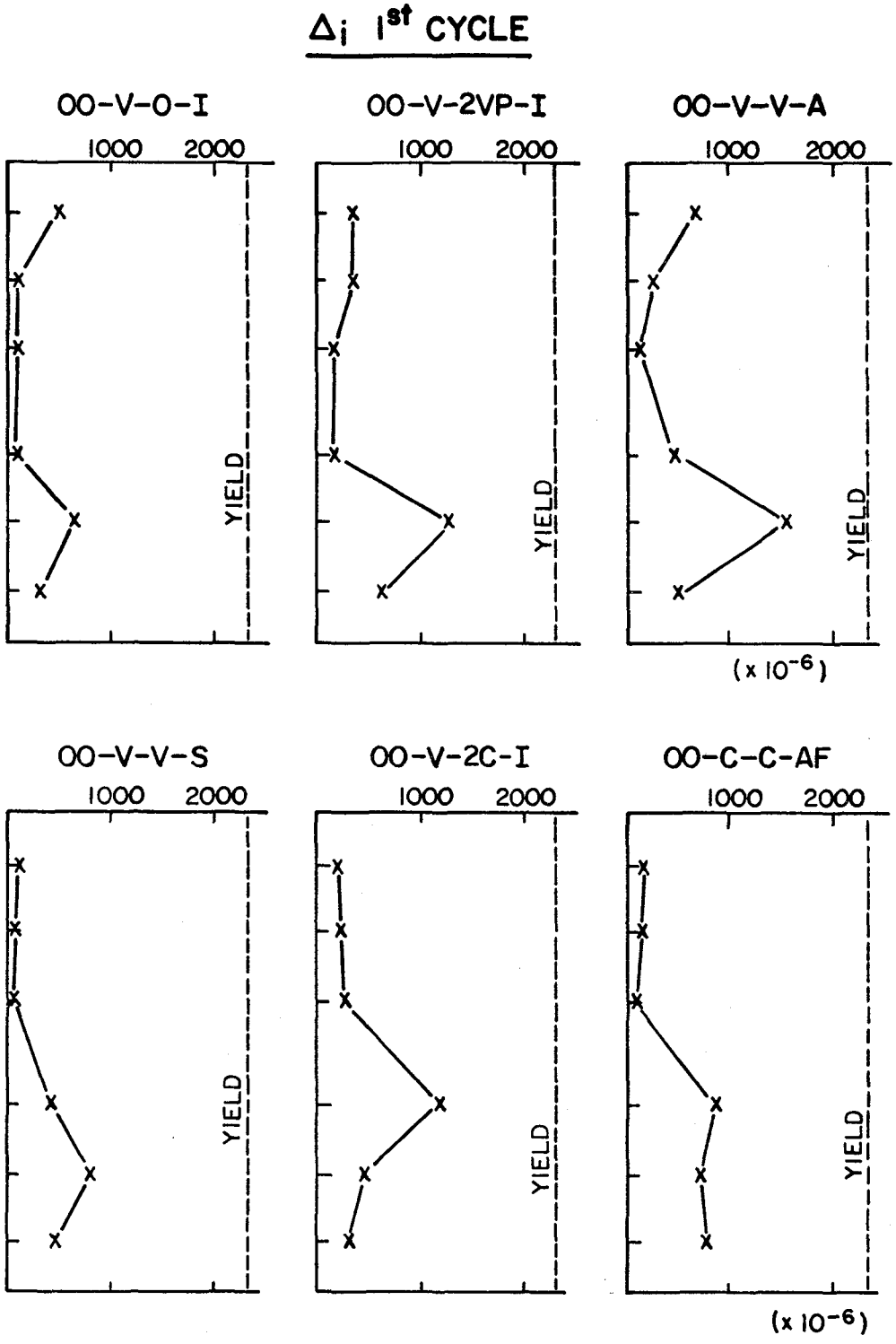

Fig. 4.27 Strain distribution in tie bars--Δ_i - 1st cycle

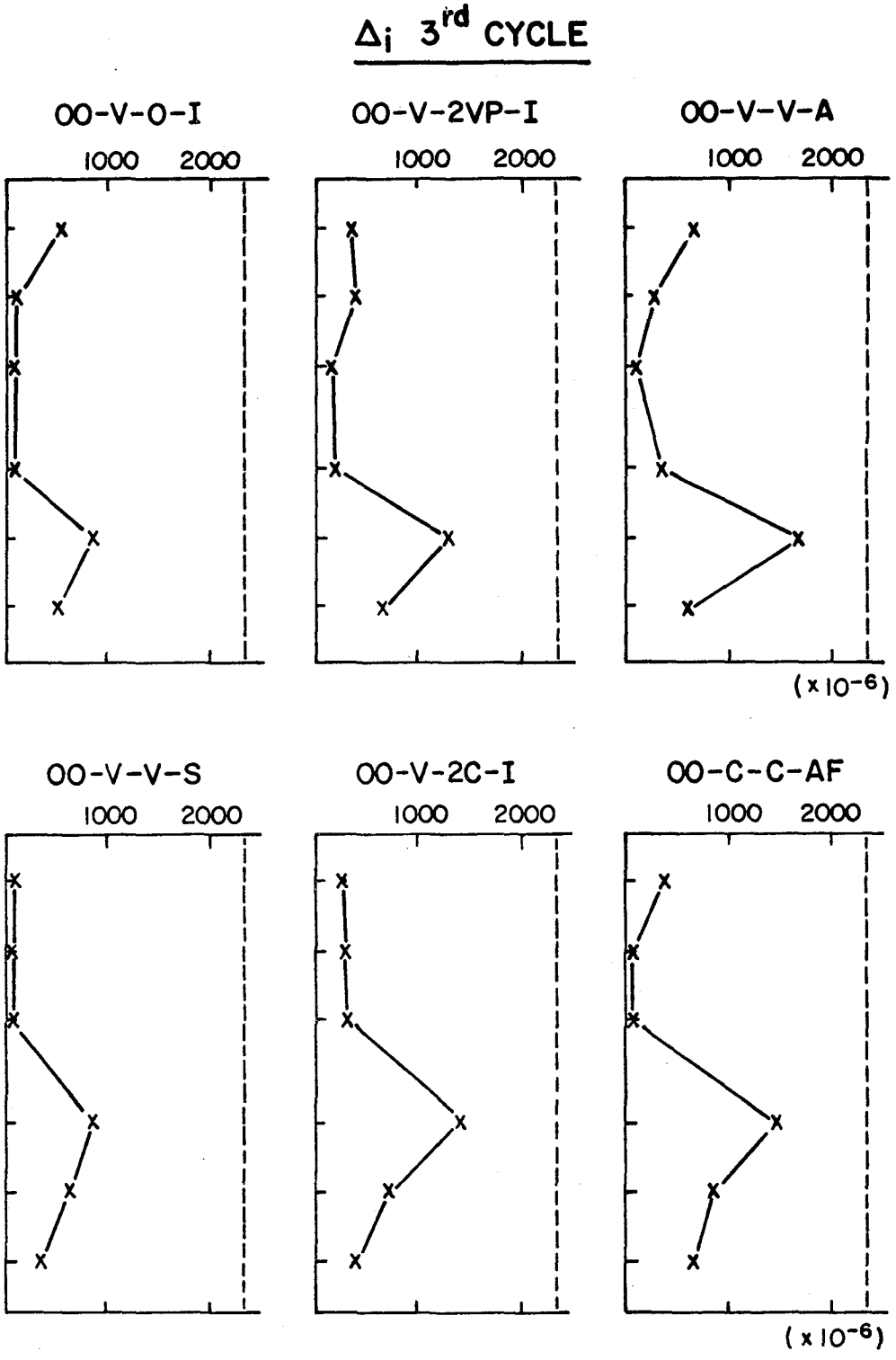

Fig. 4.28 Strain distribution in tie bars--Δ_i - 3rd cycle

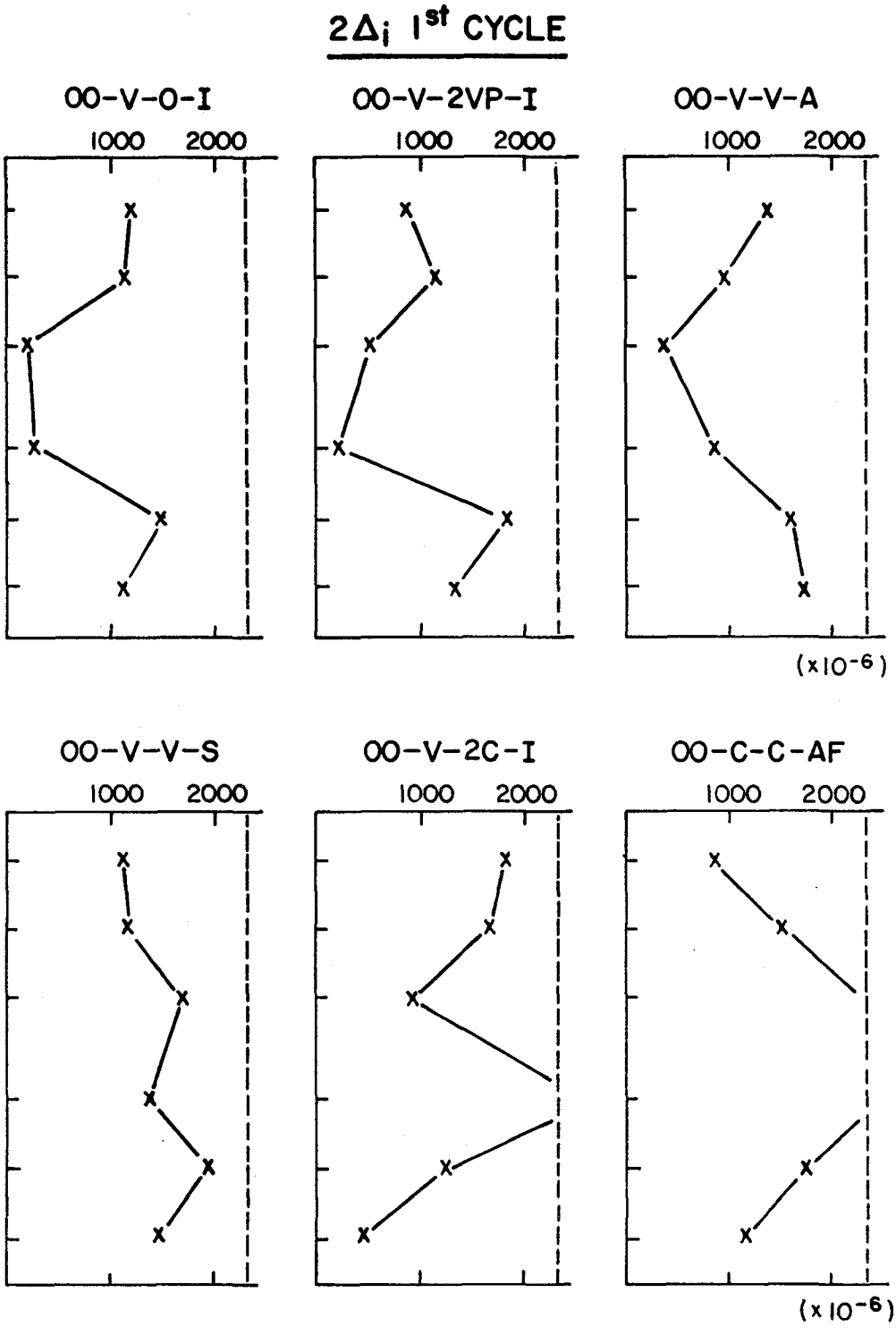

Fig. 4.29 Strain distribution in tie bars--$2\Delta_i$ - 1st cycle

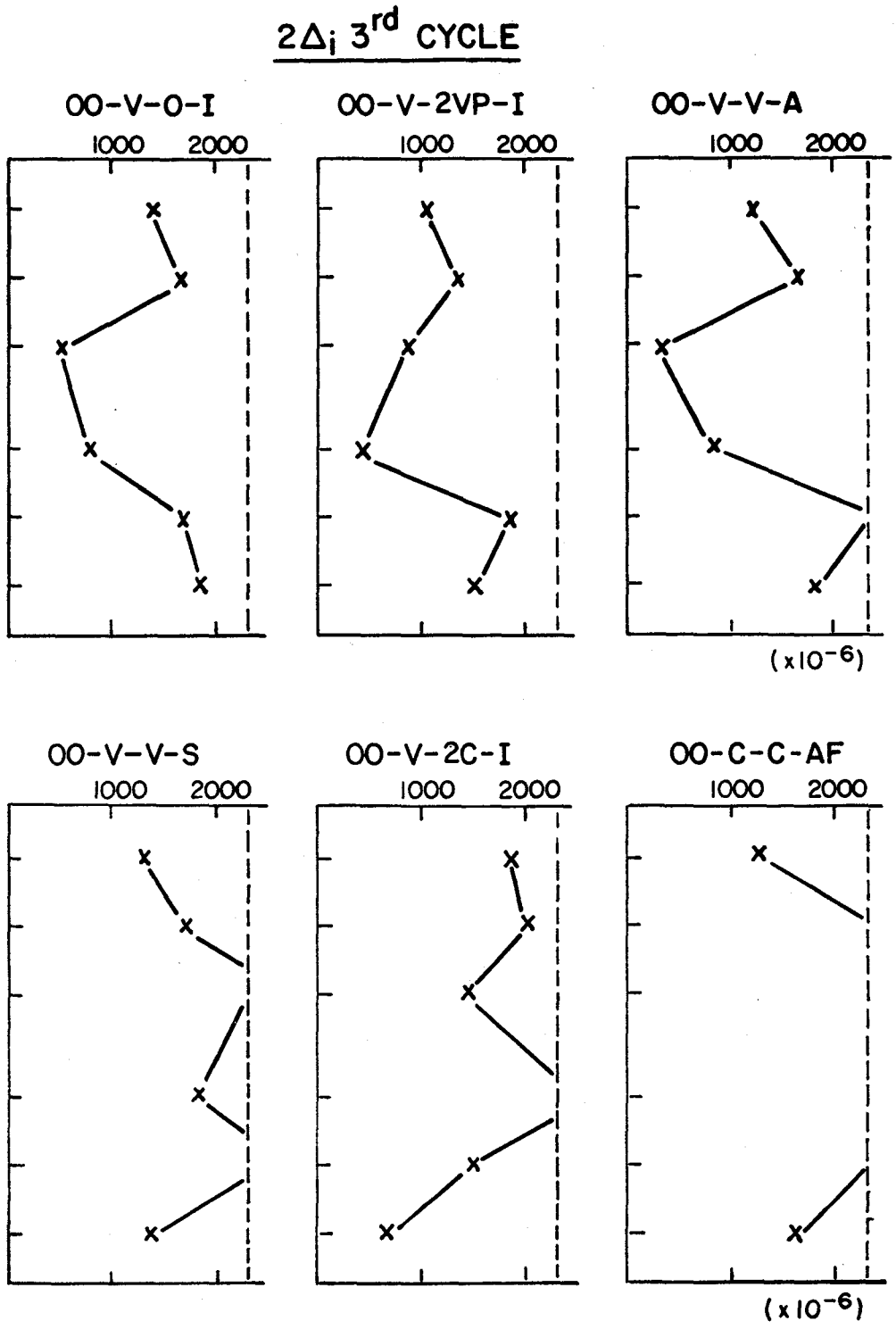

Fig. 4.30 Strain distribution in tie bars--$2\Delta_i$ - 3rd cycle

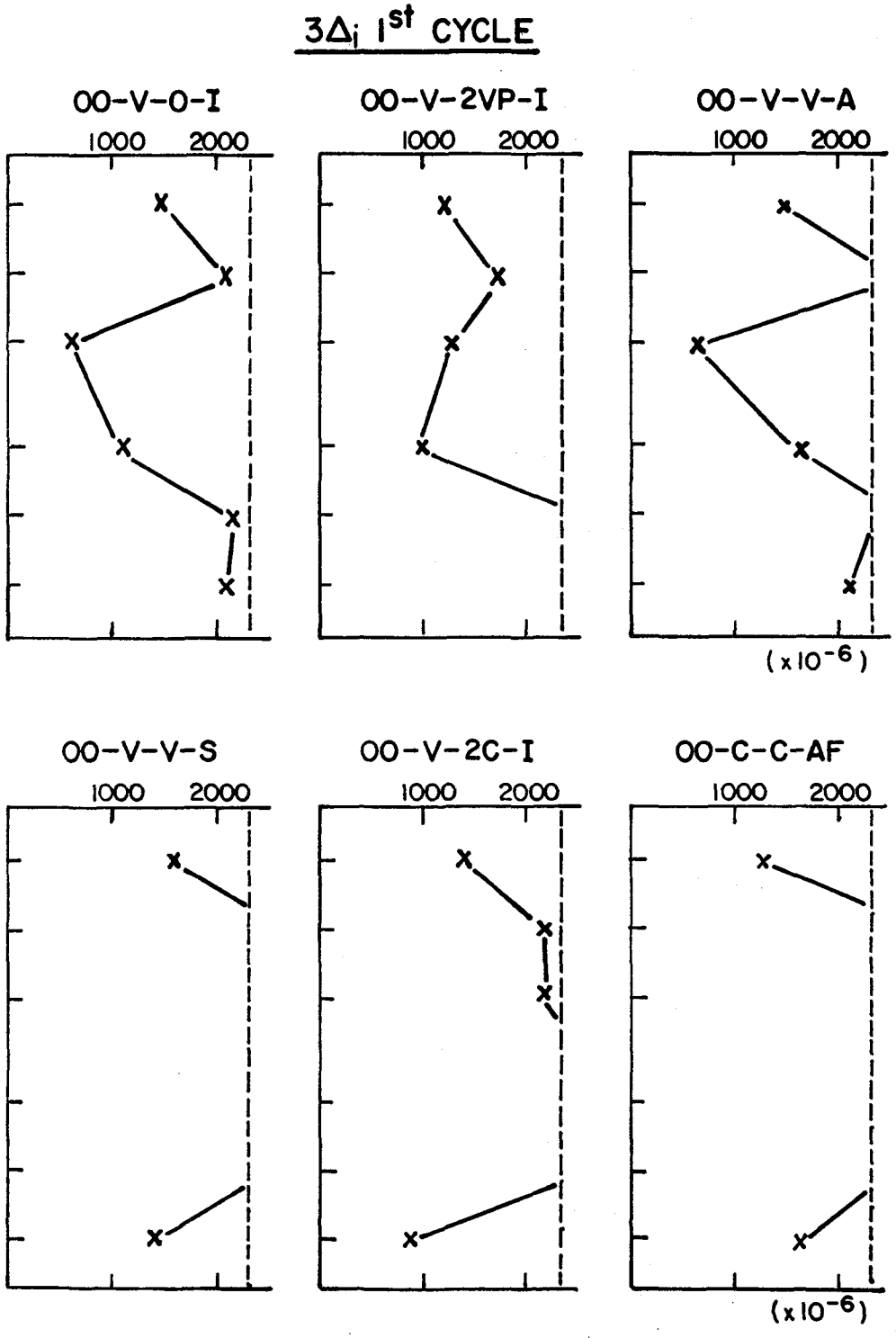

Fig. 4.31 Strain distribution in tie bars--$3\Delta_i$ - 1st cycle

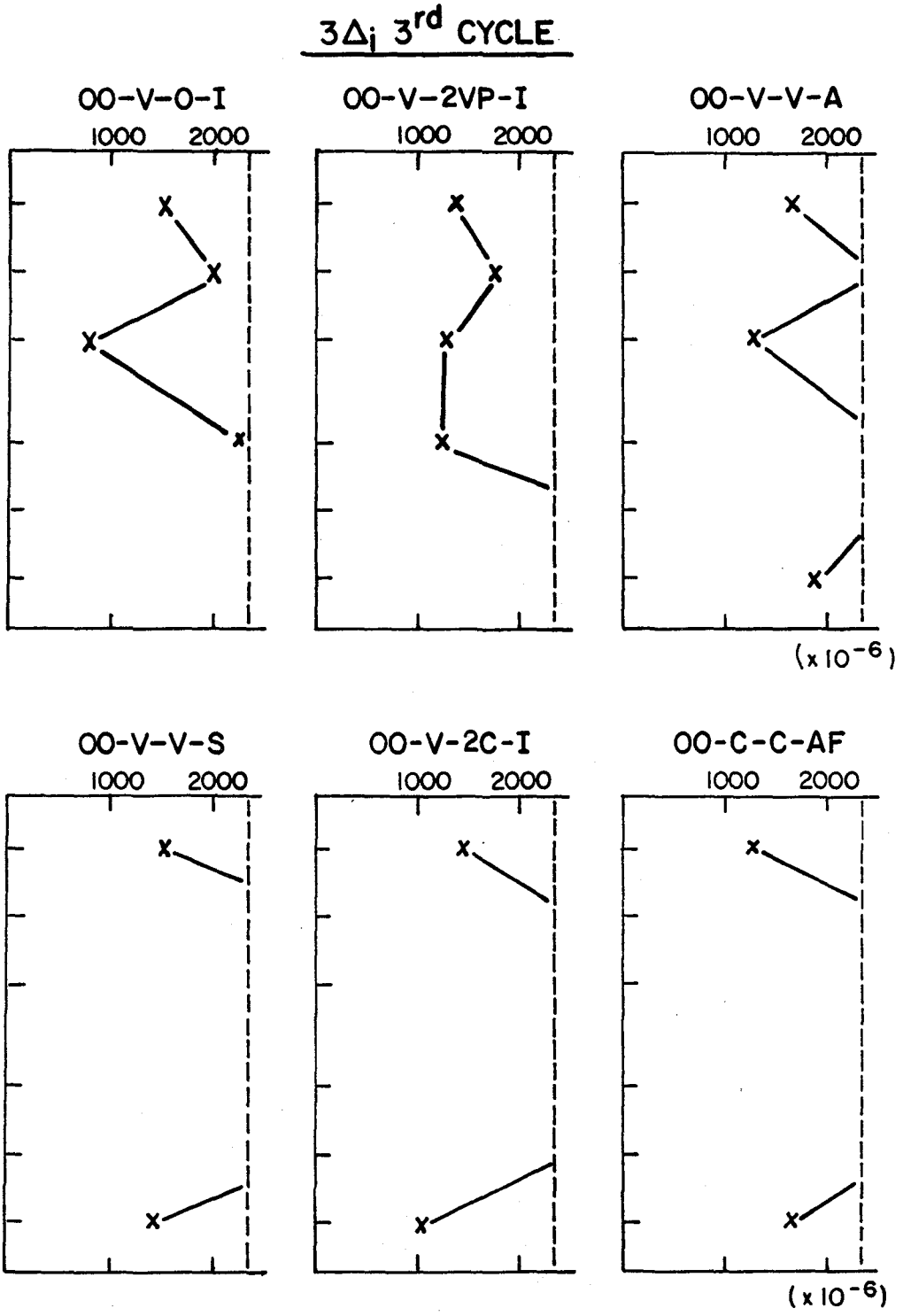

Fig. 4.32 Strain distribution in tie bars--$3\Delta_i$ - 3rd cycle

deformations in an orthogonal direction do not affect the strain distribution.

At the $2\Delta_i$ level (Figs. 4.29 and 4.30), three cases--00-V-0-I, 00-V-2VP-I, and 00-V-V-A--show similar results. The influence of previous loading still is not apparent at this level. The difference between the first and the third cycle is small; however, the maximum strain is near yield. On the other hand, the remaining three cases indicate higher strain, and the distribution patterns are different from the above three cases.

With deformation imposed simultaneously in orthogonal directions, the strain distribution is altered. The difference between the first and the third cycle becomes significant at the $2\Delta_i$ level. In the case of the square load path (00-C-C-AF), almost all ties yield in the third cycle.

At the $3\Delta_i$ level (Figs. 4.31 and 4.32), the strain is near yield in specimens 00-V-0-I, 00-V-2VP-I, and 00-V-V-A. In the three cases of simultaneous loading in both principal directions, nearly all strain gages are inoperative.

In every case the strain distribution in the transverse reinforcement along column height is not necessarily symmetrical about the middle height. The moment at the bottom of the column was a little larger than the moment at the top of the column due to the small rotation of the top column head. When cracks propagate across the position of a tie, the tie carries a larger shear force and the strain in the tie increases. Cracking was predominant at the bottom of the column at low deflection levels in every case. However, as a deflection level increased, cracks propagated across the entire region uniformly and almost all strains reached yield.

In order to see how the strain in the legs normal to the direction of loading changes during loading, the results from 00-V-2C-I are shown in Fig. 4.33. It may be helpful to refer to Fig. 4.26, which shows the relationship between the loading direction and the notation for the tie legs. When the load is applied in the N-S direction, the transverse reinforcement which contributes to the shear strength of the column is mainly the E-W legs.

A constant deflection to the east of $2\Delta_i$ was imposed in this case. As mentioned above, when the deflection level reaches $2\Delta_i$, the maximum strain reached yield for the first time. However, the strains in the E-W legs were influenced very little by the initial loading. The strain distribution in the E-W legs increases with loading to Δ_i in the N-S direction, but the maximum value does not exceed yield. This loading produces almost no change in the strain distribution in the N-S legs.

Strains in the N-S legs change rapidly after the $2\Delta_i$ level in the N-S direction is reached. At this stage, the N-S loading reduces the concrete capacity in the E-W direction as well as in the N-S direction. Therefore, the N-S legs must carry an increasing fraction of the shear. Furthermore, when the core concrete is damaged severely, ties work as confinement for loading in an orthogonal direction.

It should also be noted that the deflection at maximum shear strength under monotonic loading is about 0.6 in., and a deflection of $2\Delta_i$ to the east and $2\Delta_i$ to the north produces a resultant deflection of 0.6 in. in the northeast quadrant.

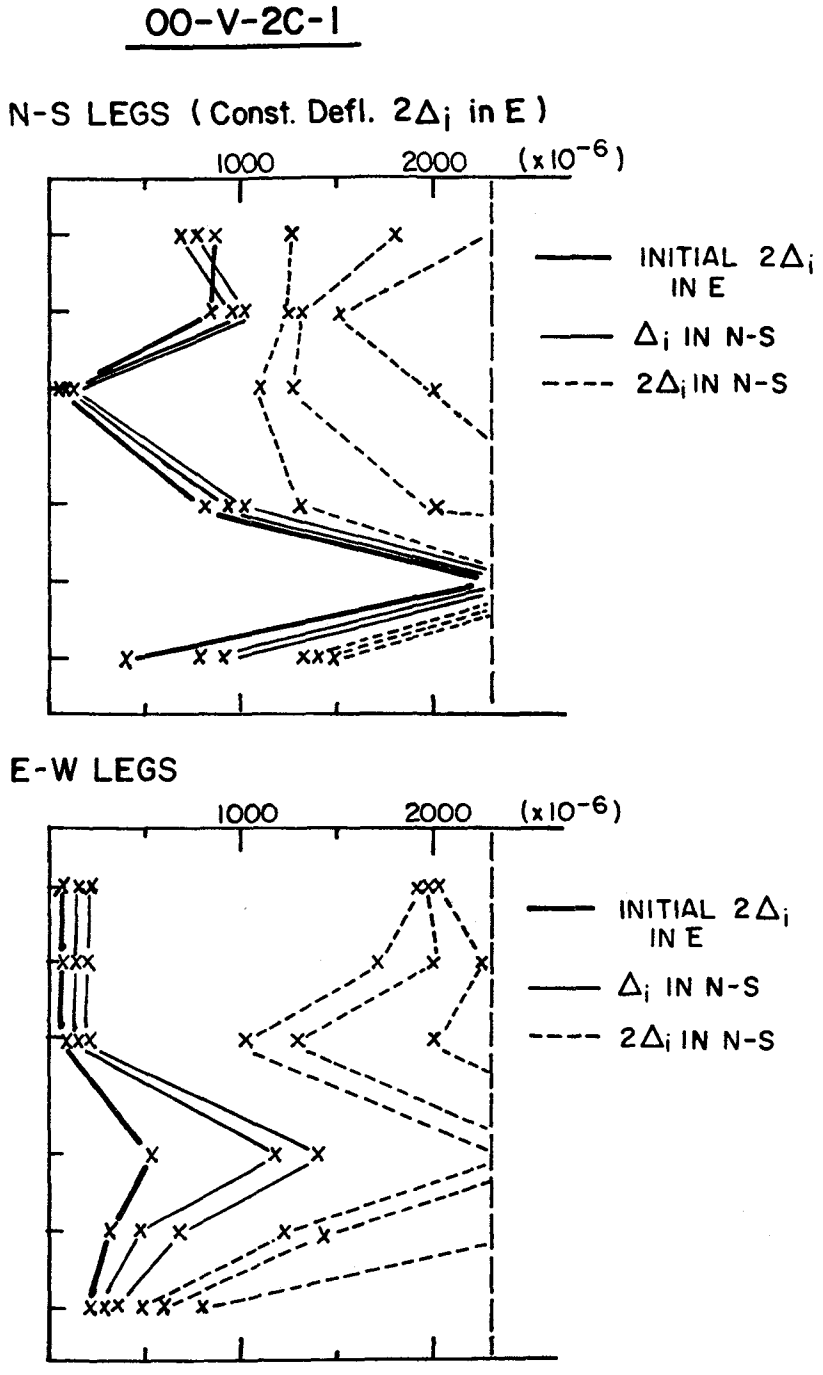

Fig. 4.33 Comparison of strain distribution in transverse reinforcing legs--00-V-2C-I

4.4 Crack Patterns

Crack patterns of the ten specimens tested are shown in Figs. 4.34 to 4.43. In the figures, Δ_i stands for the unit initial deflection (= 0.2 in.) in the principal direction. Therefore, in the case of simultaneous loading in both principal directions, the resultant deflection is larger than the initial deflection.

Cracks were marked at every peak load stage at each deflection level. The crack patterns are shown after three cycles of load reversal at each deflection level.

Although the maximum shear strength was not necessarily reached at the same deflection level in each test, the major cracks usually were apparent during the three cycles at a $2\Delta_i$ level. A couple of tests reached the maximum shear strength at a $3\Delta_i$ level; however, there were very few new cracks during that loading. Instead of initiating new cracks, the loading increased the width of several existing cracks. For these reasons, the crack patterns at the Δ_i and $2\Delta_i$ levels were traced from photographs. Major cracks at failure are also shown because they may provide a better understanding of the failure mechanism. Figures 4.44 and 4.45 show the appearance of several specimens at failure.

00-V-0-I. (Fig. 4.34) The load was applied only in the N-S direction. The diagonal shear cracks are predominant in the east and west faces of the column and are almost identical. In the north and the south sides there were several horizontal cracks and a vertical crack over the middle column longitudinal bar. At the $2\Delta_i$ level, cracks propagated toward the middle of the column and several new cracks initiated in the middle position of

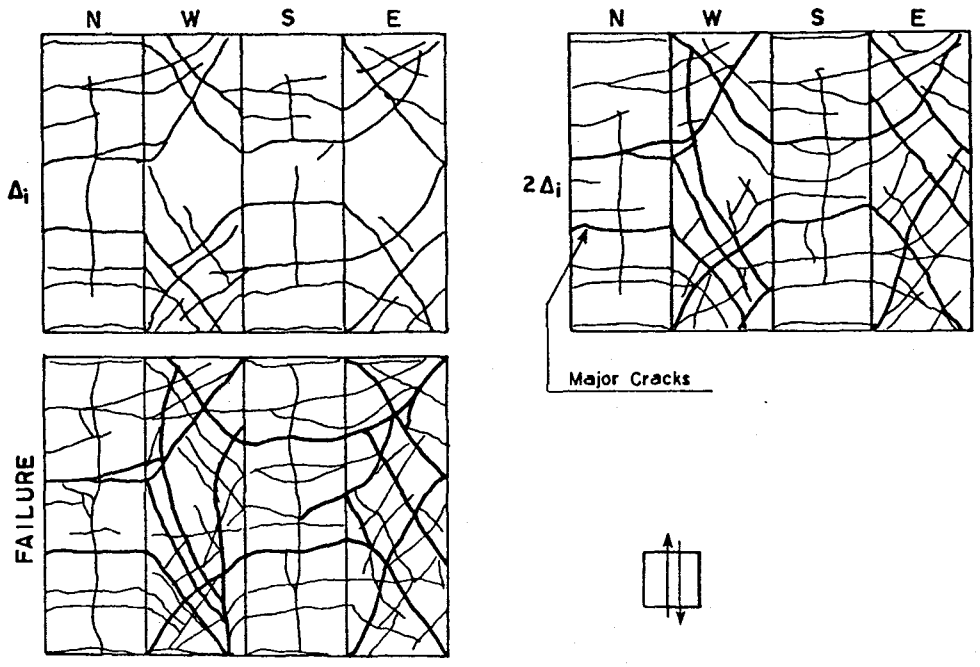

Fig. 4.34 Crack patterns--OO-V-O-I

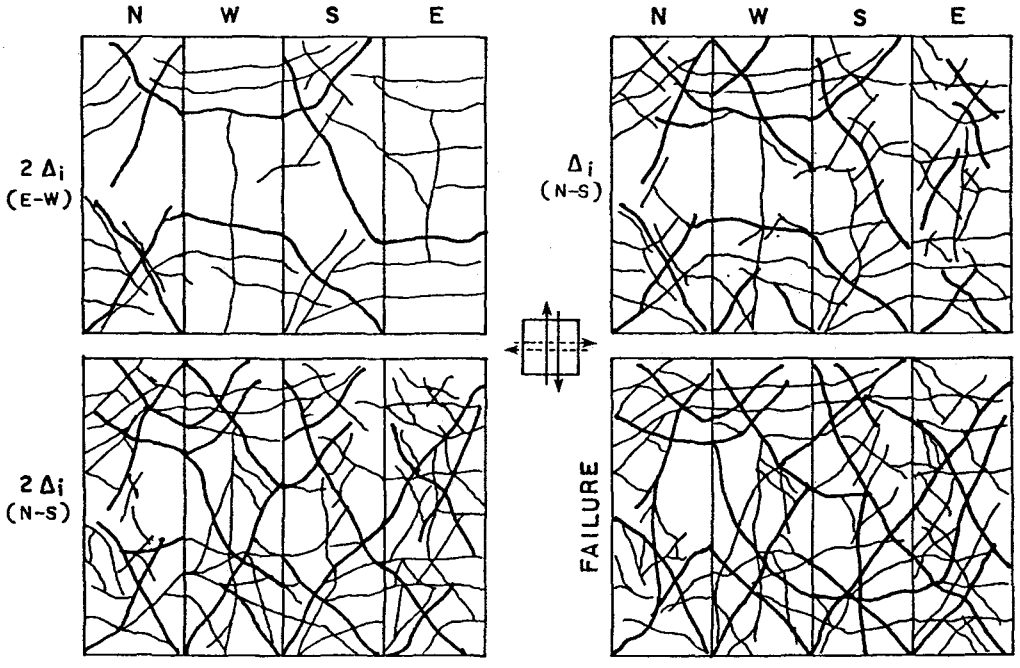

Fig. 4.35 Crack patterns--OO-V-2VP-I

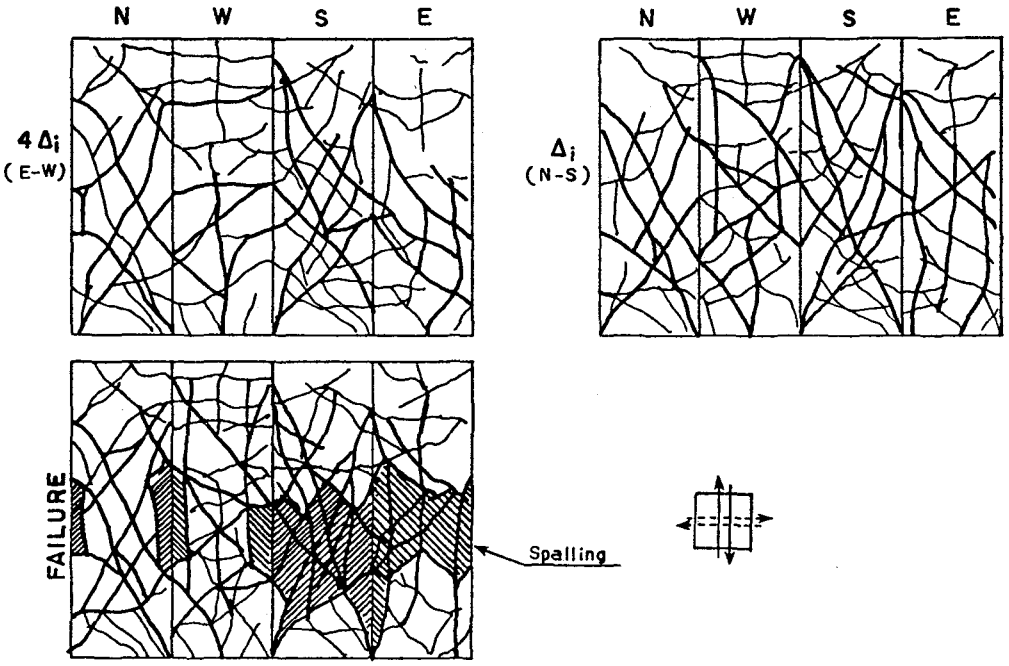

Fig. 4.36 Crack patterns--OO-V-4VP-I

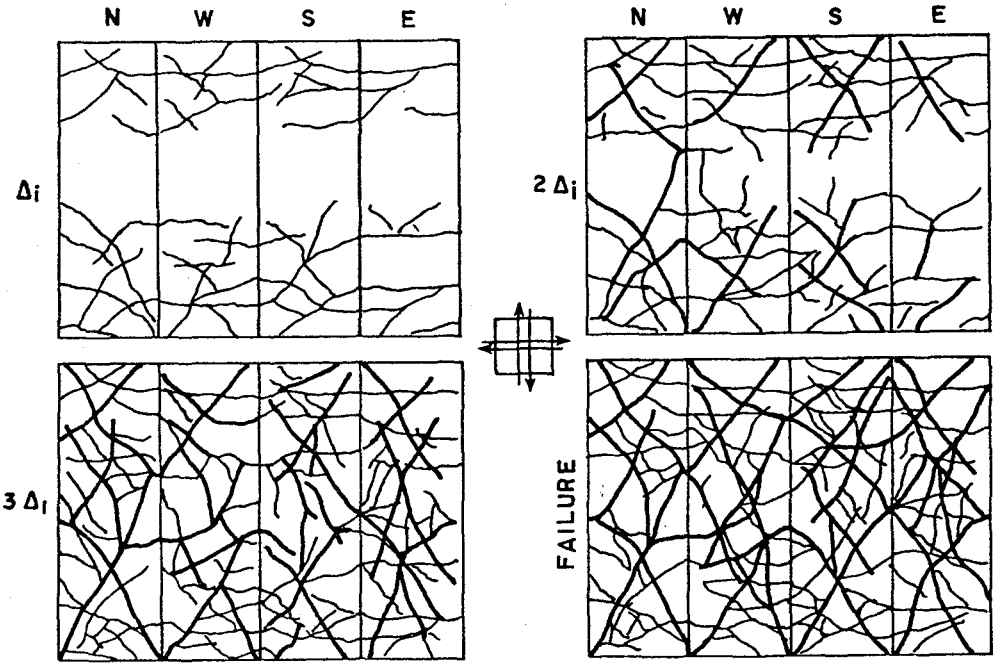

Fig. 4.37 Crack patterns--OO-V-V-A

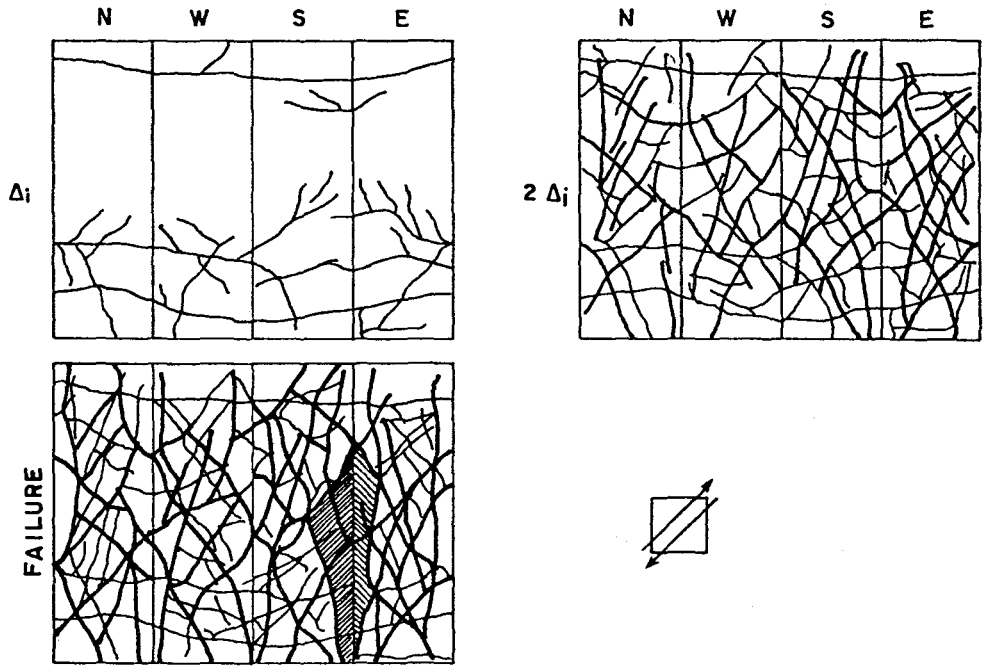

Fig. 4.38 Crack patterns--OO-V-V-S

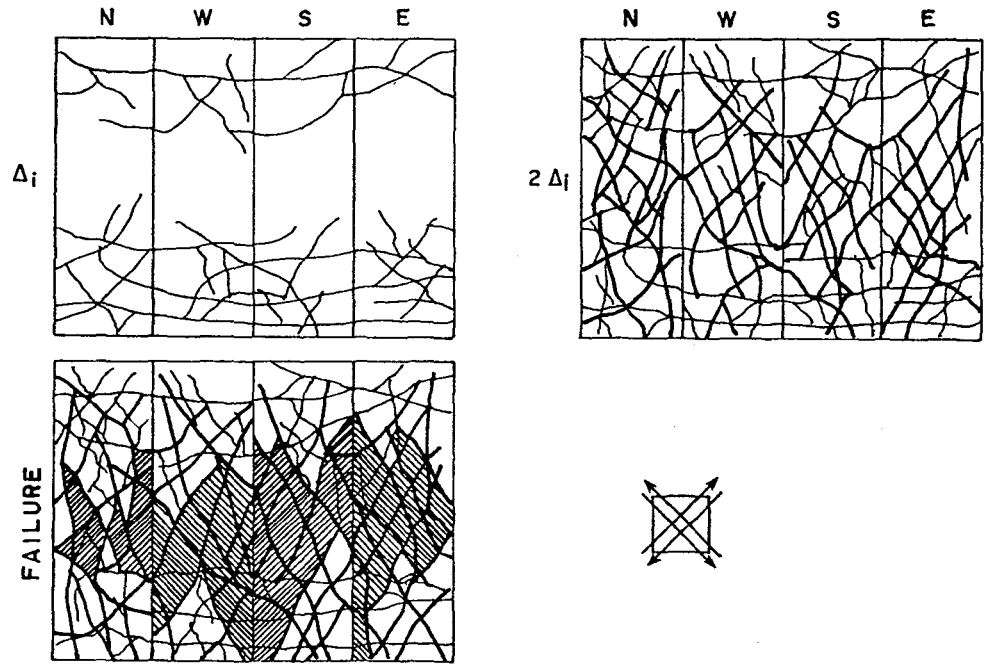

Fig. 4.39 Crack patterns--OO-V-V-SA

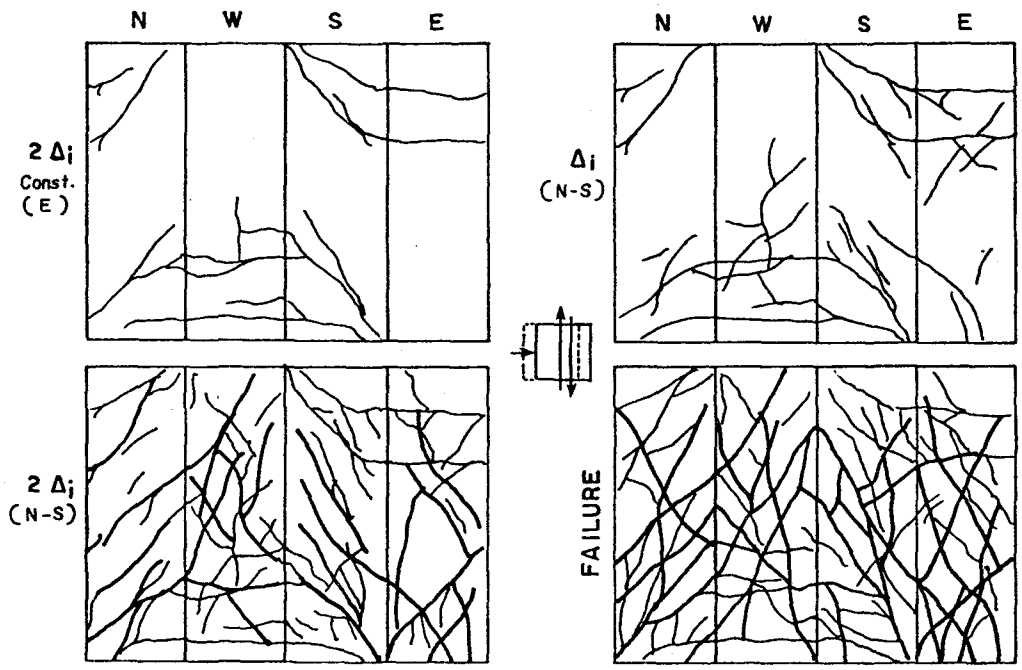

Fig. 4.40 Crack patterns--OO-V-2C-I

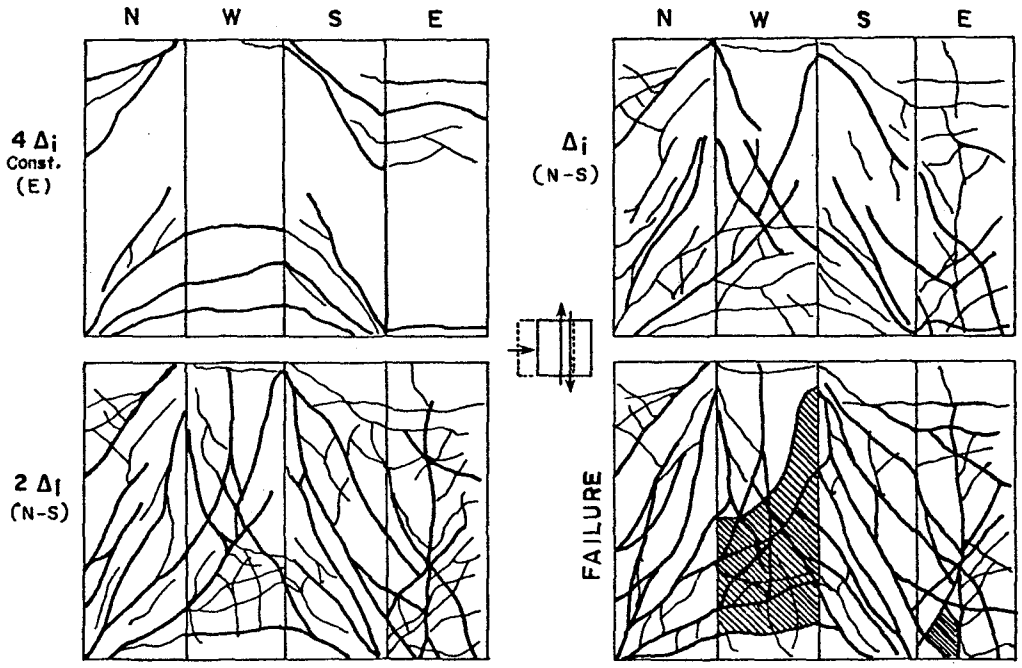

Fig. 4.41 Crack patterns--OO-V-4C-I

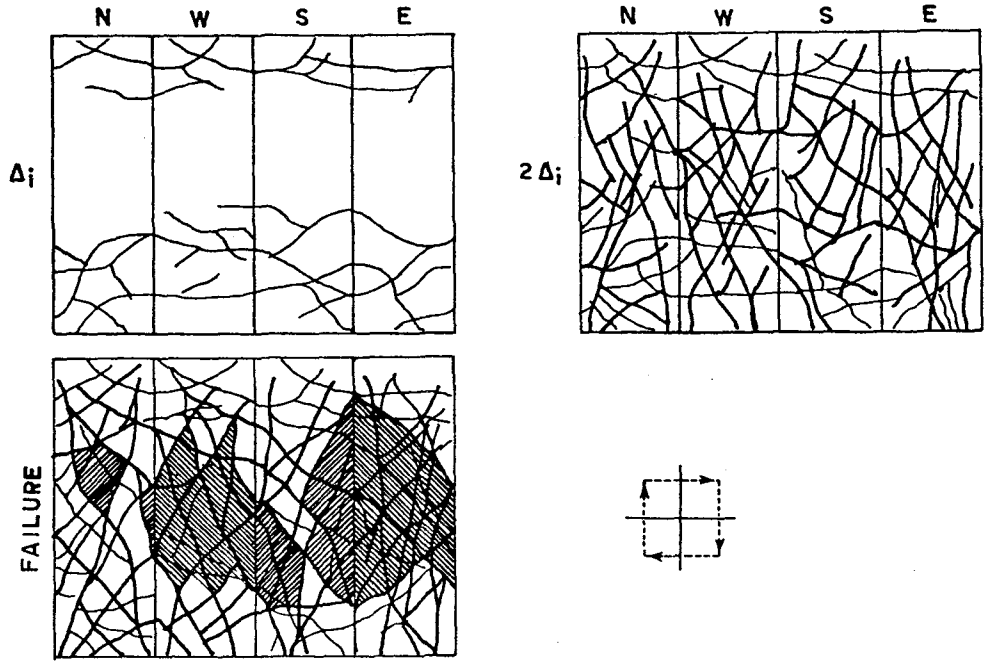

Fig. 4.42 Crack patterns--OO-C-C-AF

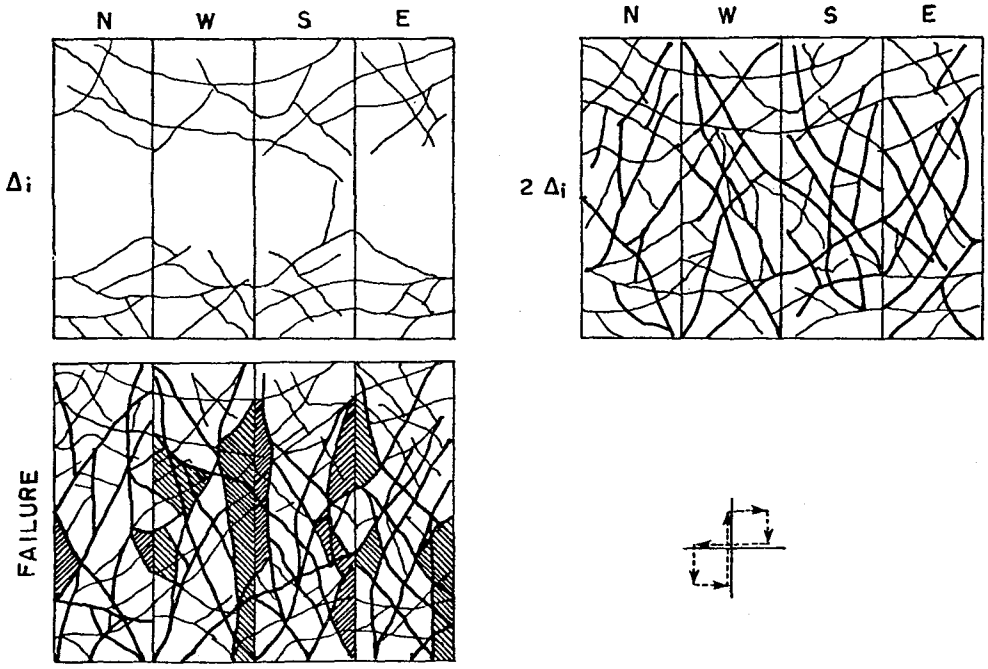

Fig. 4.43 Crack patterns--OO-C-C-AH

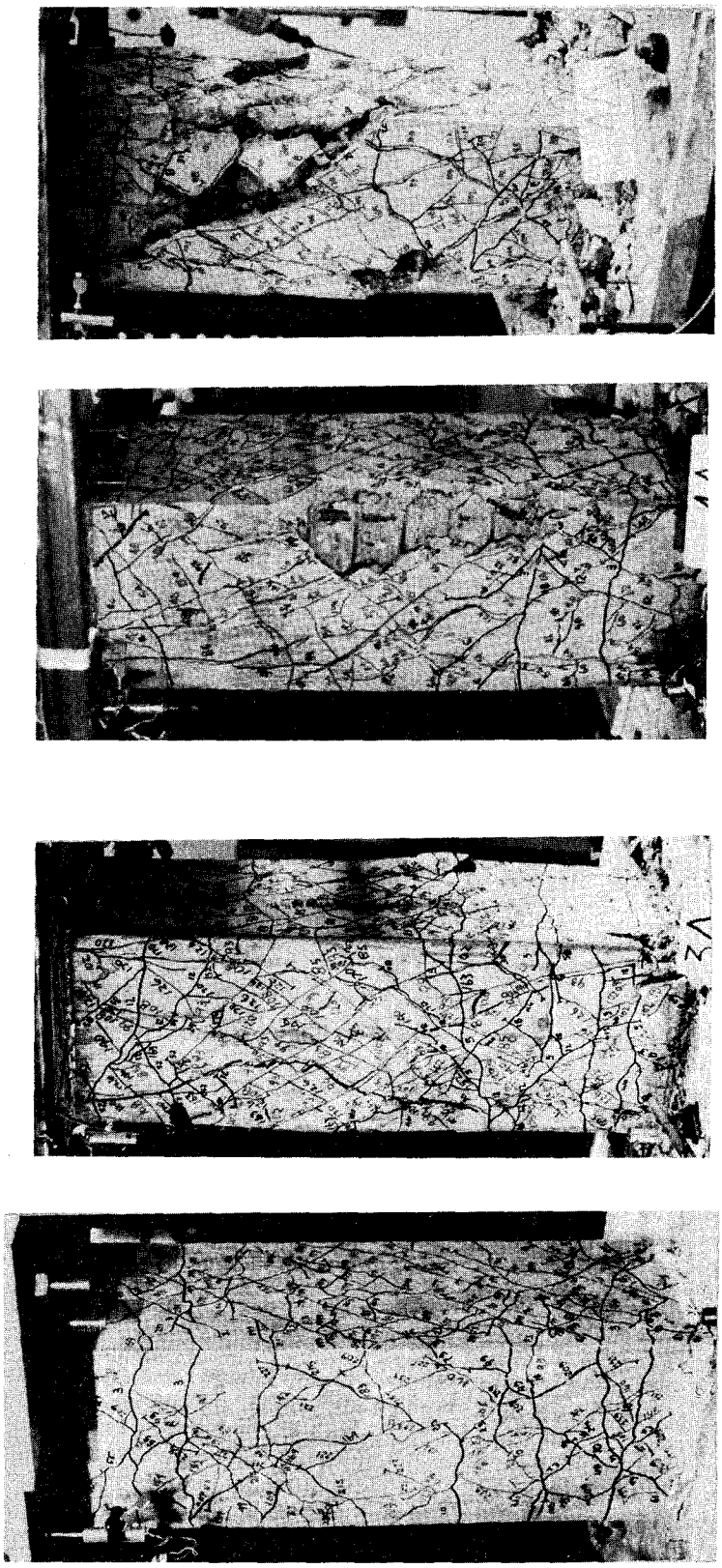

00-C-C-AF

00-V-V-S

00-V-V-S

00-V-V-A

Fig. 4.44 Failure patterns

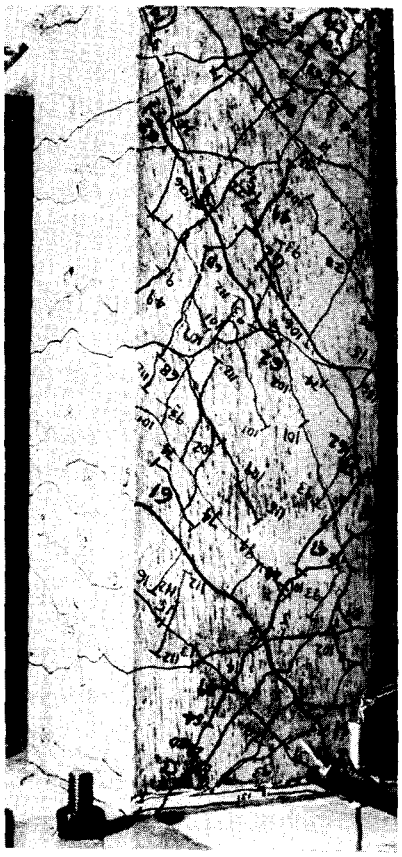

00-V-0-I

00-V-2C-I

00-V-VC-I

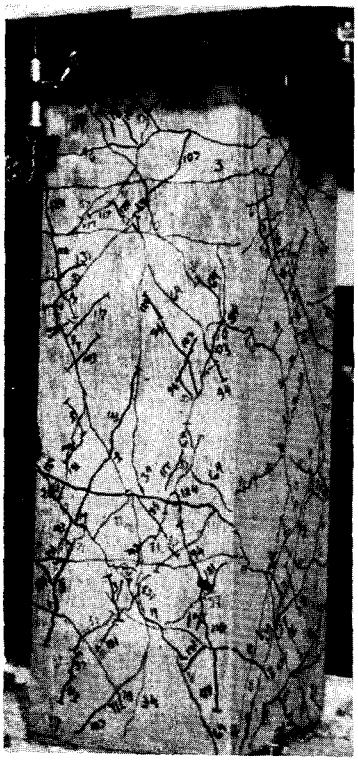

00-V-2VP-I

00-V-4VP-I

Fig. 4.45 Failure patterns

the column. Several major shear cracks can be seen at failure at an angle of about 45 degrees with the column axis.

00-V-2VP-I. (Fig. 4.35) In this case, three cycles at a $2\Delta_i$ level were imposed in the E-W direction. The crack pattern due to the initial loading is similar to the of 00-V-0-I.

These initial cracks from the E-W loading appear to influence the crack pattern for the N-S loading. Cracks newly initiated by the N-S loading are not necessarily horizontal in the north and south faces. At failure, inclined cracks at an angle slightly more than 45 degrees are predominent in all four faces of the column.

00-V-4VP-I. (Fig. 4.36) Three cycles at $4\Delta_i$ were imposed in the E-W direction before any load was applied in the N-S direction. With this reversed load, the column lost virtually all shear capacity. The load in the N-S direction after the E-W loading did not produce any change in the column because the column was so heavily damaged that the Δ_i, $2\Delta_i$, and $3\Delta_i$ deflection levels could be reached with very low load. The major cracks at failure were due to the previous $4\Delta_i$ level load.

00-V-V-A. (Fig. 4.37) Three cycles of load were applied in both the N-S and the E-W direction alternately. The crack pattern in each side is almost identical. In this case, cracks initiated and propagated very uniformly in the entire section. At failure, diagonal cracks at an angle slightly more than 45 degrees were dominant.

00-V-V-S. (Fig. 4.38) The reversed loading was in the diagonal direction, NE-SW. The diagonal cracks propagated toward the NE or the SW corners at the Δ_i level in both principal directions. With $2\Delta_i$ loading, the entire section was covered with

very steep cracks. Some of those cracks became wider at failure.

00-V-V-SA. (Fig. 4.39) The loading was applied in both diagonal directions alternately--NE-SW and NW-SE. Cracks were distributed uniformly in all directions. At failure, a large area of the cover concrete spalled off. Major diagonal cracks were present in all diagonal directions.

00-V-2C-I. (Fig. 4.40) Initially, the $2\Delta_i$ level deflection was imposed in the E direction and was held constant during the N-S loading. Under this constant deflection, the upper part in the east face of the column and the lower part in the west face exhibited flexural cracking. Therefore, those sections were easily cracked in shear by the N-S loading. Major diagonal cracks were produced by the N-S loading and led to failure.

00-V-4C-I. (Fig. 4.41) The loading pattern is almost the same as the above case, except the $4\Delta_i$ constant deflection was imposed in the E direction. Initial cracks produced by the $4\Delta_i$ deflection were not much different from those due to the $2\Delta_i$ deflection, but a large number of wide cracks were initiated with three cycles of load with the Δ_i deflection in the N-S direction. The angle of the cracks was steeper than 45 degrees. The Δ_i level in the N-S direction governed the failure pattern. The $2\Delta_i$ level in the N-S loading did not cause any serious new cracks, but resulted in a widening of existing cracks.

00-C-C-AF. (Fig. 4.42) This is the case of the square load path in all four quadrants. The main feature of the crack pattern in this case is the crack angle. Cracks initiated at Δ_i with relatively shallow angles; however, new cracks at $2\Delta_i$ are very steep and those cracks became predominant at failure. Major cracks were observed throughout the column and the large number of cracks caused a large portion of cover concrete to spall.

OO-C-C-AH. (Fig. 4.43) The load path is a square only in the first and the third quadrants. The crack pattern is quite similar to the above case (OO-C-C-AF). Cracks were distributed uniformly and across the entire section.

CHAPTER 5

DISCUSSION OF TEST RESULTS

Ten specimens were tested with different load histories. The ten load histories can be divided into two groups. The first group consists of the tests in which load was applied in only one principal direction at a time. As stated in Chapter 4, "the principal direction" implies the N-S or the E-W direction. The results of this group permit an examination of the influence of previous loadings in the same direction or in an orthogonal direction. The second group consists of the tests in which the load was applied in both principal directions simultaneously. The results of this group permit a study of the influence of load path and load sequence in the horizontal plane.

5.1 Influence of Previous Loading

In Figs. 5.1 to 5.4, the influence of the deflection level in the previous loading is examined. The shear strength is normalized using $V/A_c\sqrt{f'_c}$. V is the measured shear strength and A_c is the core area of concrete surrounded by transverse reinforcement. Shear strength of concrete is considered to be a function of $\sqrt{f'_c}$ (f'_c = concrete compressive strength in psi) [18]. The denominator $A_c\sqrt{f'_c}$ may be very good for the ultimate stage, because at the ultimate stage the concrete outside transverse reinforcement spalls off and only the core concrete can contribute to the shear strength. However, at lower deflection levels the concrete outside the transverse reinforcement can still carry shear force. Therefore, A_c may not be good for normalizing shear over the entire range of deflections.

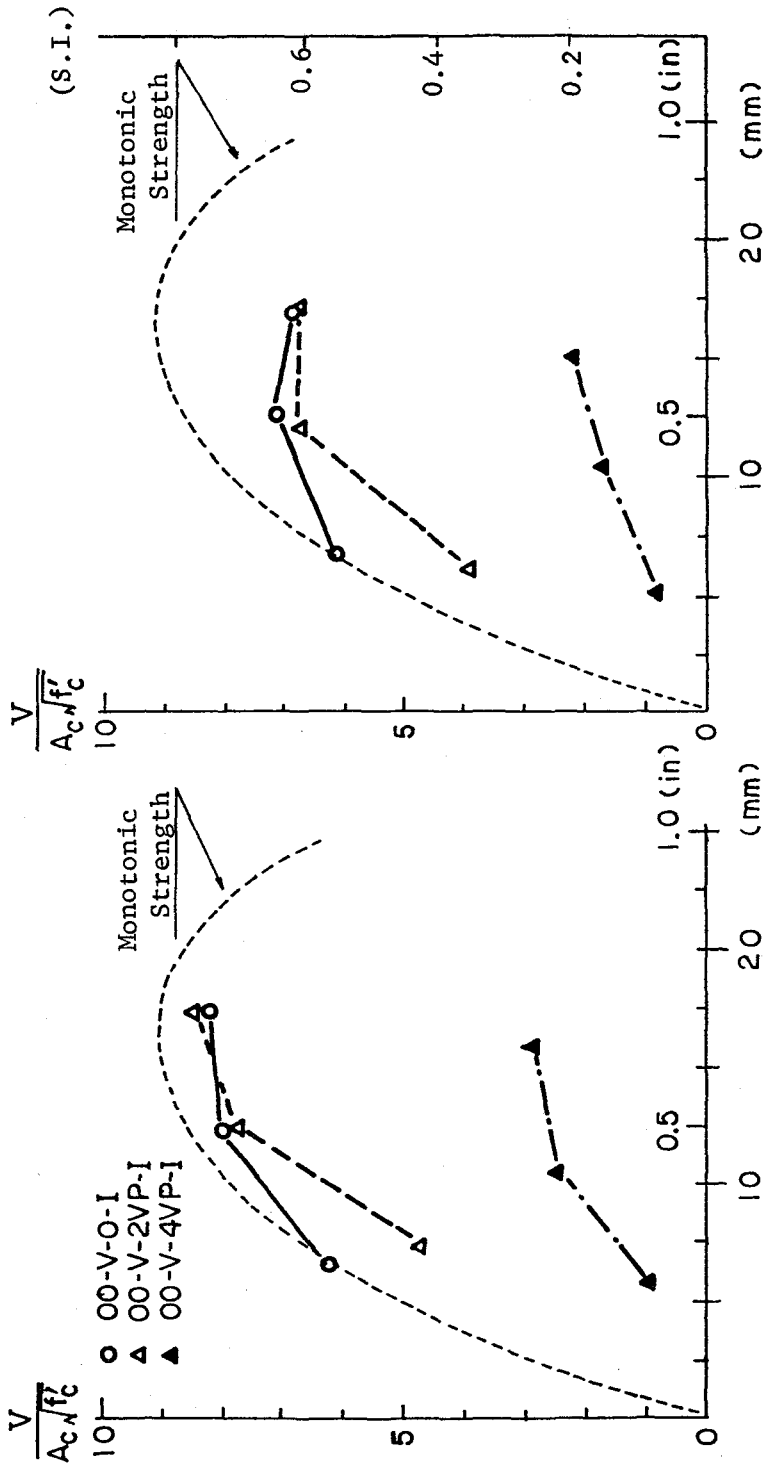

Fig. 5.1 Influence of previous loading - initial cycles

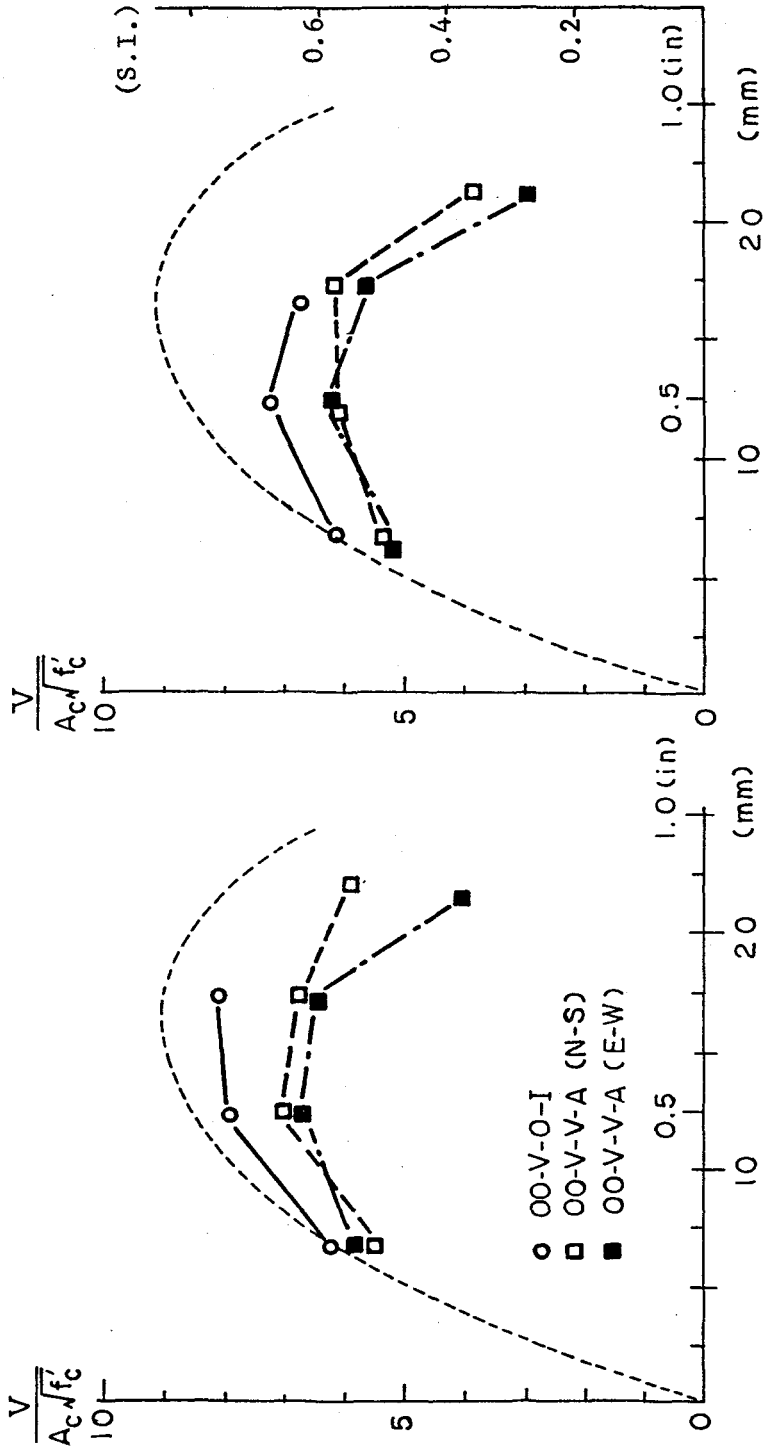

Fig. 5.2 Influence of previous loading - alternate cycles

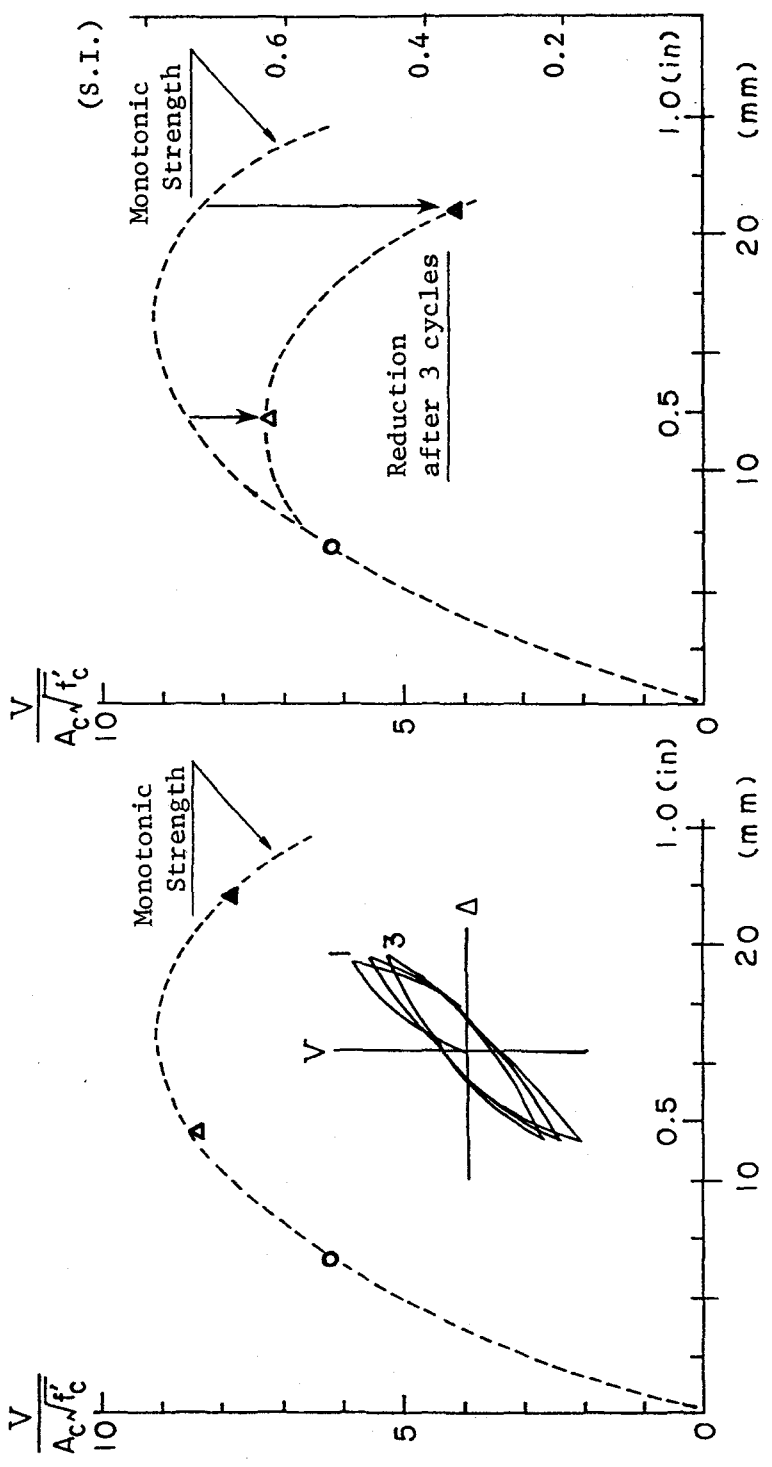

Fig. 5.3 Influence of previous loading - reference curve

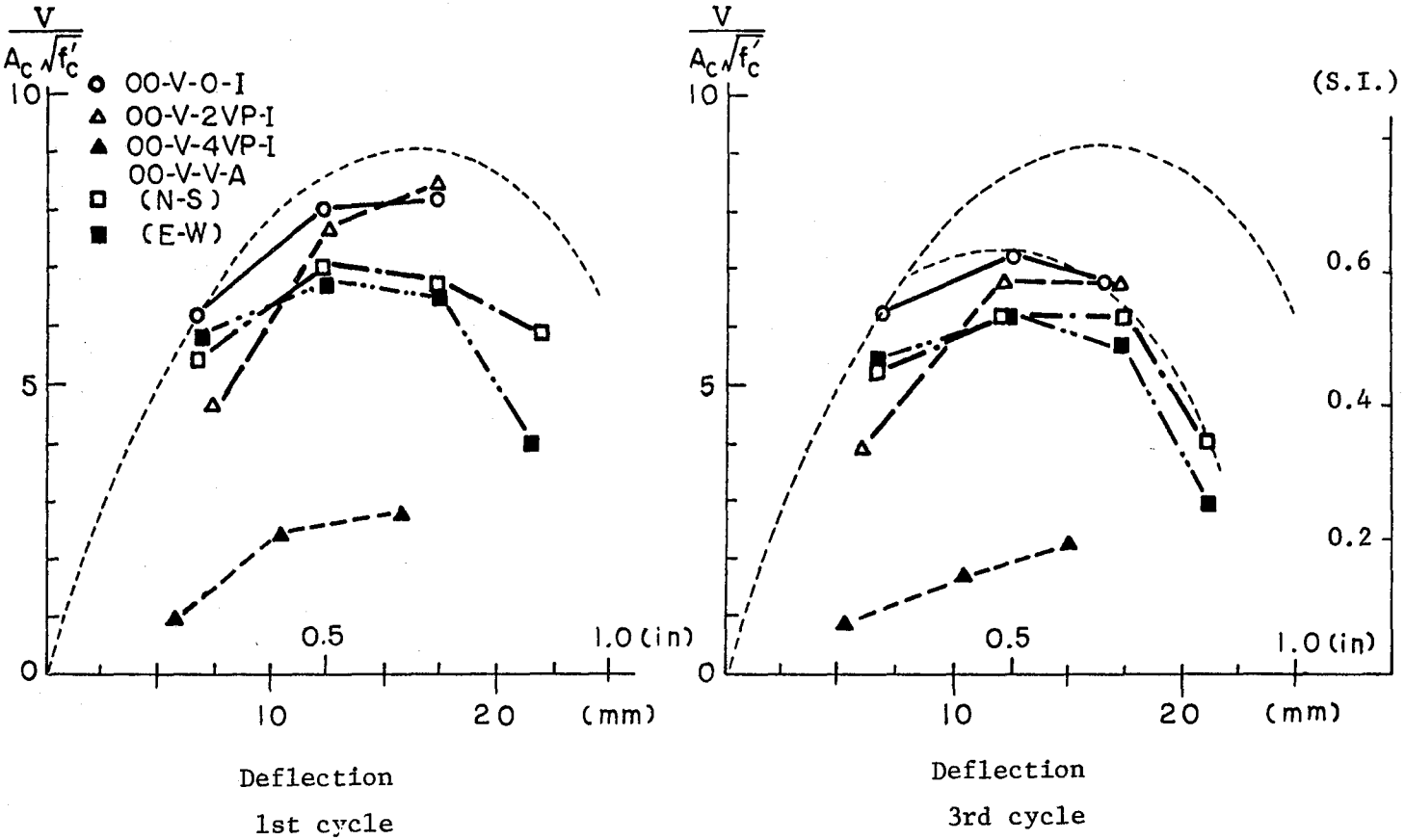

Fig. 5.4 Influence of previous loading - summary

Figure 5.1 shows the importance of the deflection level in the previous loading. When the previous deflection is $2\Delta_i$ (= 0.5 in.), the influence of that loading appears only at the low deflection level in the orthogonal direction because cracks which are initiated by the previous loading are not completely closed at equal or lower deflection levels. However, after $2\Delta_i$, the behavior of the specimen is quite similar to that of the unilateral loading case. At this stage the influence of the previous loading cannot be recognized.

On the other hand, with three cycles at a $4\Delta_i$ (= 0.9 in.) deflection level, the specimen has failed. After this loading, the remaining shear capacity is very small.

Figure 5.2 shows the shear strength deterioration in the case of alternate loading in both directions (00-V-V-A). Three cycles of load were applied in both the N-S and the E-W directions alternately at each deflection level (see Fig. 5.1). The N-S direction is loaded first and the E-W direction second. Up to the $3\Delta_i$ level, both directions show almost the same behavior. But at the $4\Delta_i$ level, the second direction (E-W) shows the influence of the N-S loading.

The curve in Fig. 5.3 is the reference against which the shear strength deterioration is evaluated. The curve indicates the shear strength at the first and the third cycle when the specimen has been subjected to three cycles of load at a certain deflection level. By comparing this curve at given deflection levels, the influence of the previous loading on the shear strength deterioration can be seen.

In order to construct the curve, three cases were studied. The data at Δ_i were obtained from the specimen 00-V-0-I (unilateral loading). The values at $2\Delta_i$ and $4\Delta_i$ were available from the specimens for the previous loading 00-V-2VP-I and 00-V-4VP-I. In those two cases, three cycles at $2\Delta_i$ or $4\Delta_i$ were initially applied.

A comparison of four cases with the reference curve is shown in Fig. 5.4. In the case of unilateral loading, the third cycle strength at $3\Delta_i$ is almost the same as the reference curve. This shows that as far as the third cycle strength is concerned, the three cycles of load at Δ_i and $2\Delta_i$ are not significant. The same thing can be said for the first direction (N-S) at the $4\Delta_i$ level. Namely, three cycles at Δ_i, $2\Delta_i$, and $3\Delta_i$ level do not significantly influence the behavior.

From these results, and with consideration that the maximum strength under monotonic loading appears at a deflection of 0.6 - 0.7 in. (= $3\Delta_i$), it can be said that the influence of previous loadings on the shear strength is not significant unless the maximum peak deflection of the previous loading exceeds 0.6 - 0.7 in. deflection level.

5.2 Influence of Simultaneous Loading in Both Principal Directions

Comparisons in Terms of Principal Direction. Figure 5.5 shows the influence of constant deflection (Fig. 5.2). Two levels of constant deflection were tested ($2\Delta_i$ and $4\Delta_i$). The higher the level of constant deflection the greater is the reduction in shear strength. When these results are compared with the influence of previous loading, it is found that the influence of the $2\Delta_i$ constant deflection is more significant than that of the previous loading at the $2\Delta_i$ or $3\Delta_i$ level. It can also be seen that at a lower deflection level the influence of the $4\Delta_i$ constant deflection is less serious than previous loading of three cycles at a $4\Delta_i$ level. This is because the three cycles of load at a $4\Delta_i$ level fail the specimen but the constant east loading to $4\Delta_i$ does not.

Figure 5.6 shows a comparison of the influence of the skewed loading with that of loading along a principal direction.

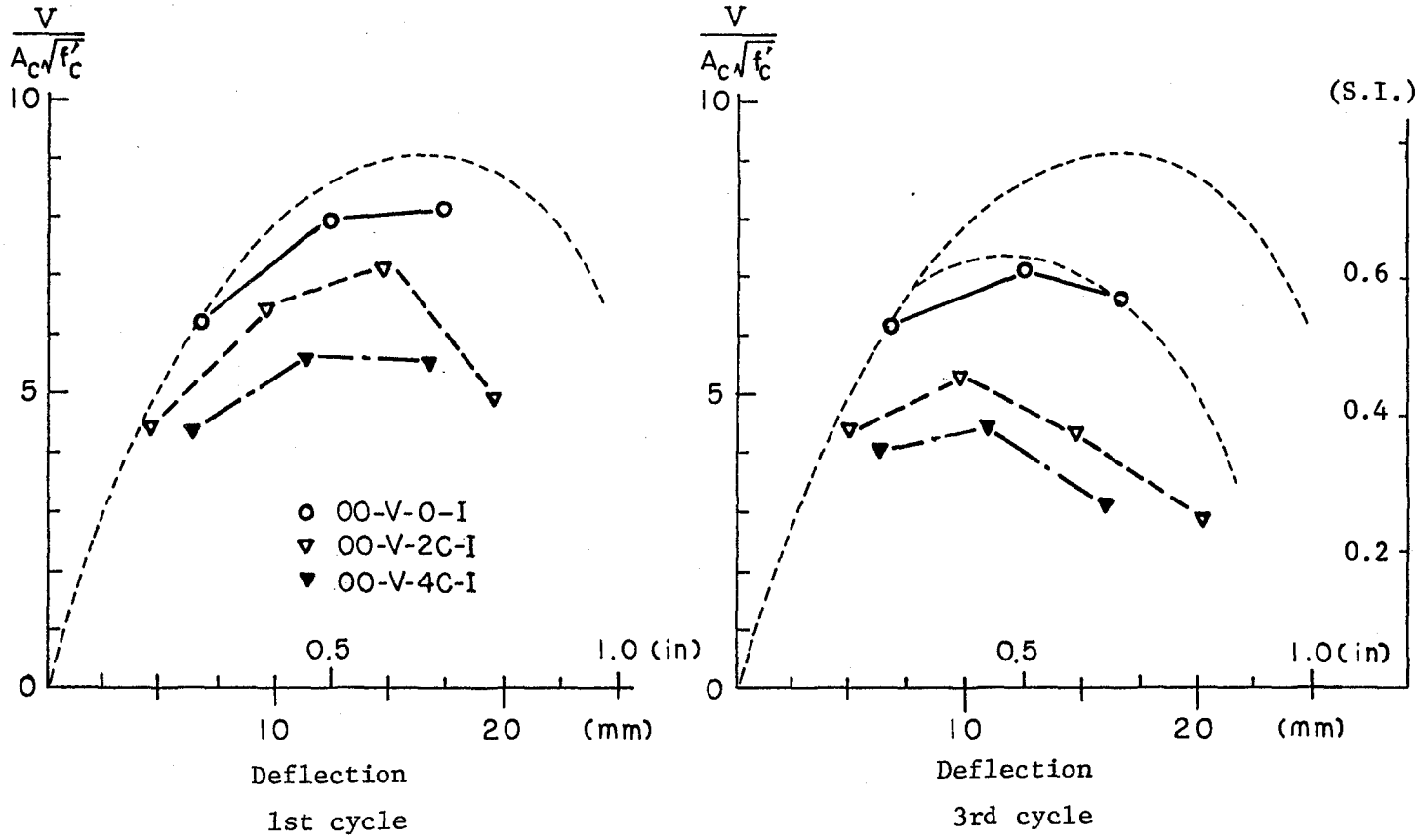

Fig. 5.5 Influence of constant deflection

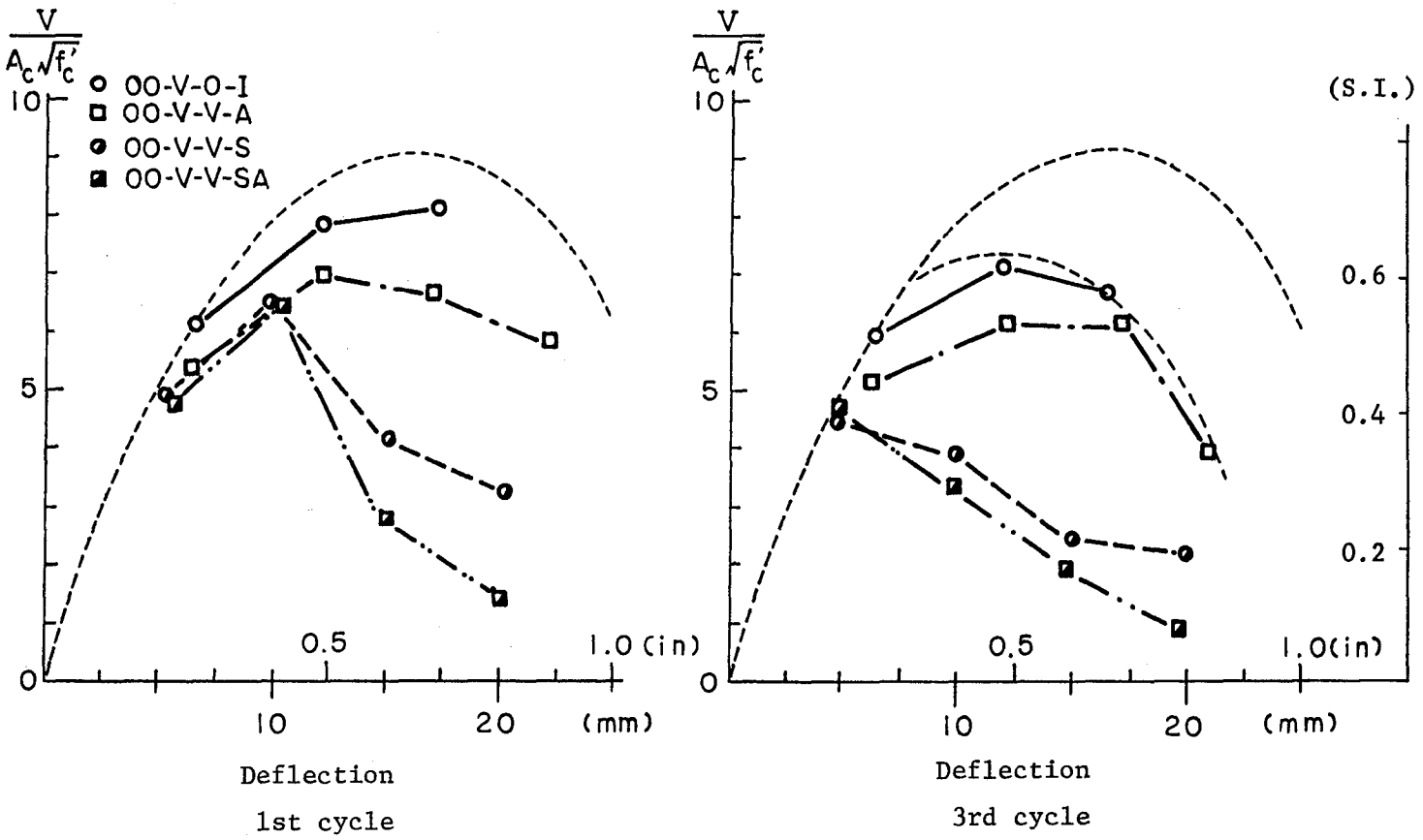

Fig. 5.6 Comparison of skewed loading with principal loading--principal direction

As mentioned before, the same deformation is applied in both principal directions. At Δ_i there is no influence of the loading in an orthogonal direction. However, above the $2\Delta_i$ level, simultaneous loading in both directions produces a significant strength reduction.

In Fig. 5.6, alternate loading in the principal directions and along the diagonals (skew) are compared. In both cases the alternate loading further reduces the shear strength. The relationship between the shear strength under unilateral loading and that under alternate loading is similar for both cases (principal axis loading and skewed loading).

The influence of load path is shown in Figs. 5.7 and 5.8. The half square load path (square load path only in the first and the third quadrants--OO-C-C-AH) and the full square load path (square load path in all four quadrants--OO-C-C-AF) are compared with the case of unilateral loading (OO-V-O-I) and the case of alternate loading in both skew directions (OO-V-V-SA). The full square load path shows severe strength reduction after the $2\Delta_i$ level, as does alternate loading (Fig. 5.7). On the contrary, the half square load path does not reduce the shear capacity much, although some strength reduction is apparent after the $2\Delta_i$ level.

In Fig. 5.8, two cases of constant deflection are added to the full and the half square load path. The first cycle behavior of the half square load path looks similar to that of the $2\Delta_i$ level constant deflection case (OO-V-2C-I). In the third cycle, the behavior under the half square load path is almost the same as that of the $4\Delta_i$ level constant deflection (OO-V-4C-I). Therefore, it can be said that the influence of the half square load path is greater than that of constant deflection at $2\Delta_i$, but less than that of constant deflection at $4\Delta_i$.

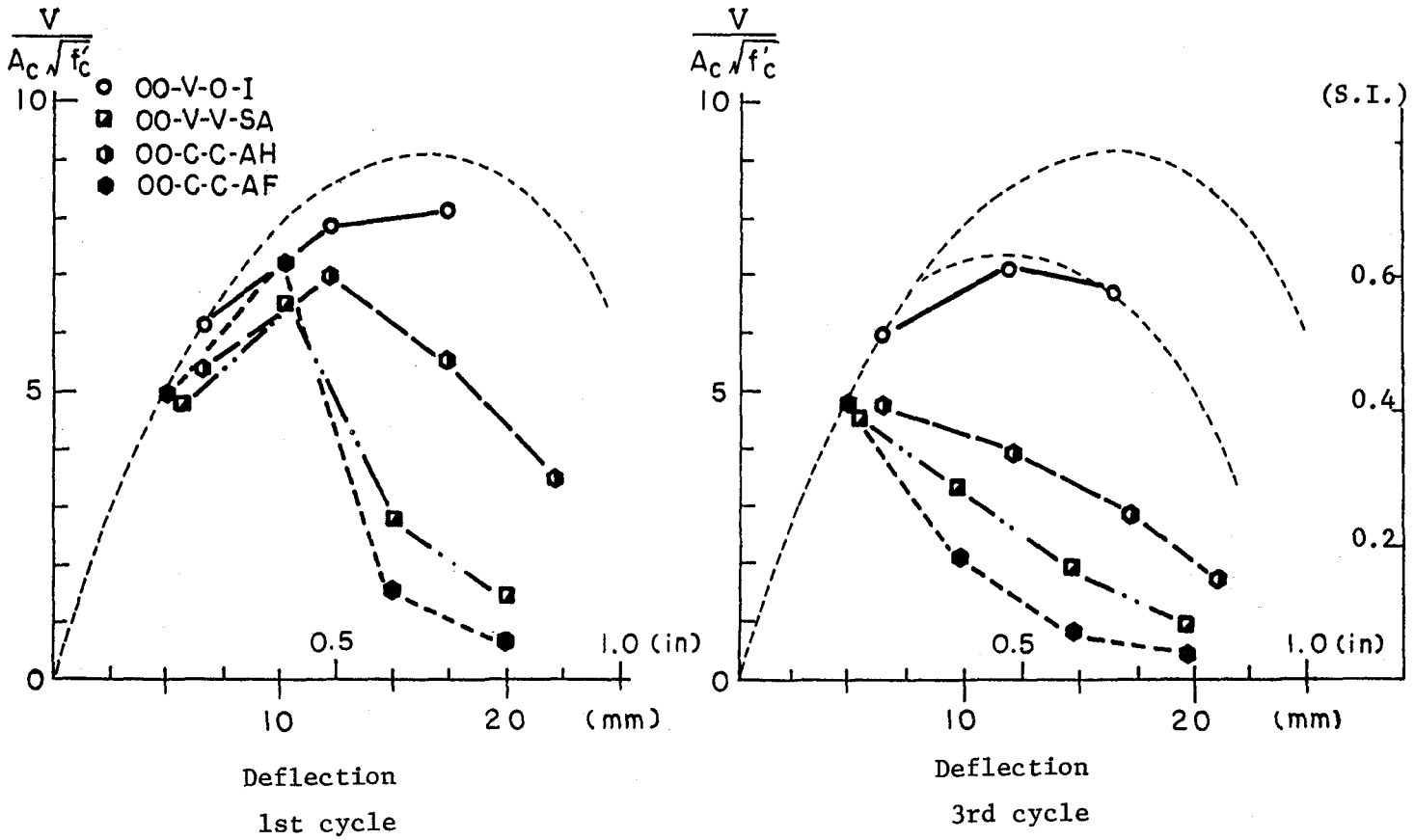

Fig. 5.7 Influence of load path (1)--principal direction

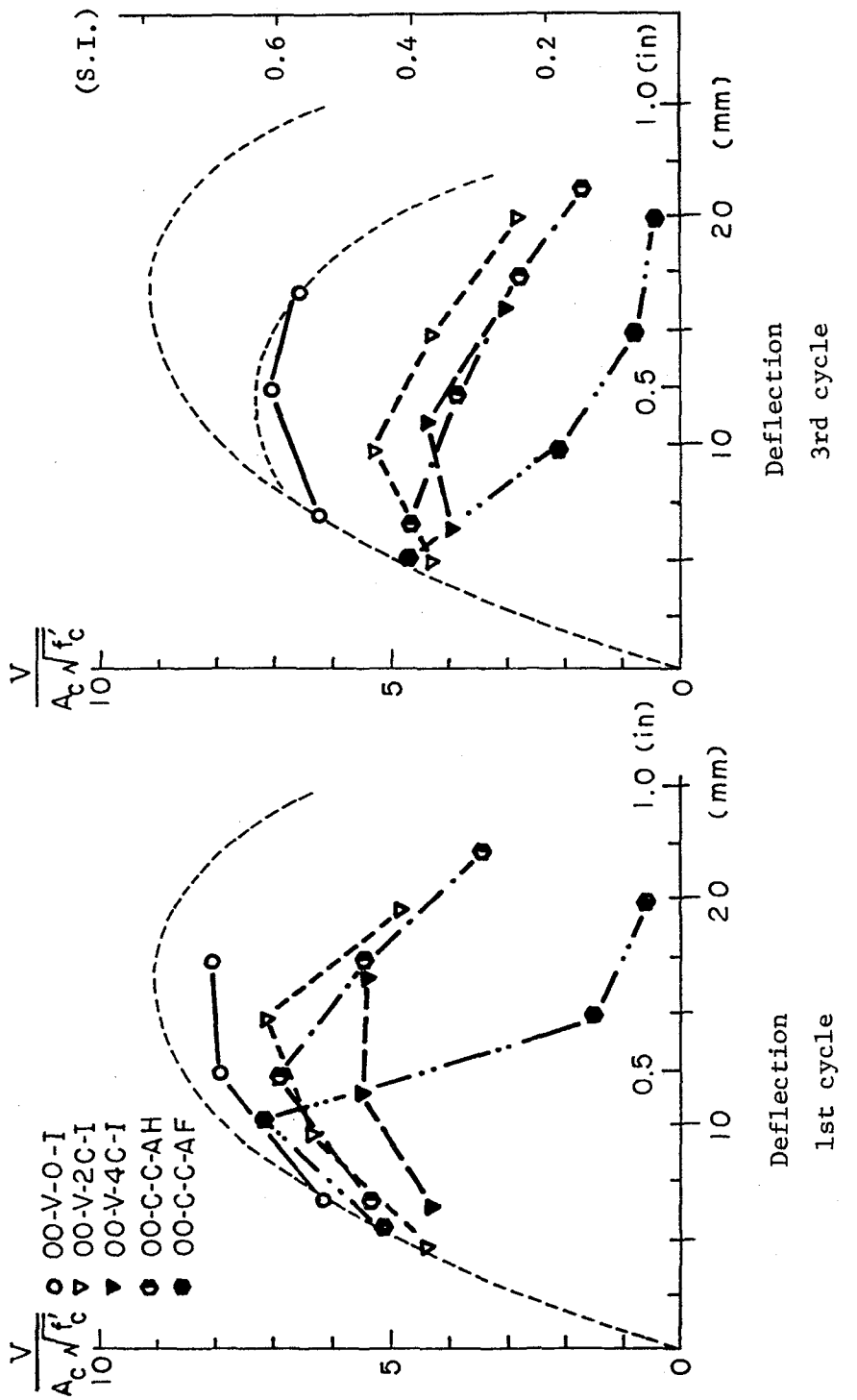

Fig. 5.8 Influence of load path (2)--principal direction

Consideration of Resultant Forces. The discussion to this point has been based on strength and deformations in the principal direction. However, in order to consider the influence of a component of force in each direction applied simultaneously, it may be useful to combine the forces in the principal directions to obtain a resultant force. The resultant force is obtained as the vector of a diagonal line in a parallelogram which is composed of the two vectors in the principal directions. Corresponding to resultant forces, resultant deflections are considered in the same manner.

Figure 5.9 shows the monotonic strength curves in the principal direction and in the skew direction at an angle of 45 degrees. In the case of skewed loading, the force and the deflection were measured along the diagonal. From Fig. 5.9 it can be seen that points from both tests lie nearly on the curve for monotonic loading. Therefore, it is possible to use the one curve as a standard for comparison of any results in this study as long as the resultant force and the resultant deflection are taken into account.

On the basis of the results shown in Fig. 5.9, the shear strength of a short square column does not appear to be influenced by the loading direction. In other words, if the imposed deflection is the same, the square specimen shows the same strength regardless of the loading direction.

When this feature is taken into account, the loading histories examined in this study can be redivided into two groups, as shown in Fig. 5.10.

Group I : Resultant load is cycled in one direction at a time.

Group II : Angle of resultant force vector varies during loading.

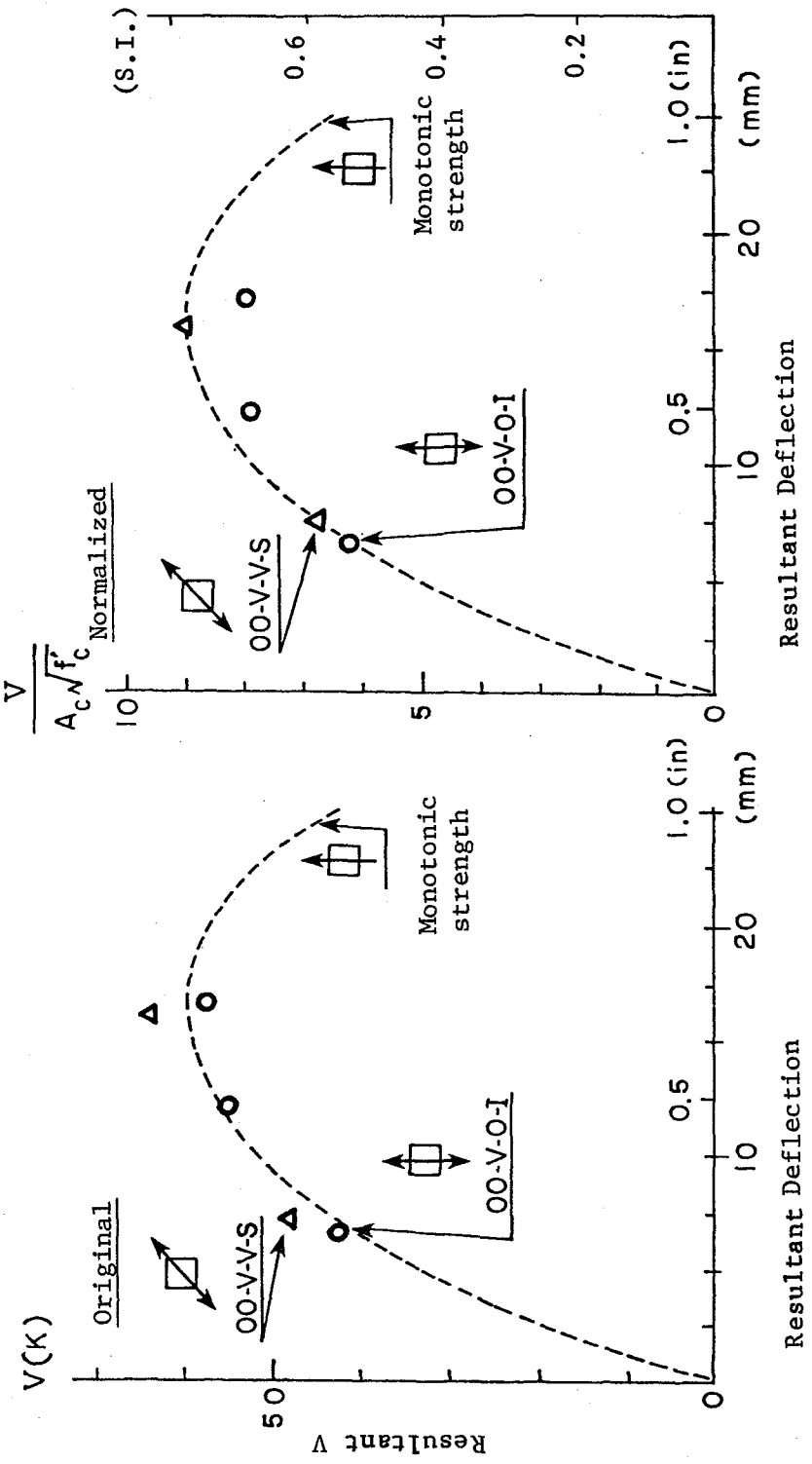

Fig. 5.9 Comparison of loading direction under unilateral loading--resultants

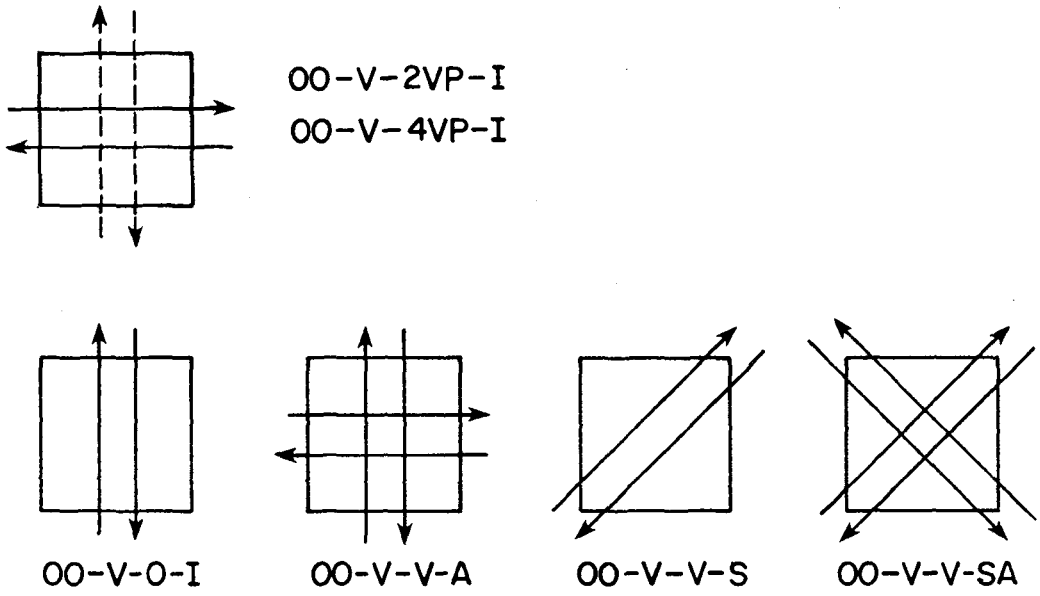

(a) Group I

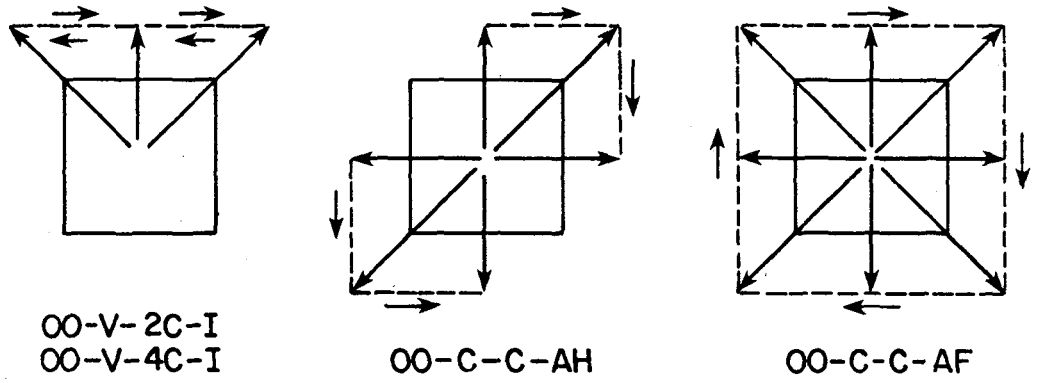

(b) Group II

Fig. 5.10 Loading direction

The influence of load history on the shear strength of a column is again discussed in terms of resultant force and resultant deflection.

Influence of Loading Direction in Group I. Four test results are compared in Fig. 5.11. Two are cases of skewed loading. In both principal and skew directional loading, the specimen exhibits a slightly lower shear strength under alternate loading than under unilateral loading. It does not appear that the shear strength depends on the loading direction. From these results it may be possible to consider the shear strength of reinforced concrete square columns as a function of the cross section properties, especially core area, and not as a function of the loading direction.

Influence of Angle Traced during Revolution of Resultant Force Vector. Figure 5.12 shows four test results in Group II compared with the unilateral loading case. Some differences can be noted, especially in the range where the resultant deflection is greater than that corresponding to the ultimate strength under monotonic loading. The range of the revolution of the resultant force vector is the smallest in the case of 00-V-4C-I (incrementally increasing load in the N-S direction with $4\Delta_i$ constant deflection in the east). This case shows the least shear strength reduction.

On the other hand, the full square load path (00-C-C-AF) causes 360 degrees revolution of the resultant force vector as seen in Fig. 5.10. This case shows the most severe shear strength reduction when the resultant deflection exceeds the deflection at ultimate strength under monotonic loading. It may be considered that when the resultant force is applied in all directions, the specimen is cracked and crushed uniformly in the entire cross section, producing the most severe strength reduction.

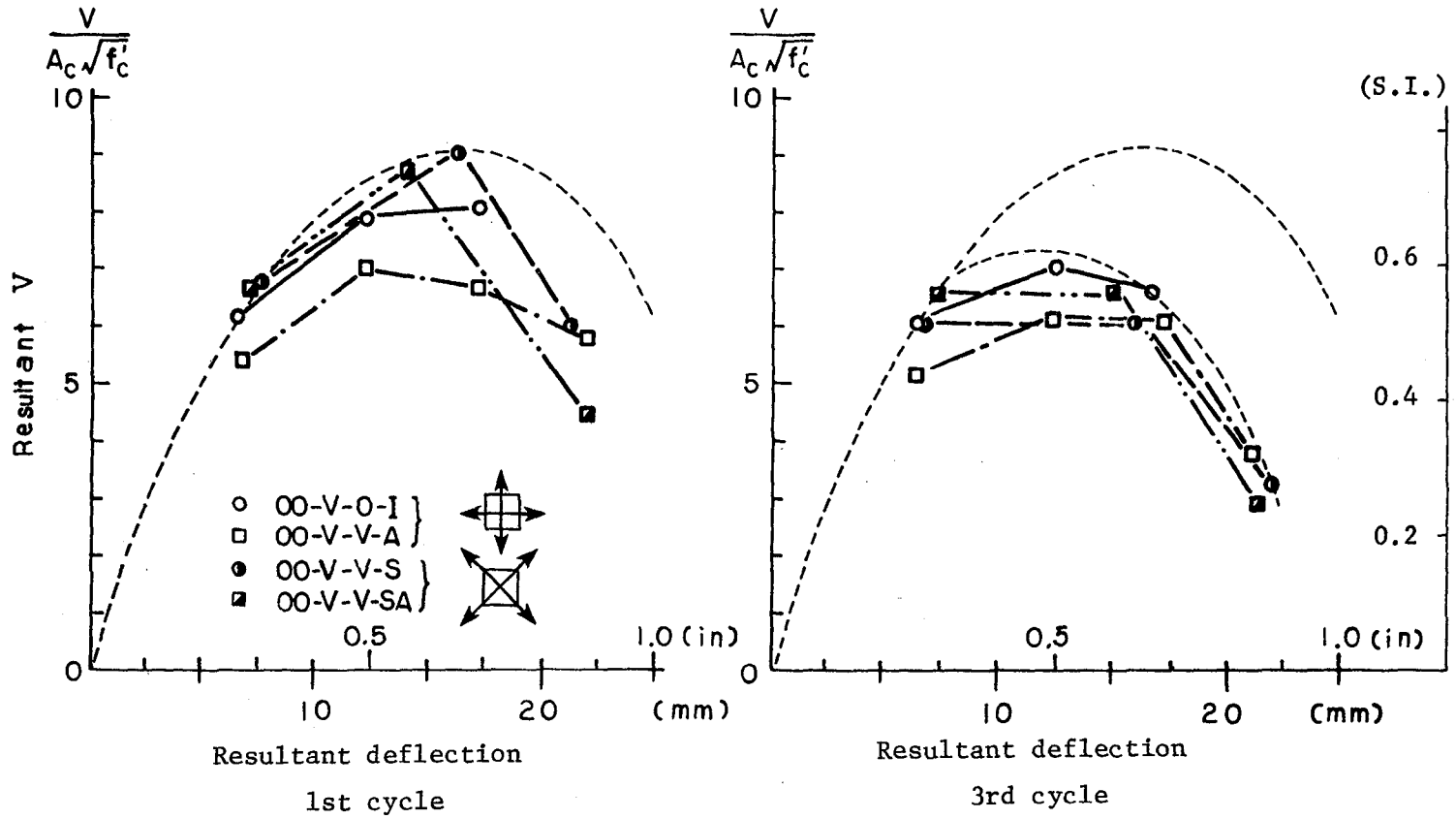

Fig. 5.11 Comparison of skewed loading with principal loading--resultants

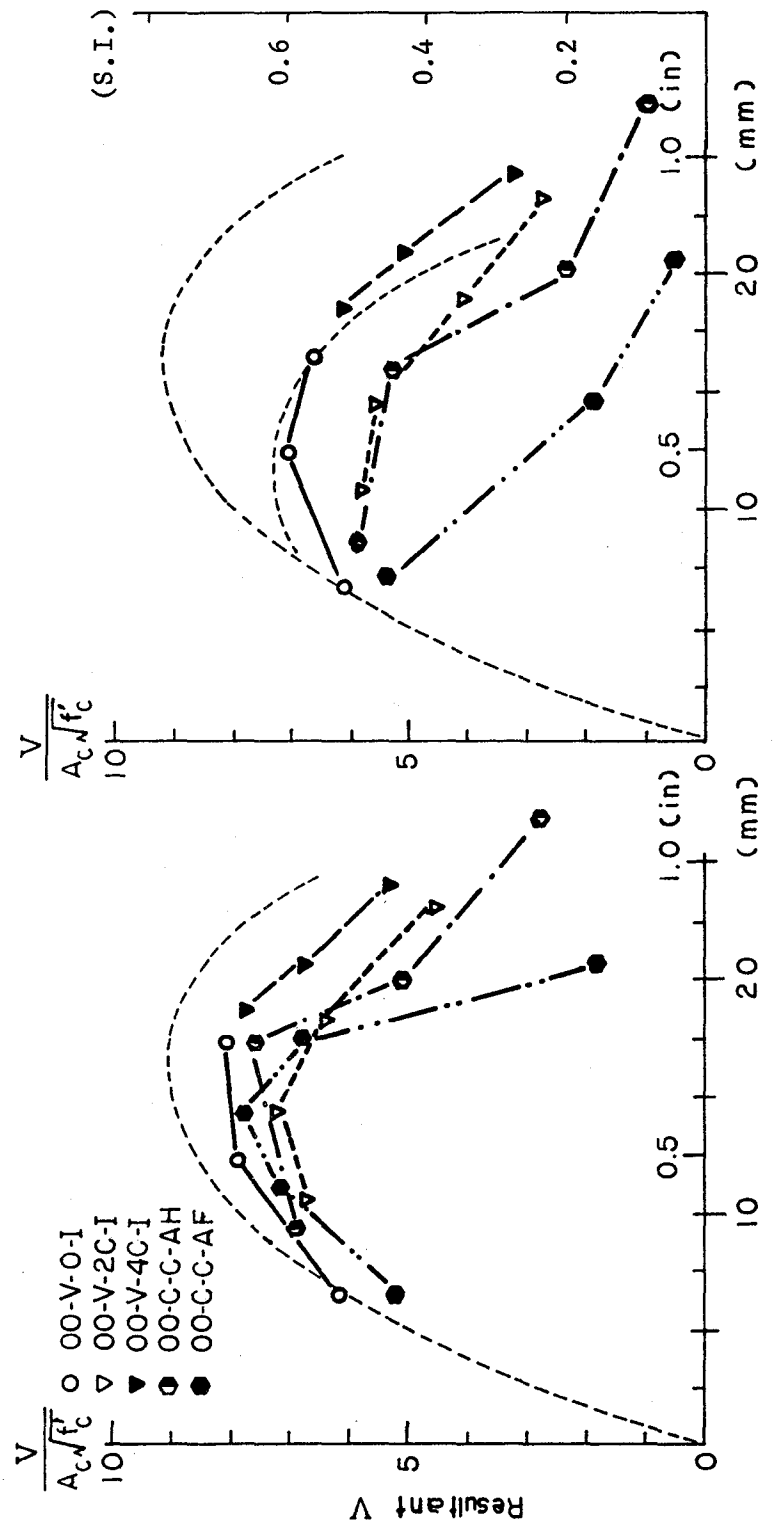

Fig. 5.12 Influence of load path--resultants

In order to see the general trend of shear strength due to different loading histories, all data except OO-V-4VP-I, which failed under cycling at $4\Delta_i$, are represented in Fig. 5.13. It seems that almost all results except the case of full square load path (OO-C-C-AF) show similar tendencies and the difference from the unilateral loading case is within about 40 percent at the ultimate stage.

5.3 Comments on Load-Deflection Curves under Different Load Paths

In the previous sections, the behavior of columns at peak deflection levels was discussed. The intermediate behavior between peaks is also of interest and will be discussed in this section.

Figure 5.14 shows an example of four different load paths and the load-deflection curves for the first cycle at the $2\Delta_i$ deflection level. Three of the paths (A, B, and C) have the same terminal deflections, point 1 (in the N-E quadrant) and point 2 (in the S-W quadrant). Path D has different terminal deflections (points 7 and 8) but the same peak deflections in the north and the south directions. Curve D is obtained from the case of unilateral loading. The load path A is a part of the loading history for OO-V-V-S. The load paths B and C are from the loading histories for OO-C-C-AF and OO-C-C-AH, respectively. The load-deflection curves are represented in the N-S direction.

In paths A and C, the peak load appears at point 2, but path B does not show the peak at that point. Although the peak load is similar in paths A and C, the load at zero deflection in the N-S direction is quite different in the two cases. The complicating factor in the load-deflection behavior is the constant deflection imposed in one direction while deformation is

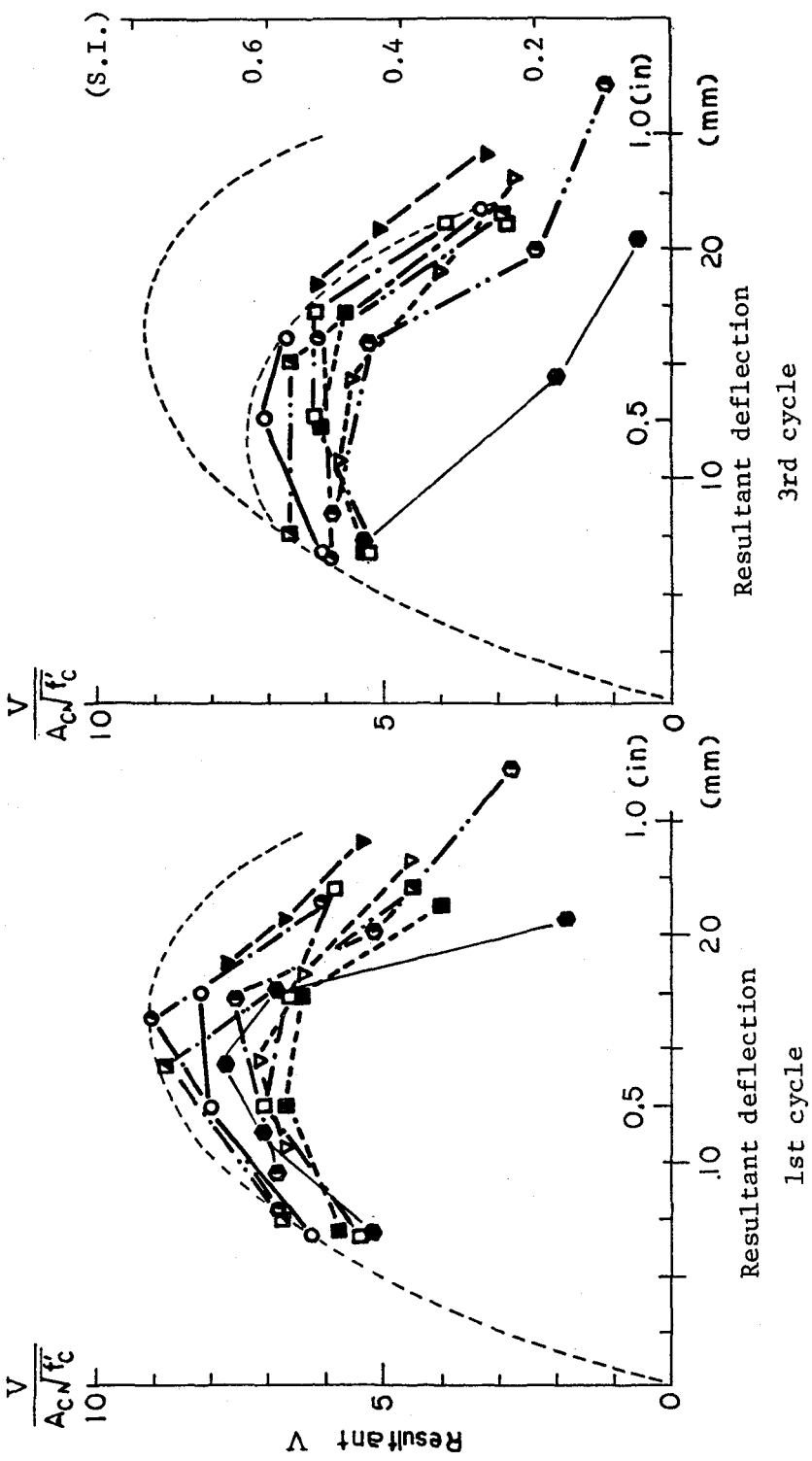

Fig. 5.13 Comparison in resultants

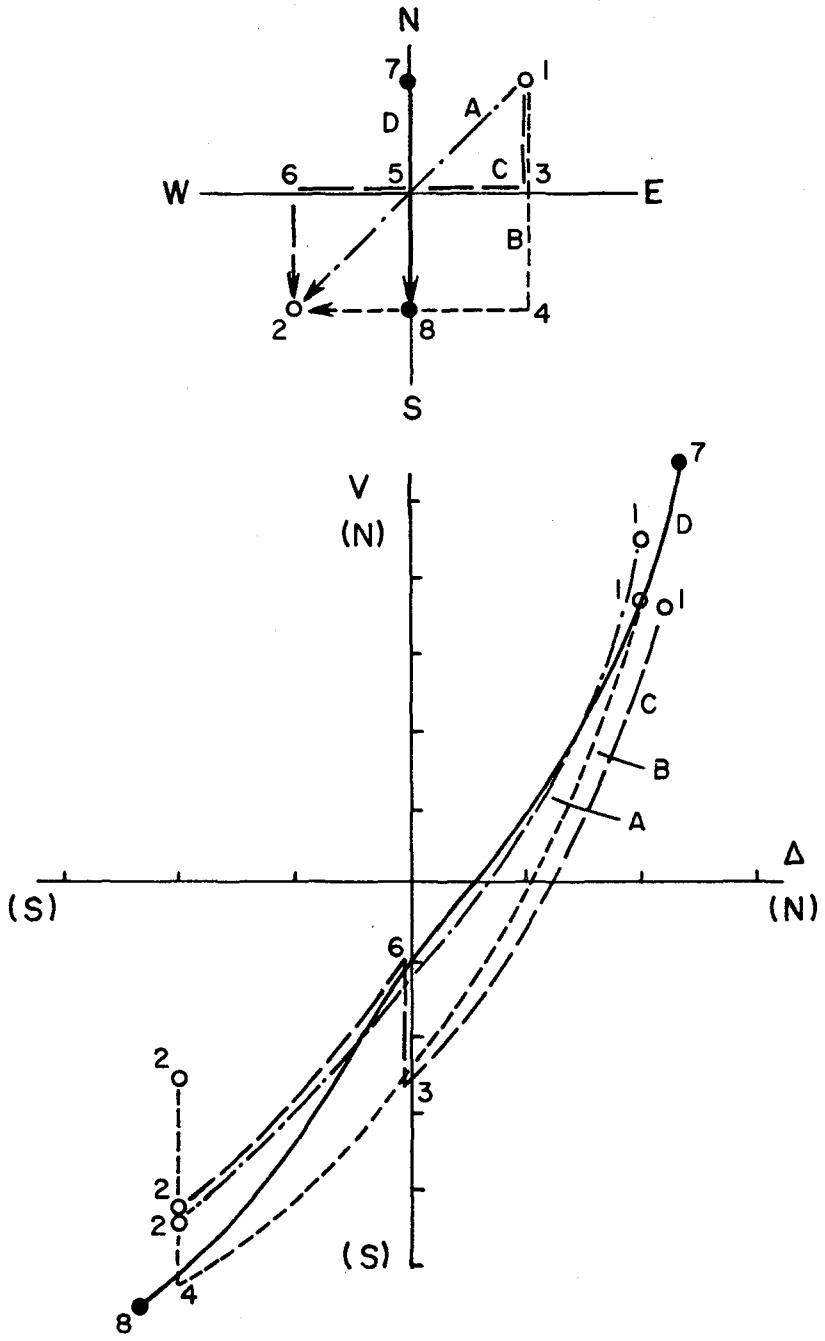

Fig. 5.14 Load path and load-deflection relationships

decreased or increased in the orthogonal direction. In the next stage the loading is switched in each direction. In other words, the decreasing or increasing load is imposed in the direction in which the constant deformation was applied previously, and the constant deflection is imposed in the direction in which the decreasing or increasing loading was applied.

However, when curves A, B, and C are compared with the case of unilateral loading (curve D), the shape of the curve from the peak in the north to that in the south is nearly the same in all four cases.

5.4 Summary

The test results were discussed with regard to the shear strength of reinforced concrete columns at peak deflection levels. The shape of the load-deflection curve as a function of load sequences and load paths was examined.

The influence of load sequence is very small at low deflection levels, but becomes significant when the deflection imposed exceeds the point at which the ultimate strength is achieved under monotonic loading.

The influence of load path on behavior along a principal axis (NS or EW direction) is large in some cases. However, when the resultant force and the resultant deflection are taken into account, the case of loading in diagonal directions can be resolved to the case of unilateral loading. The similarities are apparent when ultimate shear strength for each specimen is compared using the resultant force. Table 5.1 summarizes the test results on the basis of resultant ultimate shear and deflection at which ultimate is reached. The ultimate shear force in each test is 8 to 9 $\sqrt{f'_c}\ A_c$ at a resultant deflection of about 0.6 in. Only test 00-V-4VP-I did not fail in the range discussed, but it should be noted that the specimen had failed under previous loading.

TABLE 5.1 ULTIMATE SHEAR STRENGTH

Case	f'_c		V_u *		$\frac{V_u}{A_c\sqrt{f'_c}}$		Δ *	
	MPa	ksi	kN	kips	S.I.	U.S.	mm	in.
Monotonic	30	4.4	267	60	0.78	9.1	15	0.60
00-V-0-I Unilateral	35	5.8	258	58	0.71	8.2	18	0.69
00-V-2VP-I Previous $2\Delta_i$	30	4.4	249	56	0.73	8.5	18	0.70
00-V-4VP-I Previous $4\Delta_i$	30	4.4	84	19	0.25	2.9	16	0.64
00-V-V-A Alternate	42	6.0	240	54	0.60	7.0	13	0.50
00-V-V-S Diagonal	35	5.0	264	59	0.73	8.4	16	0.65
00-V-V-SA Alternate Diagonal	35	5.1	267	60	0.73	8.4	14	0.55
00-V-2C-I Constant $2\Delta_i$	39	5.5	247	56	0.65	7.6	14	0.57
00-V-4C-I Constant $4\Delta_i$	35	5.0	256	58	0.71	8.2	19	0.75
00-C-C-AF Square	37	5.3	255	57	0.68	7.9	14	0.57
00-C-C-AH Half Square	39	5.6	247	56	0.64	7.5	17	0.69

*All data are based on the resultant force and the resultant deflection.

The load-deflection curve differs from load path. But when the curve in each case is compared in the principal direction, the shape from the peak in one direction to the peak in the other direction is very similar.

CHAPTER 6

A CONCEPTUAL MODEL FOR SHEAR BEHAVIOR

6.1 Introduction

The behavior of reinforced concrete can be categorized broadly into two types according to the mode of failure, i.e., flexural failure and shear failure. Flexural behavior has been studied by many researchers and models have been developed for interpreting and understanding behavior of columns. Some models are successfully being extended into biaxial bending problems [8,9,12,13].

On the other hand, shear behavior is not so easily modeled because there are several factors which contribute to the shear strength of reinforced concrete members. The influence of each factor is not clearly understood at present. Several empirical formulae have been introduced for estimating ultimate shear strength [14,15]. However, in the range of inelastic load reversals, shear behavior has not been studied extensively and models have not been developed even for the case of unilateral loading.

The most difficult part in modeling shear behavior is to define a basic relationship between force and deflection analogous to the moment curvature relationship in bending analysis.

6.2 General Concept

In the range of inelastic load reversals of short columns, the bending effects on deflection may be relatively

small because of large shear cracks. The main factor in determining shear strength and deformation may be the shear cracks. The problem is to establish when and how the cracks initiate and propagate in the member.

To describe the cracking phenomena, a damage ratio is introduced which represents the magnitude or extent of shear cracking, as shown in Fig. 6.1. Figure 6.1 shows the degree of damage corresponding to varying levels of shear deformation under monotonic loading.

The basic premise in developing a model is that the shear force versus deflection relationship and the damage ratio versus deflection relationship can be defined for monotonic loading. When a deflection Δ_o is imposed on the specimen, the corresponding shear strength V_o and the corresponding damage ratio D_r can be defined as shown in Fig. 6.2. To use the damage ratio in estimating shear strength deterioration, two assumptions are introduced. The first is that D_r increases with cycles of load, even though the peak shear deformation does not increase. After several cycles of load, D_r increases as shown in Fig. 6.2 from $D_{r,o}$ to $D_{r,n}$. Under monotonic loading, the same $D_{r,n}$ would be reached when deflection is increased to Δ_n.

The second assumption introduced is that the ratio of Δ_o to Δ_n is related to the ratio of shear strength at Δ_o to Δ_n (V_n/V_o). When applied deflection is Δ_n or greater than Δ_n, the monotonic strength corresponding to the deflection can be obtained. In this model the damaged part is treated as sand. Therefore, in this case the "sand" in the damaged portion can be considered tightly packed and monolithic. When the applied deflection is less than Δ_n, the crushed part may be only partly compacted and a strength reduction results.

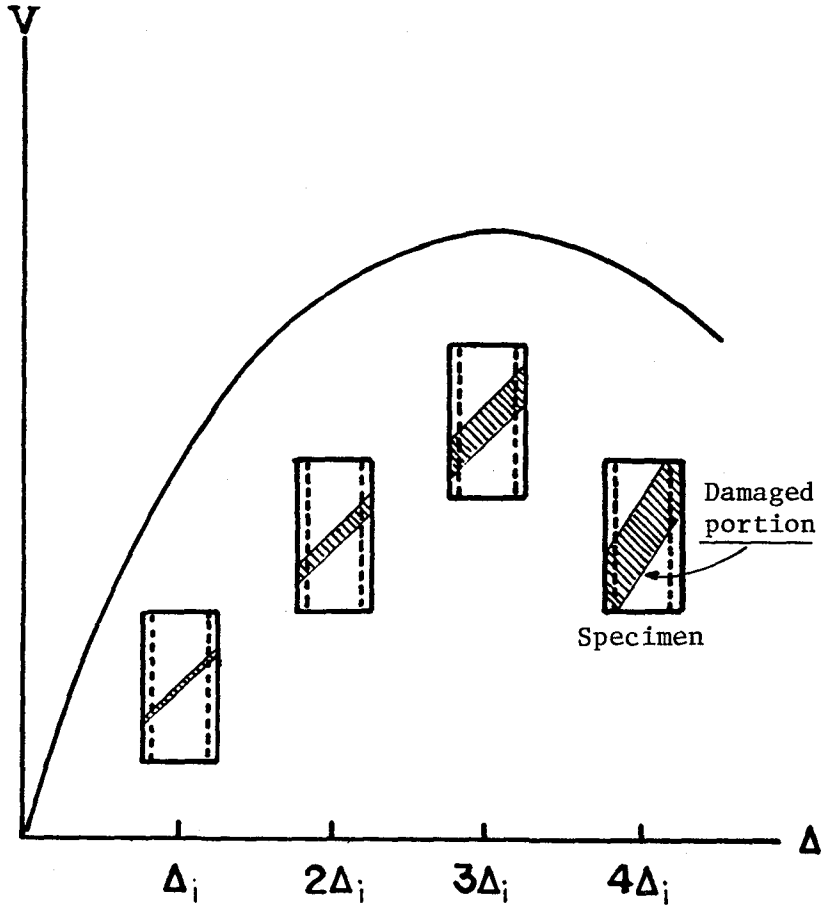

The damaged region is represented by the term D_r (damage ratio) and is a function of deflection. As an analogy, the damaged region can be considered to consist of sand particles.

Fig. 6.1 Analogy for progression of damage

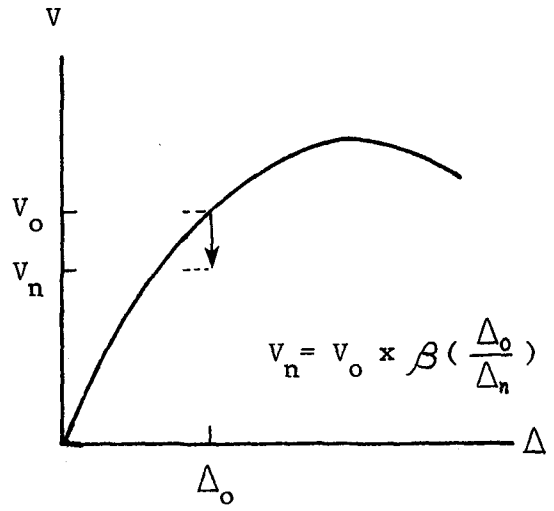

a) V-Δ relationship

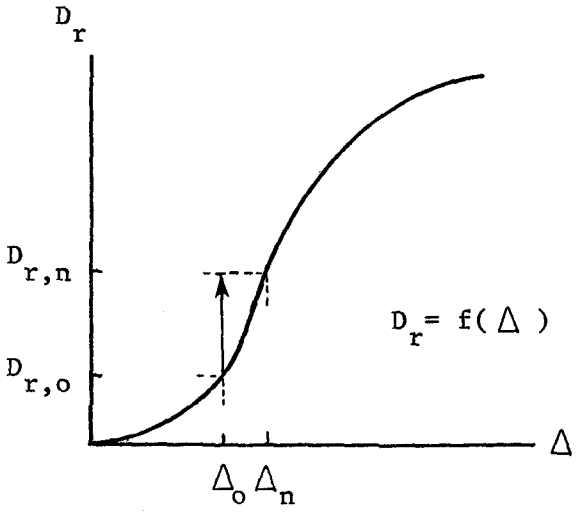

b) D-Δ relationship

Fig. 6.2 V-Δ , D_r-Δ relationships

The shear strength reduction is defined as

$$V_n = V_o \times \beta \left(\frac{\Delta_o}{\Delta_n}\right)$$

where

V_o = Monotonic shear strength corresponding to deflection Δ_o

β = Correlation function between Δ_o/Δ_n and V_n/V_o

The definition of D_r and β are discussed in the following sections.

6.3 Development of D_r and β in Conceptual Model

Although the general concept is quite simple, the details are complex because the influence of load repetition, orthogonal loading and simultaneous loading in two directions is included in the model. The model was developed in the following manner.

(1) Load-deflection relationship under monotonic loading

This relationship is defined by the monotonic loading test such as shown in Fig. 6.2a. The relationship between the applied shear force and the top displacement is considered to be the same in reinforced concrete columns with the same dimensions and cross-sectional properties.

(2) Damage ratio-deflection relationship under monotonic loading

When the deflection is very small, elastic behavior is predominant and the damage ratio D_r is small. At a certain point,

D_r becomes large with small increments of deflection. The critical deflection corresponds with the initiation and propagation of hairline cracks. In the final stages, the widening of large shear cracks results in a small change in the damage ratio.

It is assumed that at each deflection level, only one value of D_r exists. Therefore, under monotonic loading D_r can be defined given the deflection or if D_r is given, the corresponding deflection under monotonic loading can be obtained. A curve reflecting these relationships is shown in Fig. 6.2b.

(3) Influence of cycles of load on D_r

From low cycle fatigue behavior, the increase of D_r with the number of load reversals can be expressed as follows:

$$D_{r,n} = D_{r,o} \times \left(\sum_{1}^{n} \alpha_i \right)$$

where

α_i = Increment of damage occurring during i-th cycle of load

$D_{r,o}$ = Damage ratio under monotonic loading at a given deflection Δ_o

n = Number of cycles

$D_{r,n}$ = Damage ratio at n-th cycle of load

The damage increment α can be expressed as a function of the number of cycles, as shown in Fig. 6.3.

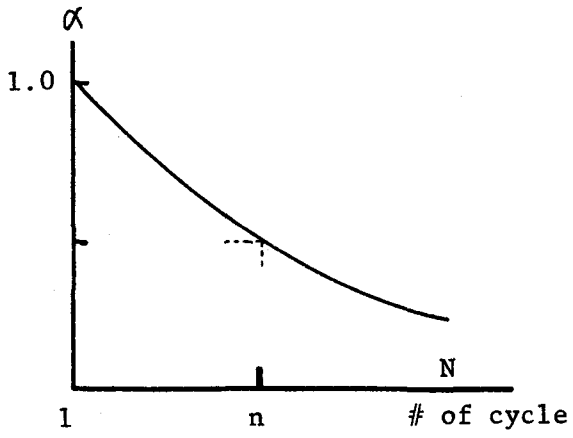

Fig. 6.3 α - N relationship

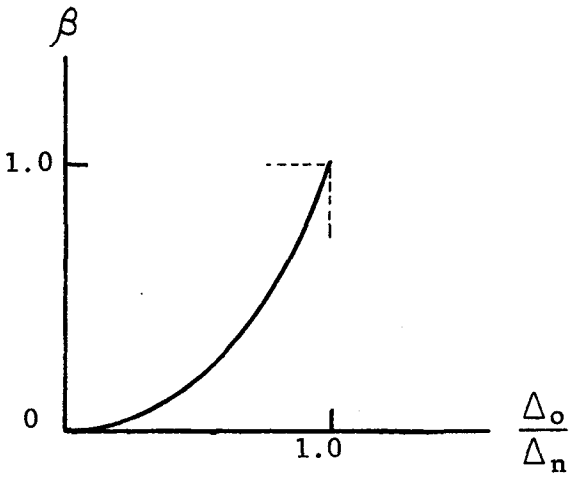

Fig. 6.4 Shear strength reduction versus deflection ratio

(4) Reduction of peak shear strength

As stated in (3), D_r increases with cycles of load. Consequently, the deflection needed to produce the same damage ratio ($D_{r,n}$) under monotonic loading increases to Δ_n, as shown in Fig. 6.2. However, the applied peak deflection stays the same in each cycle. Therefore, the shear strength at the peak deflection should be reduced with each cycle. A function β is introduced to represent this effect.

$$\beta = \beta\ (\Delta_o/\Delta_n)$$

where

Δ_o = Peak applied deflection

Δ_n = Deflection which corresponds to $D_{r,n}$ under monotonic loading

Once a function β is defined, the peak shear strength at n-th cycle can be obtained.

$$V_n = V_o \cdot \beta$$

where

V_o = Monotonic shear strength at Δ_o deflection level

V_n = n-th cycle peak shear strength

The function β has the following characteristics: $\beta = 1.0$ when Δ_o/Δ_n is 1.0. As Δ_o/Δ_n is increasing to 1.0 from zero, β approaches 1.0 rapidly. Figure 6.4 shows the relationship between β and Δ_o/Δ_n.

(5) Influence of damage ratio on behavior in orthogonal direction

It is assumed that D_r has directional properties. When the applied load is small, cracks due to that load may not affect the strength of the column in the orthogonal direction. At this level D_r is independent of direction of loading. But once large cracks develop, D_r^X, damage from loading in the X direction begins to influence the response in the Y direction. In other words, loading in the X direction produces a component of the damage ratio in the Y direction, D_r^Y.

This can be expressed as follows:

$$D_r^Y = \phi \cdot D_r^X$$

where

D_r^X = Damage ratio in the X direction.

D_r^Y = Damage ratio in the Y direction.

ϕ = Orthogonality function which defines the influence of loading in an orthogonal direction D_r.

A possible relationship for ϕ and D_r is shown in Fig. 6.5.

In the next step the combination of loadings in both directions should be taken into account. Because when a relatively small load is applied in the Y direction after a large

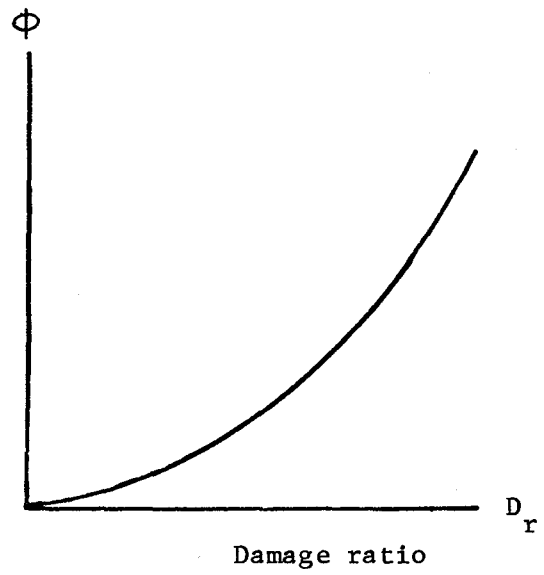

Fig. 6.5 Φ - D_r relationship

load imposed in the X direction, the damage ratio which controls behavior in the Y direction is due to the loading in the X direction, not the loading in the Y direction. On the contrary, if the load in the Y direction is much larger than that in the X direction, the influence of the loading in the X direction on behavior in the Y direction is very small. In addition, in the case that the load in the Y direction is similar in magnitude to that in the X direction, there is some mutual influence on damage ratio.

These relationships can be summarized as follows:

[Case I] Load in the Y direction is much smaller than that in the X direction. ($\Delta_o^Y \ll \Delta_o^X$)

$$\begin{cases} D_{r,n}^X = D_{r,o}^X \cdot \left(\sum_1^n \alpha_i \right) \\ D_r^Y = \phi \cdot D_{r,n}^X \quad \text{and} \quad D_{r,n}^Y = D_r^Y \cdot \left(\sum_1^n \alpha_i \right) \end{cases}$$

where

$D_{r,o}^X$ = Damage ratio under monotonic loading at a given deflection (Δ_o^X) imposed in the X direction

$D_{r,n}^X$ = Damage ratio at n-th cycle of load in the X direction.

[Case II] Load in the Y direction is much larger than that in the X direction. ($\Delta_o^Y \gg \Delta_o^X$)

$$\begin{cases} D^X_{r,n} = D^X_{r,o} \cdot \left(\sum_1^n \alpha_i \right) \\ D^Y_r = D^Y_{r,o} \quad \text{and} \quad D^Y_{r,n} = D^Y_r \cdot \left(\sum_1^n \alpha_i \right) \end{cases}$$

No influence of previous loading in the X direction.

[Case III] Magnitude of load in both directions is similar. ($\Delta^Y_o \simeq \Delta^X_o$)

$$D^X_{r,n} = (1+\psi) \cdot D^X_{r,o} \cdot \left(\sum_1^n \alpha_i \right)$$

$$D^Y_{r,n} = (1+\psi) \cdot D^Y_{r,o} \cdot \left(\sum_1^n \alpha_i \right)$$

where

ψ = Interaction function

(6) Shear strength between deflection peaks

In order to define the shear strength between deflection peaks, a sand spring analogy is proposed, as shown in Fig. 6.6. The sand represents crushed concrete and the spring represents the influence of longitudinal reinforcement in a cracked reinforced concrete column on stiffness, as shown in Fig. 6.7. In Fig. 6.6, the rigid body represents the uncracked part of concrete. As concrete is cracked with loading, that rigid body becomes smaller.

When the piston is initially compressed, large deformations occur because the loose compacted sand is being compacted. At the same time the spring is also compressed. However, once

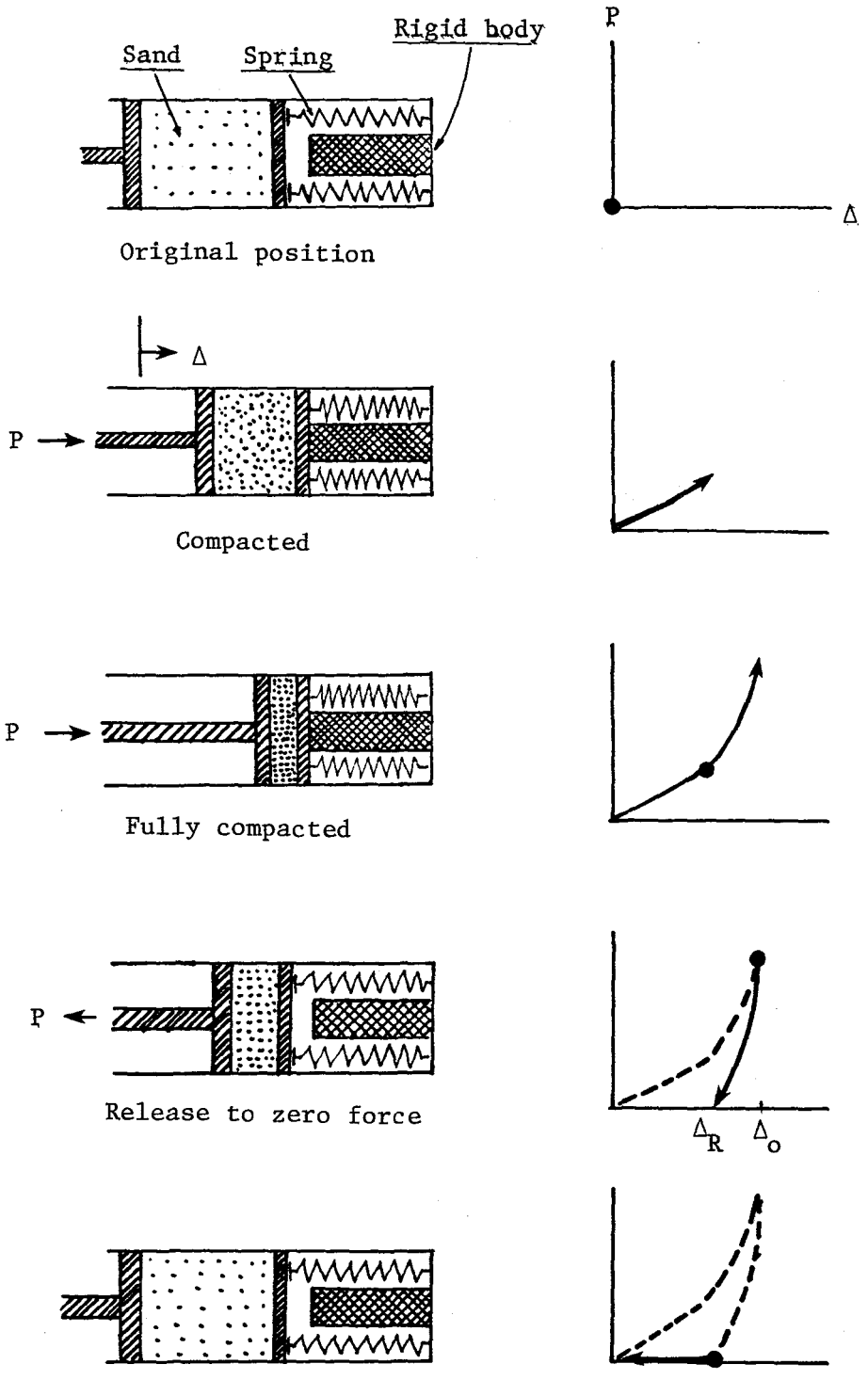

Fig. 6.6 Sand spring model for Group I

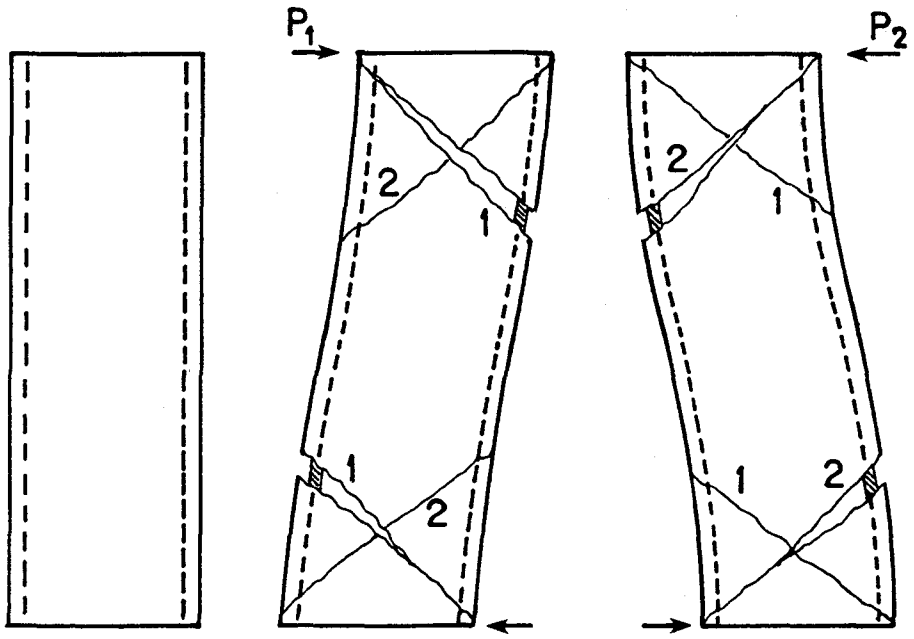

Under load P_1 , #1 cracks tend to open and #2 cracks tend to close.
Under load reversal P_2 , #1 cracks tend to close and #2 cracks tend to open.

Fig. 6.7 Actual movement of cracked section

the spring reaches its deformation limit which depends on the rigid body, a large force is developed and the sand is compacted tightly. On the other hand, when the piston is extended, the force drops suddenly because the large force which compacted the sand is released with only small deformation required and a large residual deformation is produced.

In the test specimen under load reversals, such a phenomenon can be considered to occur in both sides, as shown in Fig. 6.7. The cracks labeled 1 open under load P_1, but the #2 cracks close and transfer the force to the concrete. Under load P_2 the #1 cracks close and transfer the force. This is modeled in Fig. 6.8.

Using this model, the shear strength between deflection peaks can be defined.

$$V = S(\Delta, \Delta_o, \Delta_R, V_n)$$

where

S = Shape function as shown in Fig. 6.8

Δ = Deflection imposed

Δ_o = Peak deflection

Δ_R = Residual deformation

V_n = n-th peak shear strength

The residual deformation is considered to depend on the amount of crushed concrete; in other words, the damage ratio D_r. Since D_r is a function of the peak deflection level, it may be possible to express Δ_R as a function of Δ_o.

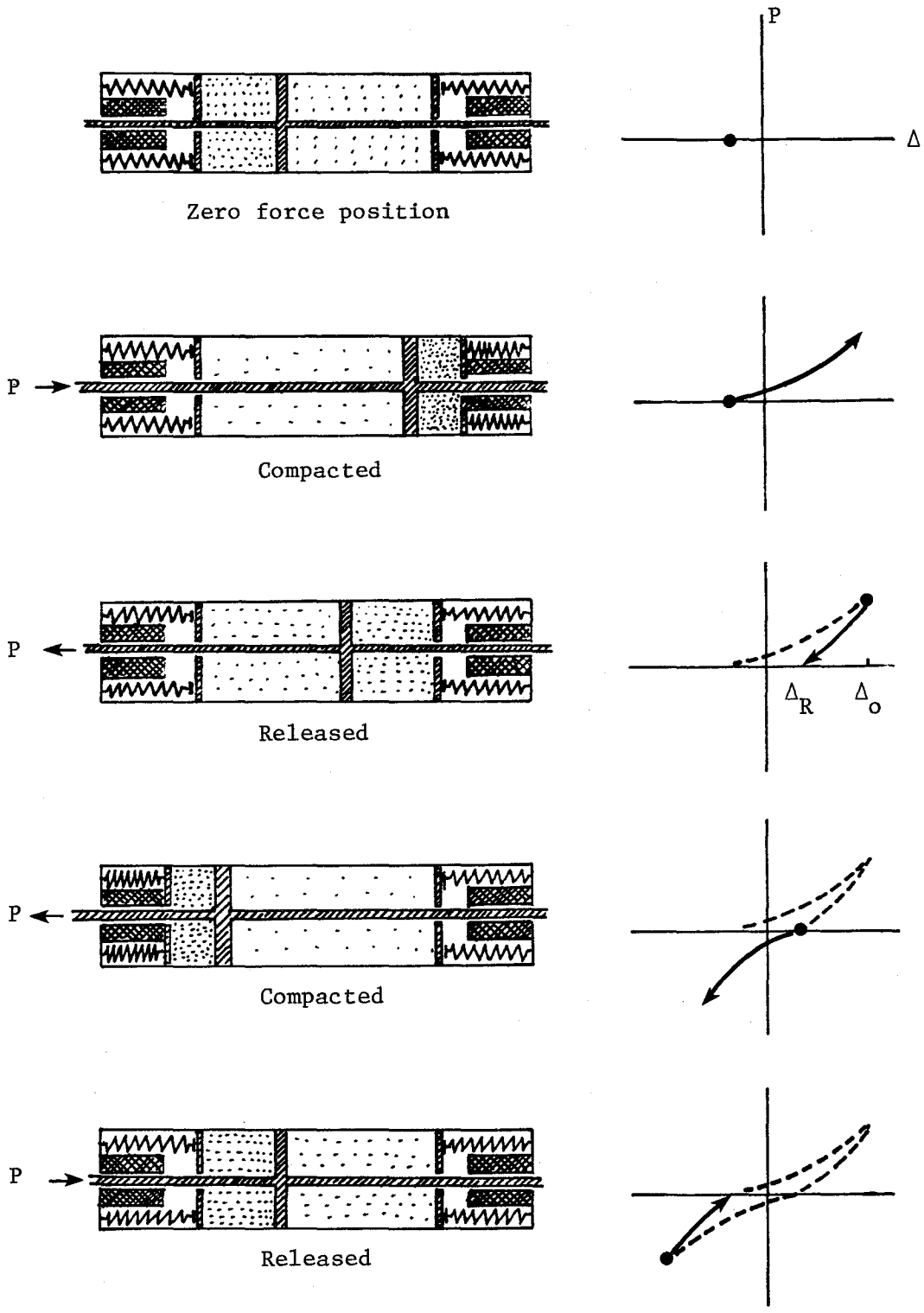

Fig. 6.8 Sand spring model for Group I--both sides

$$\Delta_R = g(\Delta_o)$$

where

g = Correlation function

It should be noted that the first cycle of load to a higher deflection level is the same as the previous cycle to the previous peak deflection. The shape of the curve between the previous peak deflection and the new peak deflection can be a straight line or a parabolic line. Obviously, the first cycle up to the first deflection level follows the monotonic loading curve.

With the relationships presented, the shear behavior of reinforced concrete short columns can be modeled. Based on these considerations the computation process is shown in Fig. 6.9.

The formulation for each relationship or function needed to define the response is discussed in the next section.

6.4 Details of Conceptual Model

In the previous section the general procedure was discussed. It is necessary to formulate each relationship or function for solving specific problems. The following discussion represents the formulation procedure for this experimental study.

In this section Group I, which is defined in 5.2, is treated. There are six cases in Group I such as 00-V-0-I, 00-V-2VP-I, 00-V-4VP-I, 00-V-V-A, 00-V-V-S and 00-V-V-SA. Load reversals were applied along a line in each case.

For Group II, constant deflection cases (00-V-2C-I and 00-V-4C-I) and square or half square load path, additional considerations are required because the direction of the resultant force varies during loading. Group II is discussed in Sec. 6.6.

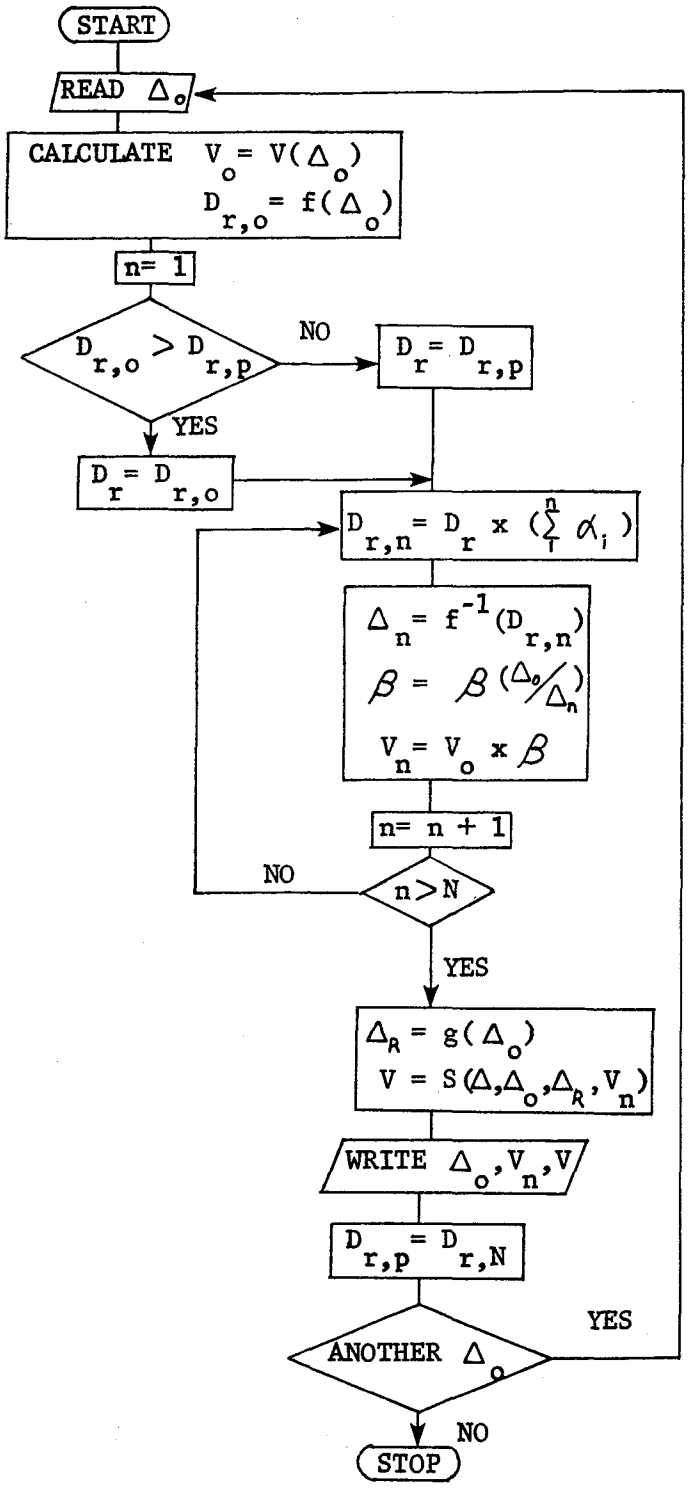

Δ_o ; Deflection level

V_o ; Monotonic shear strength

$D_{r,o}$; Damage ratio under monotonic loading

n ; Number of cycle

$D_{r,p}$; Damage ratio due to previous load

$D_{r,n}$; Damage ratio at n-th cycle

V_n ; Shear strength at n-th peak deflection

N ; Number of last cycle

Δ_R ; Residual deformation

V ; Intermediate strength

$D_{r,N}$; Damage ratio at last cycle

Fig. 6.9 Flow chart of computation process

(1) Load-deflection relationship under monotonic loading, $V = V(\Delta)$

This case is very easy to formulate because it can be obtained directly from test results under monotonic loading. The numerical equations used are as follows:

$0 \leq \Delta \leq 0.6$ in.

$$V = 200\,\Delta - 170\,\Delta^2$$

$0.6 < \Delta$

$$V = 84 - 40\,\Delta$$

where

Δ = Deflection (in.)

V = Shear strength (kips)

(2) Damage ratio-deflection relationship under monotonic loading, $D_r = f(\Delta)$

This is the most difficult curve to define, because it influences the formulation of other functions. The test results from unilateral loading OO-V-O-I were used to determine the shape of the curve by a trial and error procedure. The general shape should be the "S" type, as shown in Fig. 6.2, because of the aspects of the damage ratio discussed in the previous section.

The rate of change of D_r with Δ is very significant, because it defines the n-th cycle deflection Δ_n, which corresponds to D_r at the n-th cycle ($D_{r,n}$).

For the first trial, $D_r = 1.0$ at $\Delta_o = 1.0$ was assumed and two parabolic curves were combined to obtain the shape of the curve. After comparing the computed results with the test

results, the curve was defined. After a number of trials, the final shape was defined as

$$0 \leq \Delta \leq 0.35 \text{ in.}$$

$$D_r = 3\,\Delta^2$$

$$0.35 < \Delta \leq 0.90 \text{ in.}$$

$$D_r = -0.7 + 4.05\,\Delta - 3.15\,\Delta^2 + 0.75\,\Delta^3$$

$$0.90 < \Delta$$

$$D_r = 0.76 + 0.2\,\Delta$$

where

Δ = Deflection (in.)

D_r = Damage ratio

From the test results, the significant change in D_r occurs for deflections from 0.3 in. to 0.9 in. As stated before, the peak shear strength at each cycle is computed by the $D_r - \Delta$ curve in combination with the function β. The formulation of β influences the $D_r - \Delta$ curve. In this formulation D_r is very sensitive in the deflection range where Δ varies from 0.35 to 0.90 in.

(3) Influence of cycles of load on D_r,

$$D_{r,n} = D_{r,o} \cdot \left(\sum_{1}^{n} \alpha_i\right)$$

The damage ratio increases with cycles of load. The increment of D_r at each cycle is expressed using the function α, which represents the ratio of change in D_r between cycles. Therefore, at the n-th cycle the damage ratio can be expressed as

$$D_{r,n} = D_r \cdot \left(\sum_{1}^{n} \alpha_i\right)$$

Although α is not necessarily a continuous function, an exponential equation is used often to express low cycle fatigue behavior.

A trial and error procedure was also applied for defining α by comparing computed results with the test results from 00-V-0-I.

$$n = 1 \qquad \alpha = 1$$

$$n > 1 \qquad \alpha = e^{-1.40(n-1)} - e^{-1.48(n-1)}$$

When n is greater than 1, α is very small. For example, $\alpha = 0.018$ at $n = 2$ and $\alpha = 0.009$ at $n = 3$. However, the influence of α on strength reduction becomes significant in combination with the damage ratio and the function β. Even though the absolute change in the damage ratio is very small, its influence on strength reduction is not necessarily small, because the percentage change may be significant.

(4) Reduction of peak shear strength, $\beta = \beta(\Delta_o/\Delta_n)$

This function provides a direct relationship between the deflection ratio Δ_o/Δ_n and the shear strength reduction. From the previous section, Δ_o/Δ_n is defined in the following manner.

$$\Delta_n = f^{-1}(D_{r,n})$$

where

f = function which defines the $D_r - \Delta$ curve

$D_r = f(\Delta)$

$$\frac{\Delta_o}{\Delta_n} = \frac{\Delta_o}{f^{-1}(D_{r,n})}$$

The n-th peak shear strength is defined as

$$V_n = V_o \cdot \beta$$

where

V_o = Monotonic shear strength which corresponds to Δ_o

At the limit, $\beta = 1.0$ with $\Delta_o/\Delta_n = 1.0$ because $\Delta_n = \Delta_o$ represents monotonic loading with damage having occurred. At this stage the increment of D_r is zero ($\delta D_r = 0$) and corresponds to elastic behavior of columns.

From the sand spring model shown in Fig. 8.6, it is expected that β will decrease rapidly with decrease of Δ_o/Δ_n. As the first trial, $\beta = (\Delta_o/\Delta_n)^4$ was used with good results.

$$\beta = (\Delta_o/\Delta_n)^4 \quad \text{for} \quad \Delta_o/\Delta_n \leq 1.0$$

$$\beta = 1.0 \quad \text{for} \quad \Delta_o/\Delta_n > 1.0$$

It should be remembered that $\beta = 1.0$ represents the monotonic strength.

(5) Influence of damage ratio on behavior in orthogonal direction, ϕ, ψ

In order to determine the orthogonality function ϕ, two test cases of previous loading, 00-V-2VP-I and 00-V-4VP-I were examined. In the case of 00-V-4VP-I, large deflections were first imposed in one direction, and after that small deflections were imposed in the orthogonal direction. The results from this case give a good estimate of ϕ for a first trial.

Initially the assumption that $\phi = 1.0$ at $D_r = 1.0$ was used because the deflection which corresponds to a damage ratio $D_r = 1.0$ produces failure. A parabolic curve was developed and refined.

$$\phi = 1.05\, D_r^2 - 0.07\, D_r$$

The interaction function ψ was determined using the test results from the case of alternate loading (00-V-V-A). When the damage ratio D_r is small, the response in each direction is independent of the other direction and $\psi = 0$.

After several trial and error calculations, the following value was found to adequately express the interaction function.

$$\psi = 0 \quad \text{for} \quad D_r < 0.5$$

$$\psi = 0.02 \quad \text{for} \quad D_r \geq 0.5$$

(6) Shear strength between deflection peaks, $S(\Delta, \Delta_o, \Delta_R, V_n)$

According to the observation of the load-deflection curves, residual deformation is almost constant in each cycle at a given deflection level. Moreoever, the amount of the residual deformation at a given deflection level seems to be quite similar in all test cases.

From these results, it was assumed that the residual deformation depends on the peak deflection level. The case of 00-V-0-I was examined and the following equation was derived (see Fig. 6.10).

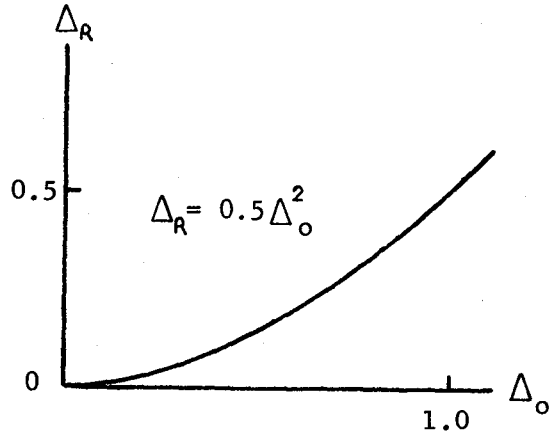

Fig. 6.10 Residual deformation versus peak deflection

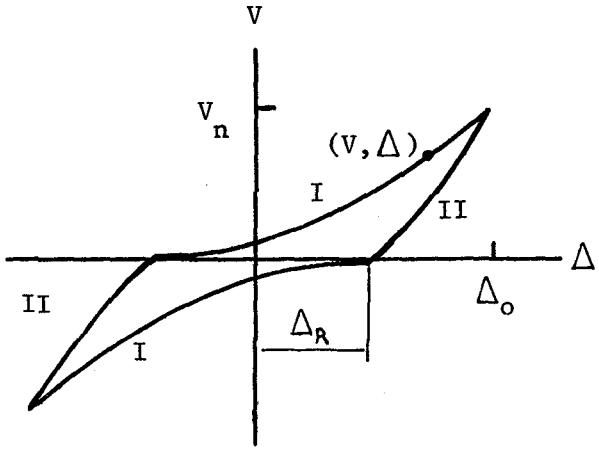

$$\text{CURVE I ;} \quad \frac{V}{V_n} = 0.53 \times \left(\frac{\Delta + \Delta_R}{\Delta_o + \Delta_R} + 0.5 \right)^2 - 0.13$$

$$\text{CURVE II ;} \quad \frac{V}{V_n} = 0.15 \times \left(\frac{\Delta + \Delta_R}{\Delta_o + \Delta_R} + 2.5 \right)^2 - 0.94$$

Fig. 6.11 Shape function

$$\Delta_R = 0.5\,\Delta_o^2$$

where Δ_R = Residual deformation (in.)

Δ_o = Peak deflection (in.)

In order to apply the same shape function for any case, the shape function was normalized with respect to Δ, Δ_o, Δ_R, and V_n. As a typical load-deflection curve, the curve for the second cycle to the $2\Delta_i$ level (from 00-V-0-I) was selected and normalized as shown in Fig. 6.11.

Curve I

$$S = V_n \times \left[-0.13 + 0.53 \times \left[\frac{\Delta + \Delta_R}{\Delta_o + \Delta_R} + 0.5\right]^2\right]$$

Curve II

$$S = V_n \times \left[-0.94 + 0.15 \times \left[\frac{\Delta + \Delta_R}{\Delta_o + \Delta_R} + 2.5\right]^2\right]$$

(7) Adjustment for simultaneous loadings

The case of loading in diagonal directions is treated with resultant forces and deflections. However, test results show that the resultant shear strength is a little less than the shear strength under principal loadings such as 00-V-0-I and 00-V-V-A. This difference is very small and it may be neglected. But it can be considered that the difference comes from the simultaneous loadings in both principal directions. The direction of the resultant force in simultaneous loadings is diagonal. In this case the effect of transverse reinforcement on shear

strength may not be the same as that in the principal loading.

Although the effect of difference in loading direction is very small, it is possible to treat that in the computer program very easily, as follows:

$$D_r = \gamma \cdot D_r$$

where D_r = Damage ratio

γ = Coefficient for simultaneous loadings ($r \geq 1.0$)

For the cases of 00-V-V-S and 00-V-V-SA, $\gamma = 1.015$ was used and provided good correlation with test results. In fact, the difference between the results due to D_r and $\gamma \cdot D_r$ is less than 10 percent.

6.5 Comparison of Computed and Test Results: Group I

The specimens in Group I were defined in Sec. 5.2. The computed results are plotted in Figs. 6.12 to 6.19. The main parameters for the model were determined from the test results of the specimen under unilateral loading (00-V-0-I). In Fig. 6.12, the case of unilateral loading is shown. In that figure the solid lines stand for test results and the symbols for computed results. In each cycle, at each deflection level, the computed results represent the test results very well as would be expected. Good correlation between computed results and test results was also obtained for the cases of previous loading (00-V-2VP-I and 00-V-4VP-I, Figs. 6.13 and 6.14) and the case of alternate loading (00-V-V-A, Figs. 6.15 and 6.16).

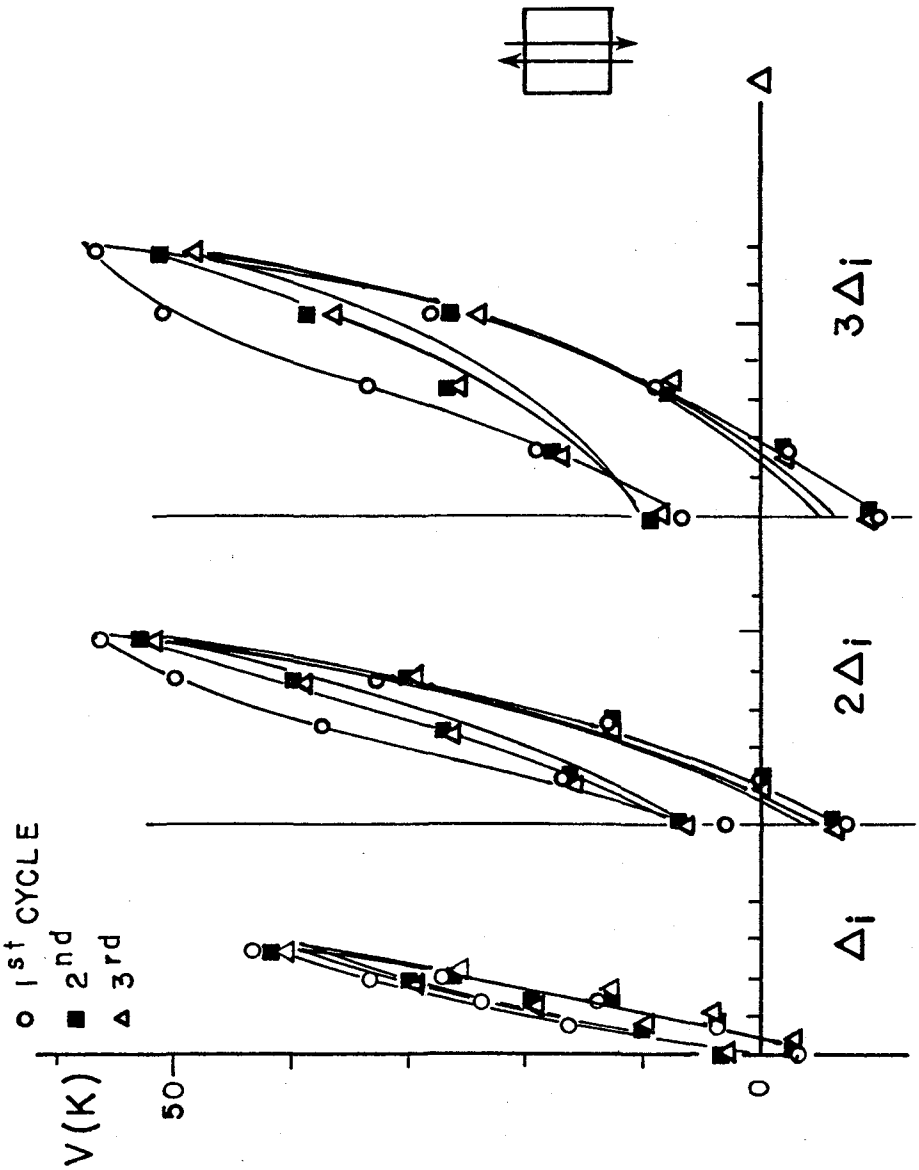

Fig. 6.12 Comparison of computed results with test results--00-V-0-I

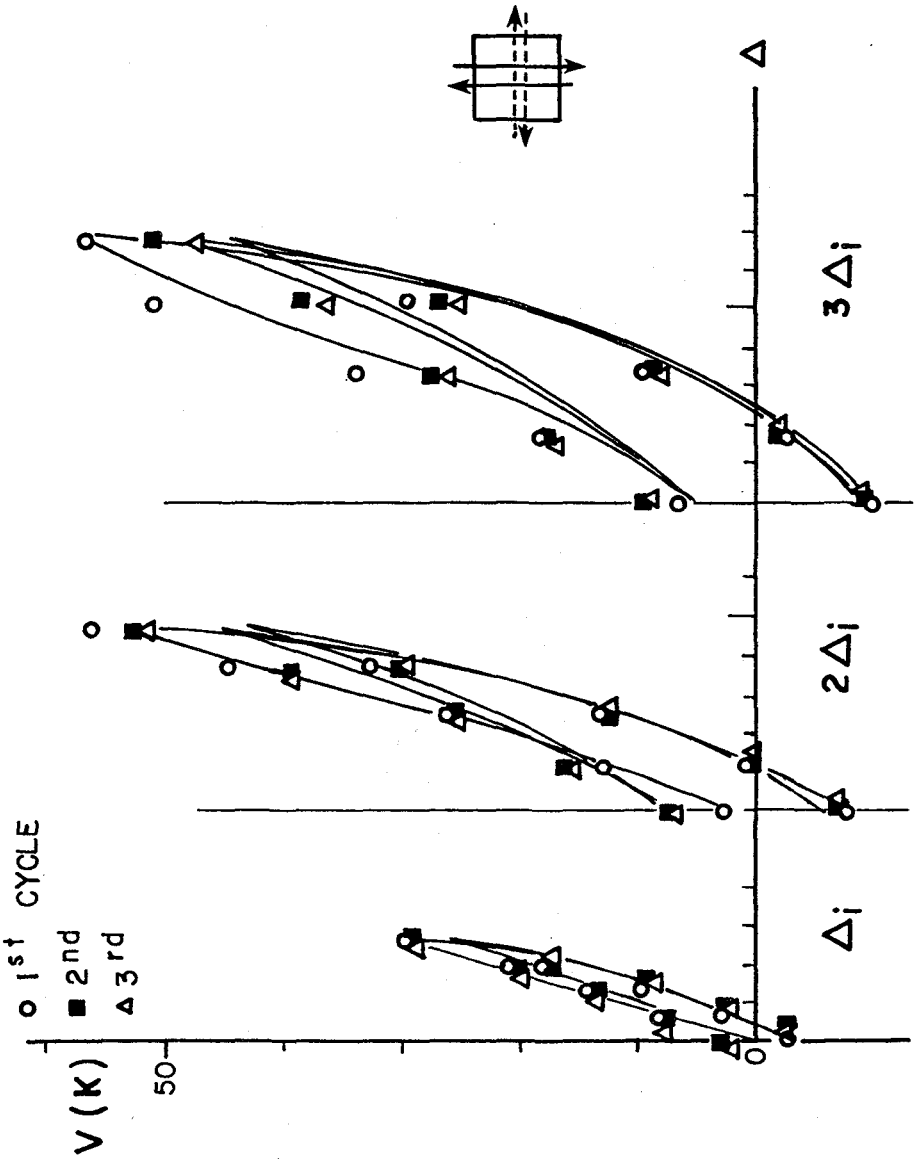

Fig. 6.13 Comparison of computed results with test results--00-V-2VP-I

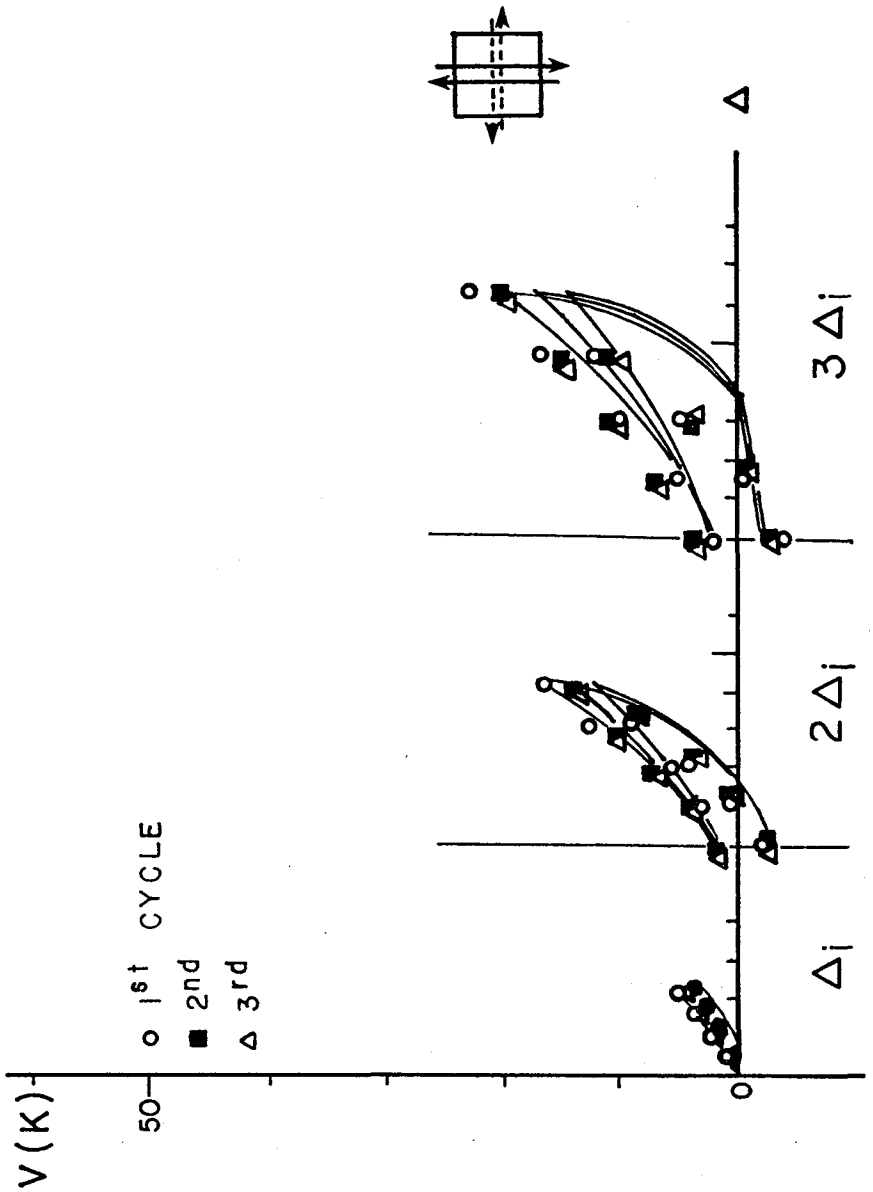

Fig. 6.14 Comparison of computed results with test results--00-V-4VP-I

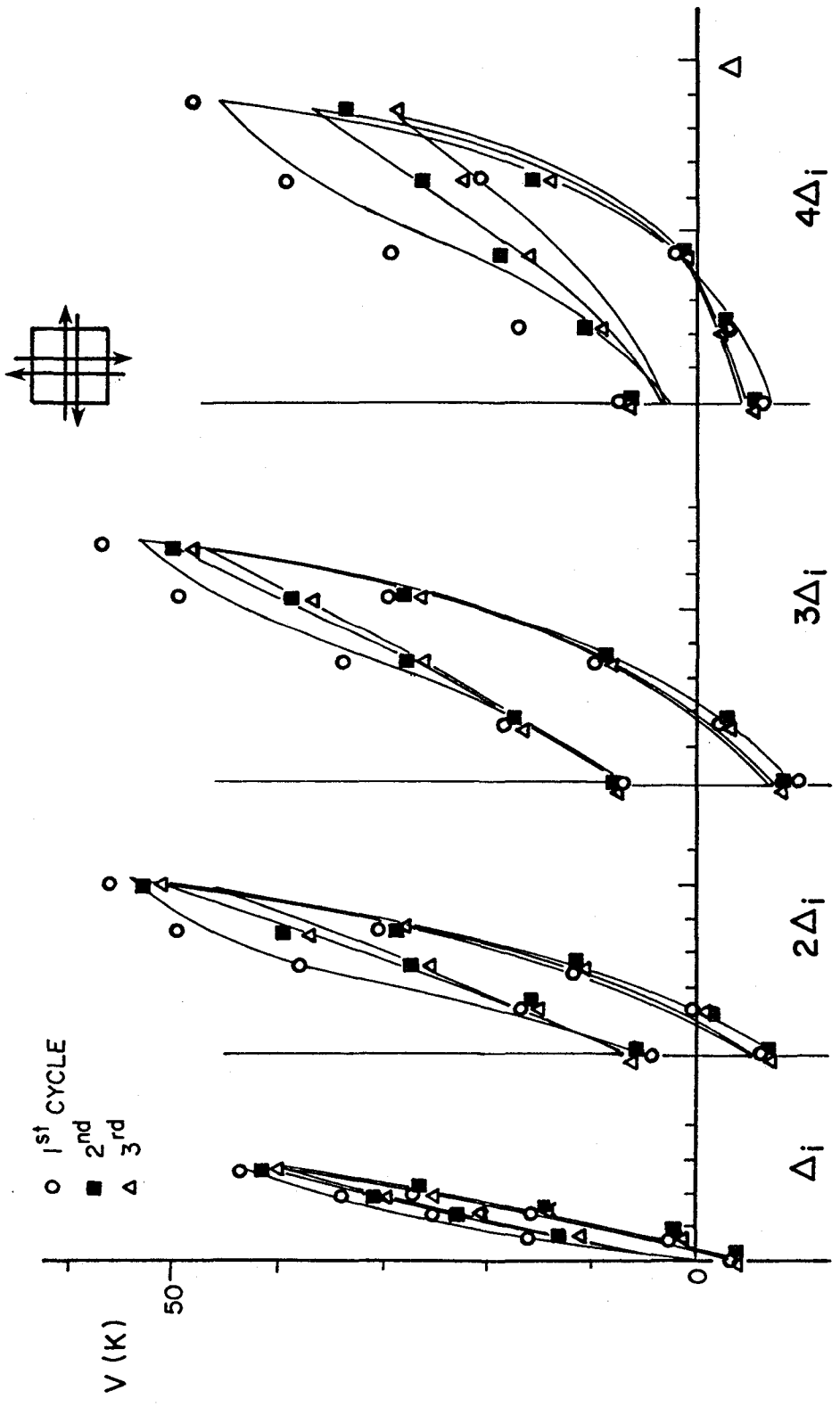

Fig. 6.15 Comparison of computed results with test results--OO-V-V-A (N-S)

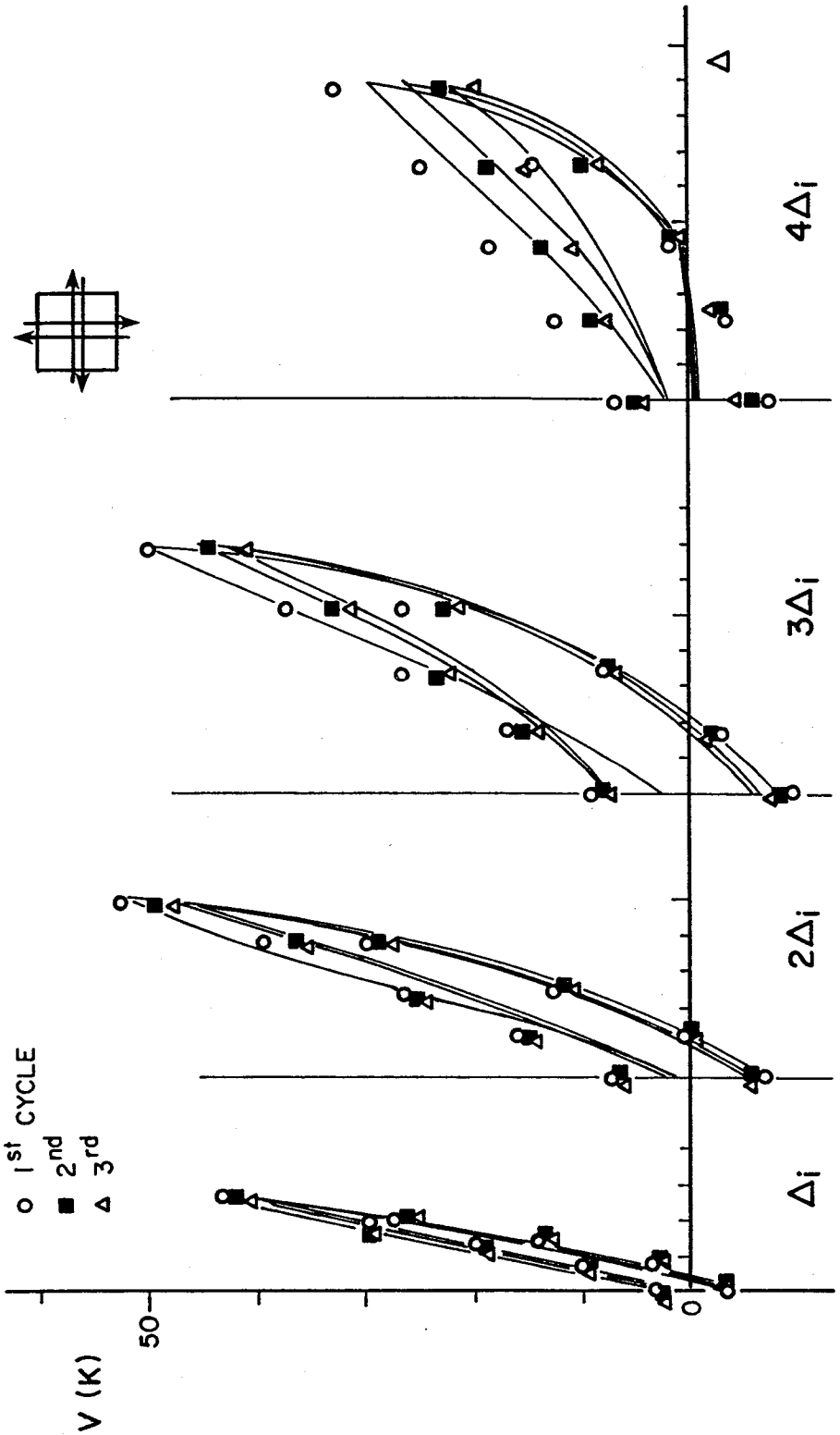

Fig. 6.16 Comparison of computed results with test results--OO-V-V-A (E-W)

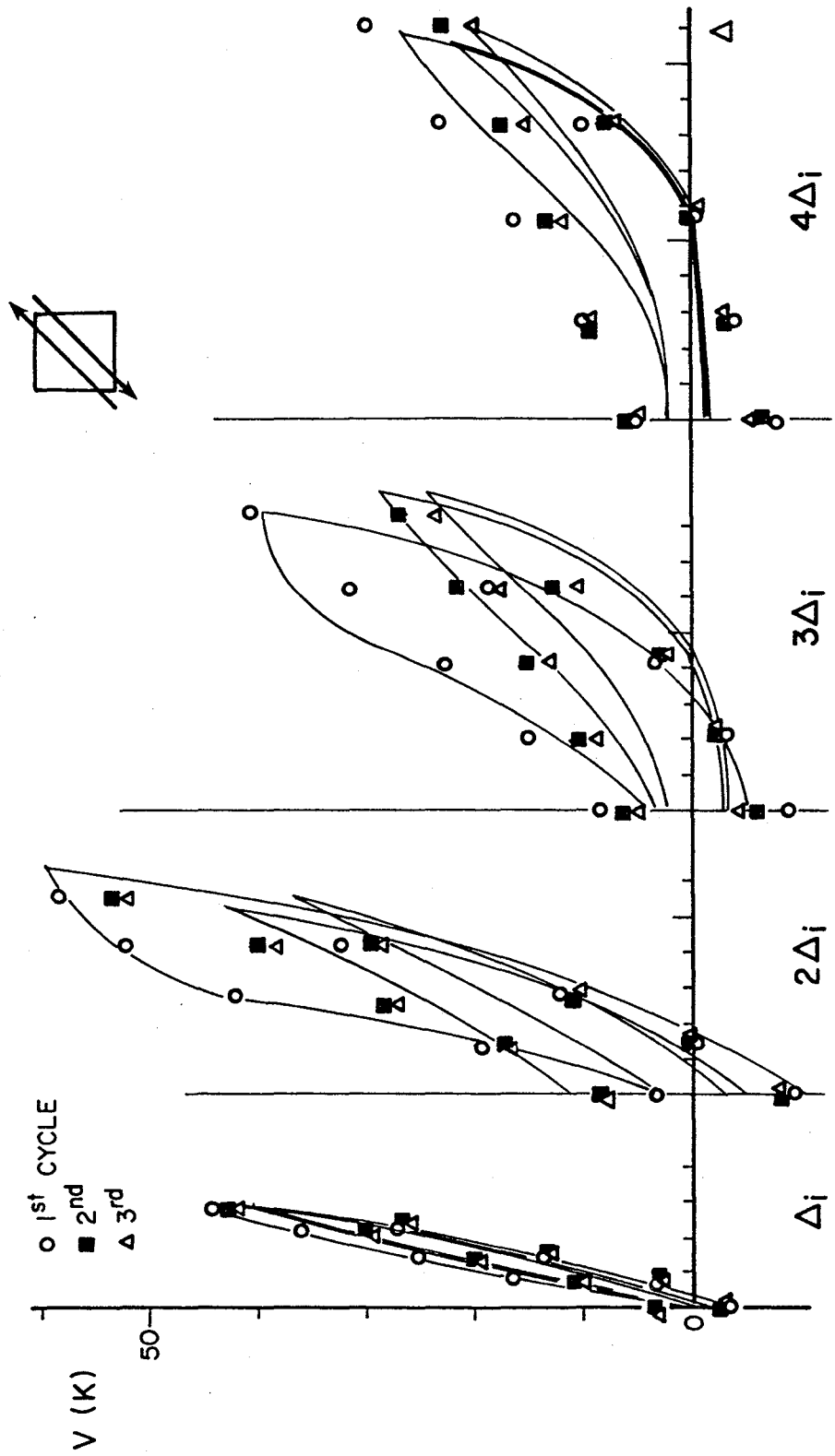

Fig. 6.17 Comparison of computed results with test results--OO-V-V-S (NE-SW)

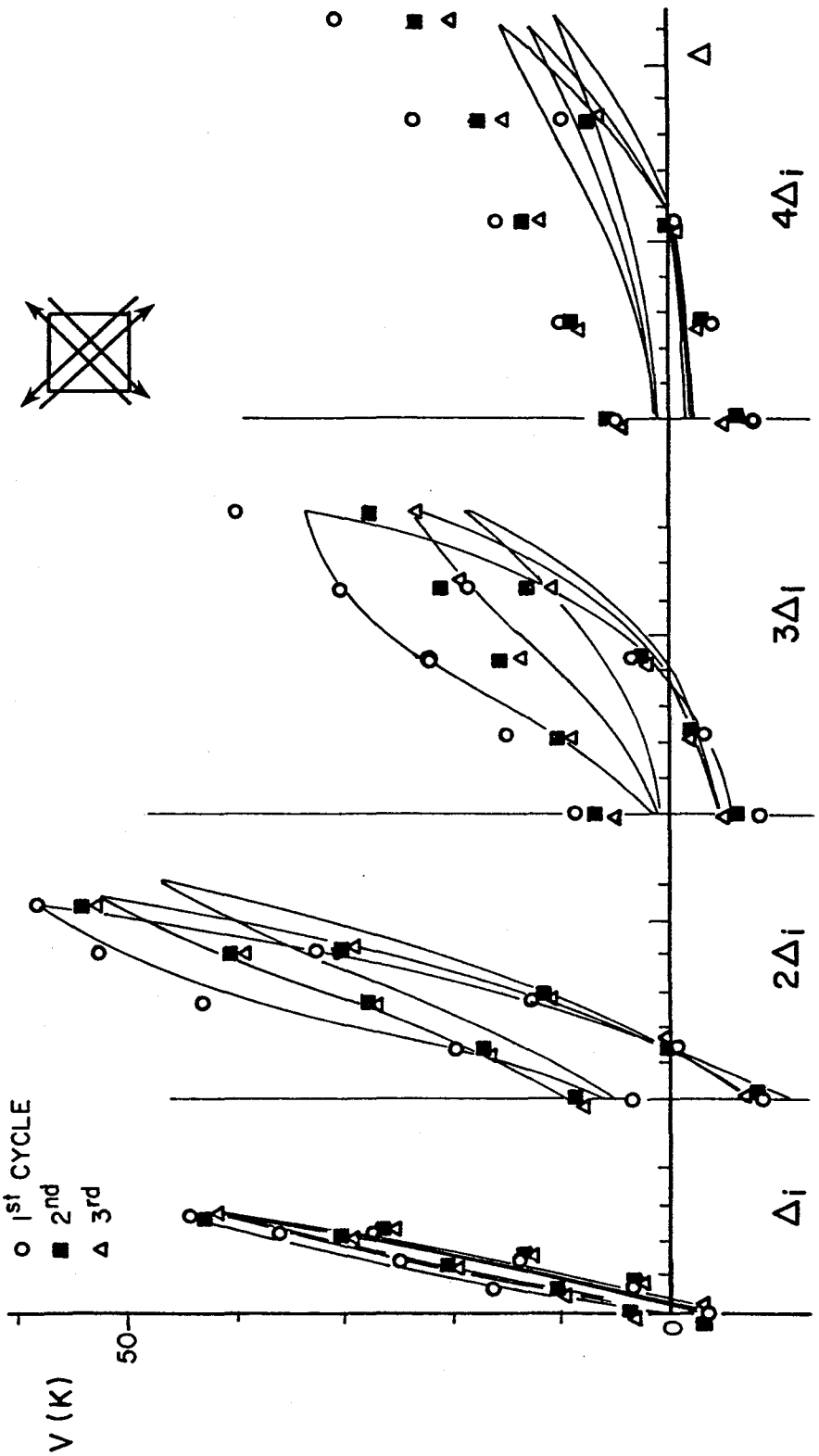

Fig. 6.18 Comparison of computed results with test results--OO-V-V-SA (NE-SW)

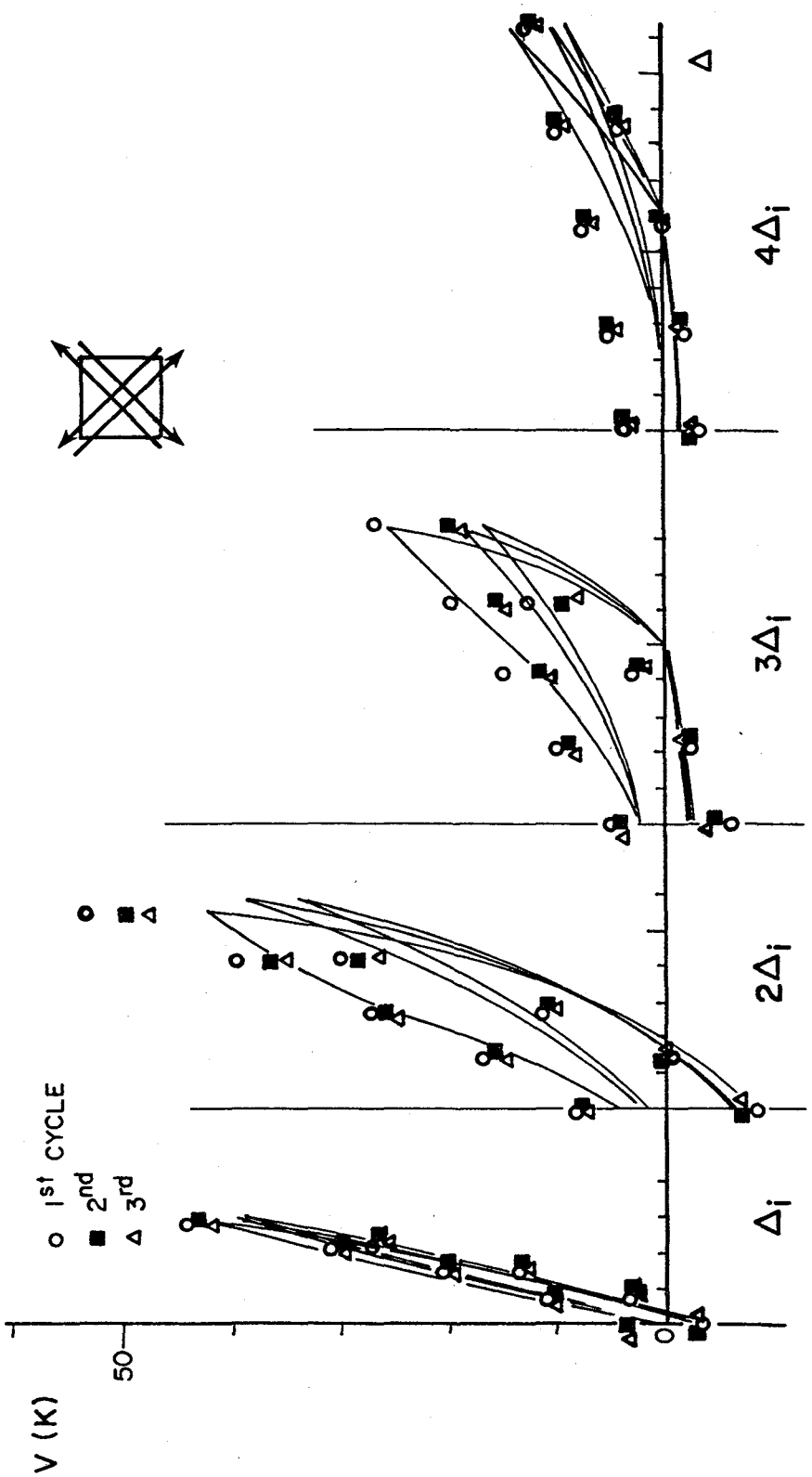

Fig. 6.19 Comparison of computed results with test results--OO-V-V-SA (NW-SE)

In the cases of diagonal load paths (OO-V-V-S, Fig. 6.17, and OO-V-V-SA, Figs. 6.18 and 6.19), both test results and computed results are treated in terms of the resultant force and the resultant deflection. The proposed model provides a good estimate of response.

6.6 Extension of Model to Group II

There are four specimens in Group II: constant deflection in one direction (OO-V-2C-I and OO-V-4C-I), square load path (OO-C-C-AF), and half square load path (OO-C-C-AH). The loading is such that response cannot be estimated using the model developed without some modification. Each specimen has a load path which consists of the loading with a constant deflection in one direction while the deflection in the orthogonal direction is changing (see Fig. 5.10b).

Of the four cases, the first two (OO-V-2C-I and OO-V-4C-I) are the simplest and form a basis for the other two cases. Therefore, the case of loading with a constant deflection in an orthogonal direction will be considered first.

The difference between Group I and Group II should appear in the expression of the damage ratio. In Group II force exists in an orthogonal direction during loading while no force in the orthogonal direction was present in Group I. The existence of force in the orthogonal direction compacts the crushed concrete and reduces the influence of the damage ratio on the behavior in the orthogonal direction.

This phenomenon may be explained using the extended sand spring model shown in Fig. 6.20c. For better understanding of that model, the composite model is introduced for the intermediate process from the basic sand spring model to the extended sand spring model (Fig. 6.20b).

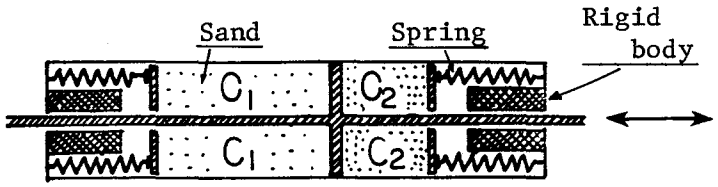

(a) Basic sand spring model

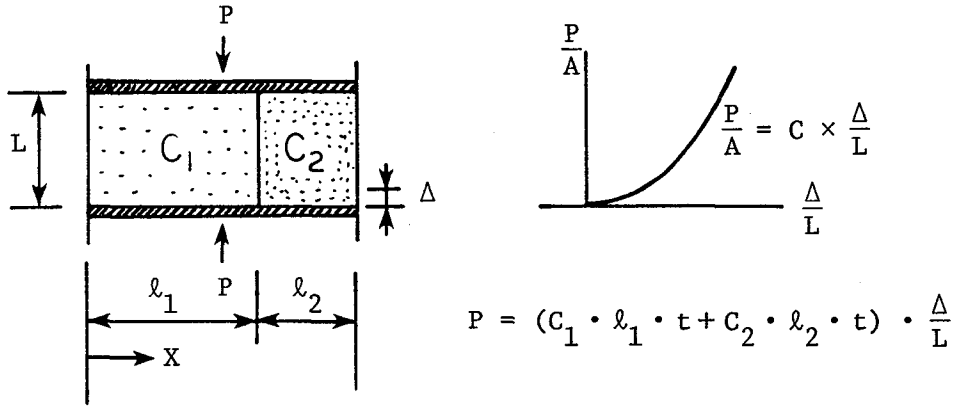

(b) Composite model

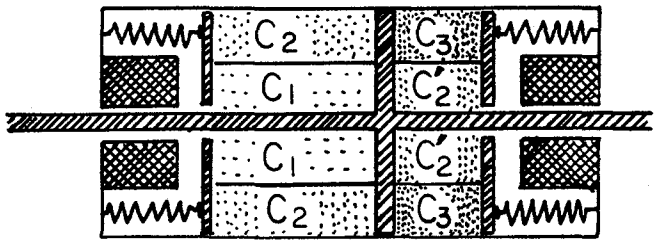

(c) Extended sand spring model

Fig. 6.20 Revised sand spring model for Group II

Under a given load two, different compacted sand portions are produced in the sand spring model. The condition of compaction may be expressed using a pseudo modulus C. The load-deflection curve (P-Δ curve) for sand compaction is shown in Fig. 6.20(b) and the above modulus C is defined as $\frac{P}{A} = C \cdot \frac{\Delta}{L}$. C is also a function of Δ/L.

Holding the sand condition (C_1 and C_2) constant, a force P is applied in the orthogonal direction. If the thickness of sand is t and the width of each portion is ℓ_1 (for C_1) and ℓ_2 (for C_2), the required force P for compacting an amount Δ is expressed as

$$P = (C_1 \cdot \ell_1 \cdot t + C_2 \cdot \ell_2 \cdot t) \cdot \frac{\Delta}{L}$$

With this model the influence of the condition of precompression of sand on the force P can be examined. If the partition, which divides sand into two portions with moduli C_1 and C_2, moves toward the right by $d\Delta$, the movement increases C_2 and decreases C_1. However, in the sand spring model when one part is compressed, there is no force in the other part. Therefore, $C_1 = 0$. In addition, C_1 does not pick up tensile force.

From these considerations, the required force is

$$P' = (C_2 + d\,C_2)(\ell_2 - d\,\Delta) \quad \frac{t \cdot \Delta}{L}$$

In the case that C is linear to Δ ($P = K \cdot \Delta^2$),

$$dC_2 = C_2 \cdot d\Delta$$

and

$$P' = (1+d\Delta)(1-\frac{d\Delta}{\ell_2}) \cdot C_2 \cdot \ell_2 \cdot \frac{t \cdot \Delta}{L}$$

$$= (1+d\Delta)(1-\frac{d\Delta}{\ell_2}) \cdot P$$

$$\simeq (1+d\Delta-\frac{d\Delta}{\ell_2}) \cdot P > P$$

Therefore, such movement requires more force. As a matter of fact, C_1 and C_2 will increase with increase in Δ. But, as seen in Fig. 6.20b, the increment of C_2 is much larger than that of C_1 and the relationship $P' > P$ does not change.

The movement of the partition toward the opposite direction reduces the required force. However, in the sand spring model, when the partition moves over some point, the sand in volume 1 (C_1) begins to be compressed. If the position of the partition is related to X, as shown in Fig. 6.20b, the P - X curve can be expressed as shown in Fig. 6.21. The minimum value P is given at the position where no compressive force exists in either portion of sand ($C_1 = C_2 = 0$).

The composite model appears to represent the phenomenon observed in the test. The extended sand spring model is obtained by modifying the basic sand spring model to include the composite model. However, this model is very difficult to express in mathematical form because the modulus C is influenced by the deflections in both directions.

$$P = \{C_1(\Delta x, \Delta y) \cdot \ell_1 + C_2(\Delta x, \Delta y) \cdot \ell_2\} \frac{t \cdot \Delta}{L}$$

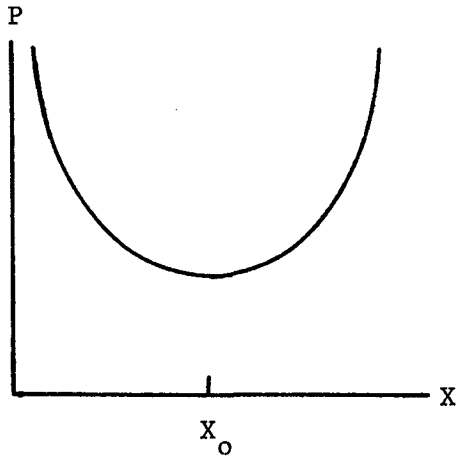

Fig. 6.21 Influence of the position of cylinder partition

6.7 Modification of Model for Cases of Constant Deflection in One Direction

The general behavior of shear strength under loading with constant deflection in an orthogonal direction can be expressed by the extended sand spring model developed in the previous section. However, it proved too complicated to formulate mathematically. In this section a simpler modification to the basic analogy is discussed.

From the test results of OO-V-2C-I and OO-V-4C-I, it was observed that shear strength at low deflection levels was not influenced by constant deflection in an orthogonal direction; however, the force required to hold the deflection constant was decreasing during cycles of load even at low deflection levels.

These observations indicate how force in an orthogonal direction influences the shear strength. One observation is that the damage ratio due to the constant deflection does not affect

the behavior in the orthogonal direction as much as is indicated in the basic model.

A second observation is that the damage ratio in the direction of the constant deflection increases with loading in the orthogonal direction even though the applied deflection level is much smaller than the constant deflection level.

These two aspects can be reasonably modeled by considering that the existence of force in the direction of constant deflection compacts the crushed concrete.

A modification of the model is needed only on the orthogonality functions in the damage ratio concept. The modification is traced step by step as follows.

[Stage I] Initially the constant deflection is applied in the Y direction.

$$\begin{cases} D_r^X = \phi \cdot D_{r,o}^Y \\ D_r^Y = D_{r,o}^Y \end{cases}$$

[Stage II] Load reversals are applied in the X direction with deflection in the Y direction held constant.

$$\begin{cases} D_{r,n}^X = (\phi \cdot D_{r,o}^Y \text{ or } D_{r,o}^X) \cdot \left(\sum_1^n \alpha_i \right) \\ D_r^Y = D_{r,o}^Y + \mu \cdot \phi \cdot D_{r,n}^X \qquad \mu \leq 1 \end{cases}$$

Here, a function μ is introduced. According to the previous definition (6.3), $\phi \cdot D^X_{r,o}$ should be used when $\phi \cdot D^X_{r,n}$ is much larger than $D^Y_{r,o}$. In addition, load reversals are applied only in one direction at a time. Therefore, $\phi \cdot D^X_{r,n}$ tends to be too big at a high deflection level in the X direction. In order to adjust the influence of loading in the X direction on the behavior in the Y direction, the function μ ($\mu \leq 1$) is introduced.

[Stage III] Due to the increase in the damage ratio, the force under constant deflection decreases and crushed concrete becomes less compacted. This influences the behavior in the X direction at the (n+1) cycle.

$$D^X_{r,n+1} = (\phi \cdot D^Y_{r,o} \text{ or } D^X_{r,o}) \cdot \left(\sum_{1}^{n+1} \alpha_i \right) \cdot h$$

A function h treats the reduction of compaction in the Y direction. If the force in the Y direction drops to zero, D_r should be treated as is defined in the previous section (8.3). At that time, h should be 1.0. The ratio $D^Y_{r,o}/D^Y_r$ can be considered an index for representing degree of compaction.

After comparing computed results with test results from 00-V-2C-I and 00-V-4C-I, functions μ and h were defined as follows.

$$\mu = (D^Y_{r,o}/D^Y_r)^4$$

$$h = 1.00 + 0.05 \cdot (D^Y_r/D^Y_{r,o})$$

6.8 Comparison of Computed Results with Test Results: Group II

As stated in Sec. 6.6, Group II is very difficult to formulate in mathematical equations. The case of constant deflection is the simplest in Group II and basic for others in Group II. Force deformation curves for two cases (OO-V-2C-I and OO-V-4C-L) were computed and compared with test results (Figs. 6.22-6.25). Figures 6.22 and 6.23 show good correlation between computed results and test results in the direction of load reversals. The shear strength reduction in the direction of constant deflection (Figs. 6.24 and 6.25) can also be traced by the model very well.

The cases of square load path and half square load path could not be formulated because of the complicated load histories. With additional tests future studies may offer the potential for extending this model.

6.9 Summary

The conceptual model was developed for shear behavior of reinforced concrete short columns. The damage ratio was introduced as the basic concept.

As is often the case of shear behavior of reinforced concrete members under inelastic load reversals, many shear cracks are present, and they produce large shear deformations. There is no well-established model because the relationship between inelastic shear deformation of a member and material properties is not easily defined. In order to solve this problem, an index which can represent the behavior of materials in an aggregate sense was sought and finally the damage ratio was introduced as an index which indicates the progress of shear cracks or severe crushing of concrete.

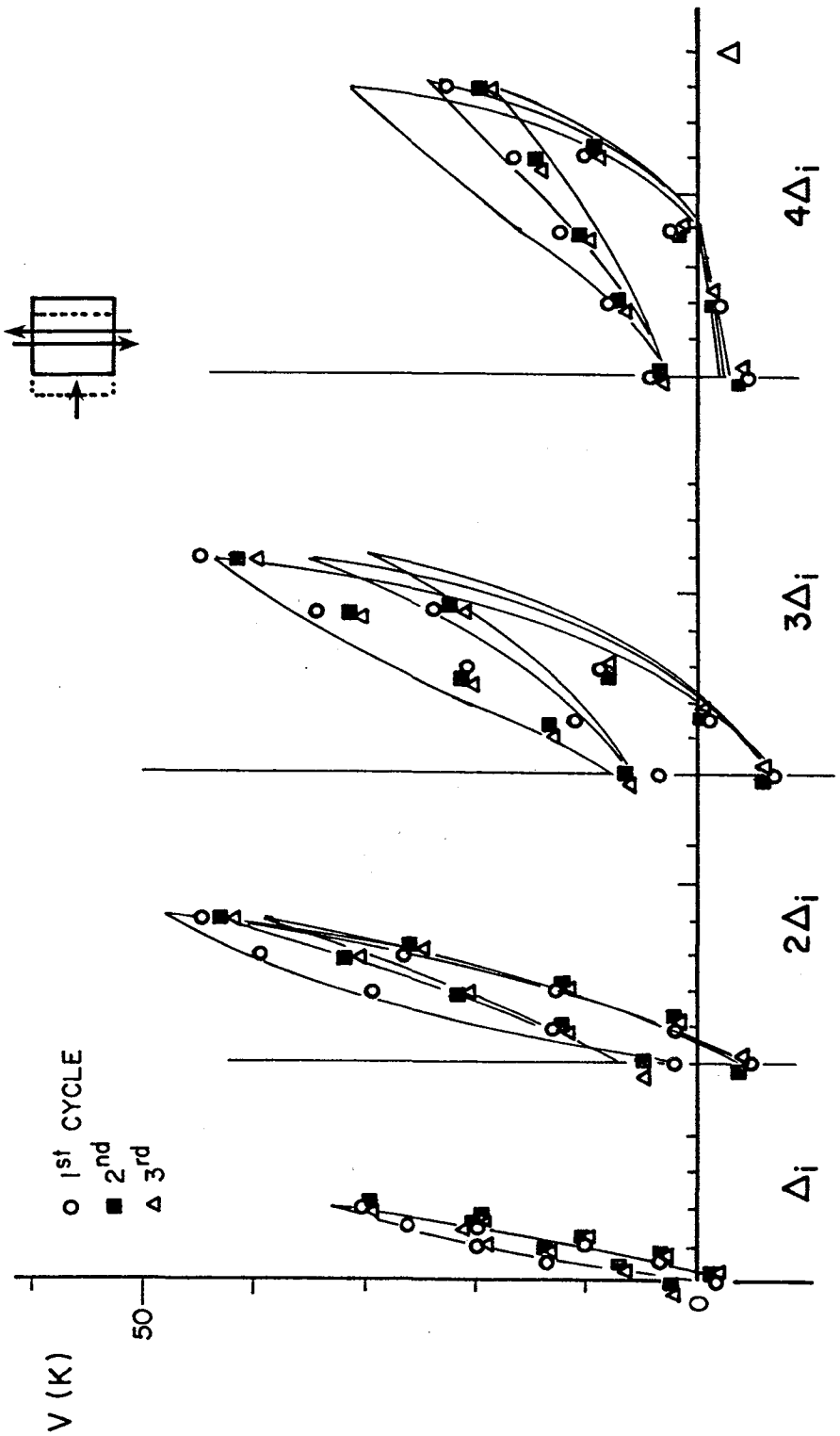

Fig. 6.22 Comparison of computed results with test results--00-V-2C-I (N-S)

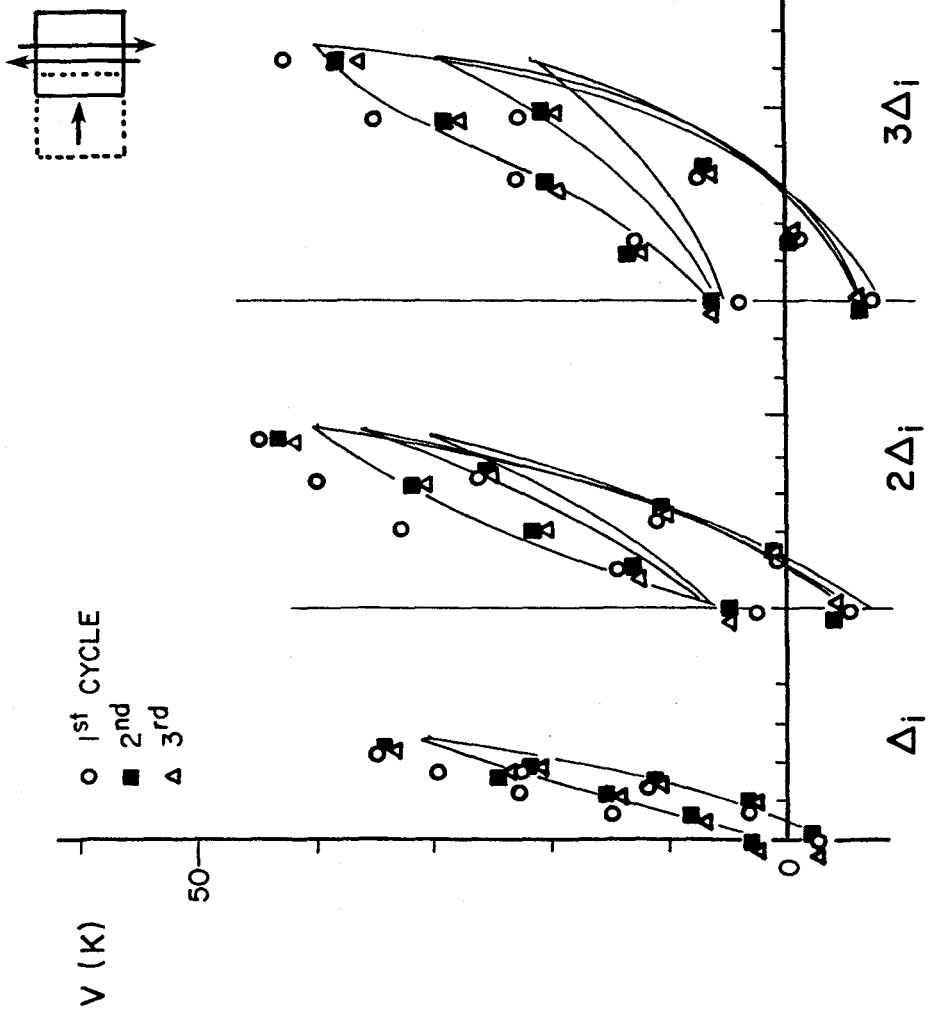

Fig. 6.23 Comparison of computed results with test results--00-V-4C-I (N-S)

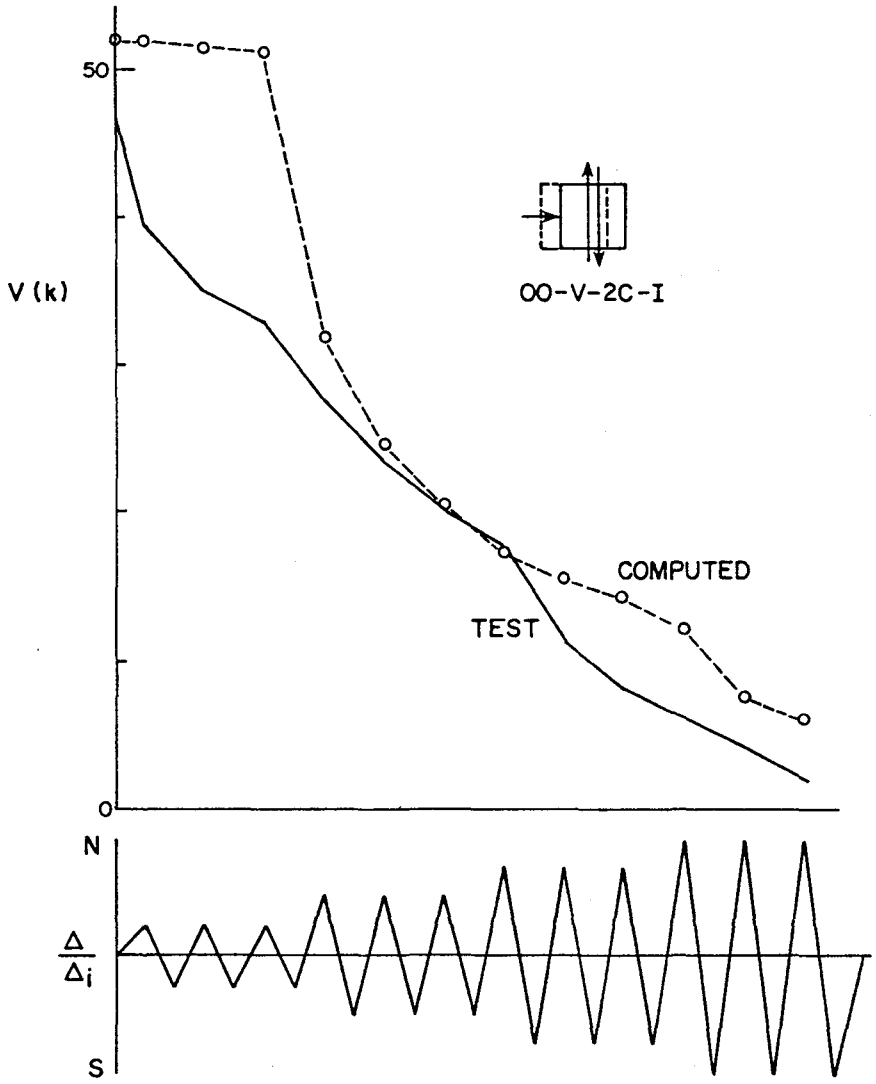

Fig. 6.24 Shear strength reduction in the direction of constant deflection (E-direction)--00-V-2C-I

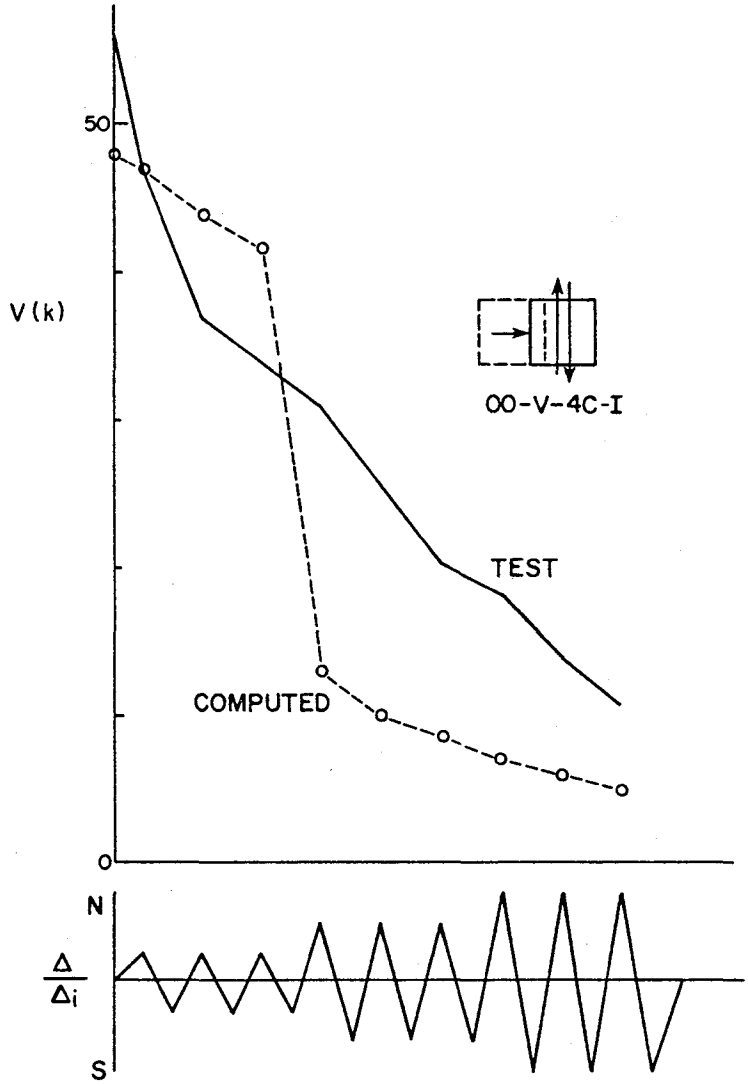

Fig. 6.25 Shear strength reduction in the direction of constant deflection (E-direction)--00-V-4C-I

The basic idea is that the shear behavior under cyclic loading can be explained using the damage ratio. In order to relate the damage ratio to the actual behavior, several relationships and functions were introduced and determined by comparing computed results with test results.

The proposed model provided a good estimate of response in each case. This may indicate that the general concept and the additional relationships introduced are reasonable for explaining the characteristics of shear behavior, but there is still the problem of applying the general concept to specific problems because the formulation was based on the tests in this study. In addition, the geometry and the cross section properties of the specimen were fixed in this study. Therefore, those influences on each relationship of the proposed model have not been studied. An extension to this study is required in the future for improving the model. Especially, the influence of transverse reinforcement should be studied because the model does not include a parameter for transverse reinforcement. With more experimental tests in this area (shear behavior), the model can be revised in a more general form.

Other researchers are investigating this area and, with much more extensive study, an understanding of the mechanism of shear failure and the development of more general and well-organized models will be possible.

INTENTIONALLY BLANK

CHAPTER 7

SUMMARY AND CONCLUSIONS

7.1 Summary

The shear behavior of reinforced concrete members under bidirectional loads was studied. Very little information is available in this area and many variables need to be studied to define the problem.

The objectives of the overall investigation were to examine the importance of bidirectional lateral load histories on the response of members in reinforced concrete structures and to develop models which can be used to predict the behavior of columns subjected to large shear forces.

Test Specimen. The test specimen was a 2/3-scale model of the prototype column. The test specimen had a 10 in. square section with eight #6 (28 mm) longitudinal bars ($\rho_g = 0.025$). The dimensions and the cross-sectional properties of the test specimen were held constant throughout this test program. The shear span-to-depth ratio for the specimen was 1.8, based on the effective column depth.

Loading System. In order to accomplish the objectives, a special loading system was constructed. This system can apply loads on the specimen with any combination of three principal directional forces or deflections. The loading fixtures controlled all rotations at the ends of the specimen, while permitting lateral translations.

A special positioning system was devised which can restrict the rotation of the column specimen in three orthogonal directions. With the use of double-rodded hydraulic actuators and the chambers of the actuators cross-coupled, the loading frame can translate but rotation is prevented.

Test Schedule. In the test program, ten different load histories were selected to examine the influence of load sequence and the influence of load path on shear strength of members. Variations in axial load were not considered and axial load was zero.

The lateral load was controlled by deformation. Three load cycles were applied at each deflection level and the deflection level was incrementally increased. A unit deflection (Δ_i) was defined as the deflection when the strain in the longitudinal bars at the bottom of the column indicated a large increase with a small increase in load.

Four of the ten specimens were tested to study the influence of previous loadings in either direction using different load sequences. In two specimens the effect of skewed loadings was studied. In four specimens the influence of load path was examined. Of the last four specimens, two specimens were tested under loading with constant deflection in one direction and cyclic reversals in the orthogonal direction. The other two specimens were subjected to square load paths in which deflections in one direction were always held constant while the other direction was varied.

In each specimen the applied forces, lateral deflection, strain in longitudinal and transverse reinforcing bars, and rotations of the column ends were measured. Cracks were marked at every peak deflection level.

From the measured data, the load-deflection curves, the strain distributions in transverse reinforcement along the column height, and crack patterns were plotted.

Discussion of Test Results. The influence of load sequence is very small at low deflection levels, but becomes significant when the deflection imposed exceeds the point at which the ultimate shear strength is achieved under monotonic loading.

The influence of load path on shear behavior along a principal direction (N-S or E-W direction) is large in some cases. However, using the resultant force and the resultant deflection, behavior under loading along diagonal directions is similar to the case of unilateral loading.

The load-deflection curves differ with load path; however, when comparisons are made using load-deflection relationships along the same axis of reference, the shape from the peak in one direction to the peak in the other direction is very similar.

A Conceptual Model. Based on the test results, a conceptual model was developed. In order to express the shear strength deterioration of columns, the concept of a damage ratio was introduced to reflect the response characteristics of the model. The damage ratio represents the progression of damage in the specimen. By constructing relationships between the damage ratio and the load history (including the influence of load reversals, the influence of loading in an orthogonal direction, and the influence of simultaneous loading), the shear behavior of the columns tested under bidirectional lateral loadings was modeled.

The shear behavior under cyclic loading can be explained using the damage ratio. In order to relate the damage ratio to the actual behavior, the relationship between the deflection level, the number of cycles and direction of loading, and the damage ratio

were established by comparing computed results with test results. A sand-spring analogy was introduced as one component of the analytical model.

The proposed model provided a good estimate of response and indicated that the approach selected was acceptable for representing the shear behavior. There is still a problem of applying the general concept to other members with different geometry because the formulation was based on the test results in this study.

7.2 Conclusions

Based on the results of this study in which square specimens with moderate transverse reinforcement ($\rho_{(s)} = 0.0033$) were tested, the following conclusions were made:

(1) Previous loading in either direction did not significantly affect the ultimate shear strength of the columns unless the maximum deflection of any previous loading exceeded the deflection at which the ultimate shear strength of columns under monotonic loading was reached. However, when the deflection level imposed was lower than the maximum deflection of the previous loading, the shear resistance at a given deflection was less than the shear resistance under monotonic loading to the same deflection level (reduction in stiffness).

(2) In the case of square columns with square tie arrangements, loading along a principal direction (E-W or N-S) or loading along a diagonal direction (NE-SW or NW-SE) did not make any difference in response if the resultant force and the resultant direction were taken into account.

(3) In the case of complex load paths such as the square load paths, the resultant force and the resultant deflections

cannot be easily defined because the direction of the resultant force vector was changing with the load path. For example, the square load path produced a 360^{o} revolution of the direction of the resultant force vector. Therefore, the behavior of the resultant force vector in cases of complex load paths was quite different from those in which forces are reversed along the same line. The revolution of the force vector produced a grinding effect across the cracked sections of the column. When the angle of revolution was large (e.g., 360^{o}), the grinding effect caused much more severe damage in the column than did the reversed load. On the other hand, when the angle of revolution was very small (such as the case of loading with large constant deflection in one direction), the grinding effect was small and the members exhibited less damage.

(4) In order to express the shear behavior of reinforced concrete elements under bilateral loading, a conceptual model was developed to include response to variations in load history. Although the idea of the model is very general, the formulation of each relationship in the model was calibrated against the test specimen. The formulation of each general relationship was time-consuming, but computed results showed very good correlation with test results. The model offers an approach on which future investigations may be able to expand as more test results become available. Additional work is needed to define the influence of variations in transverse and longitudinal reinforcement, axial load, cross section, and shear span-to-depth ratio on the response of members under more complex load histories than were considered in this study.

INTENTIONALLY BLANK

REFERENCES

1. Okada, T. et al., "Analyses of the Hachinohe Library Damage by '68 Tokachi-Oki Earthquake," Proceedings, U.S.-Japan Seminar on Earthquake Engineering with Emphasis on Safety of School Buildings, Sendai, Japan, September 1970, pp. 172-189.

2. Aoyama, H., and Sozen, M. A., "Dynamic Response of a Reinforced Concrete Structure with Tied and Spiral Columns," Proceedings, Fifth World Conference on Earthquake Engineering, Rome, 1973, Paper No. 15.

3. Karlsson, B. I., Aoyama, H., and Sozen, M. A., "Spirally Reinforced Concrete Columns Subjected to Loading Reversals Simulating Earthquake Effects," Proceedings, Fifth World Conference on Earthquake Engineering, Rome, 1973, Paper No. 93.

4. Aktan, A. E., Pecknold, D. A. W., and Sozen, M. A., "Effects of Two-dimensional Earthquake Motion on a Reinforced Concrete Column," Civil Engineering Studies, Structural Research Series 399, University of Illinois, May 1973.

5. Pecknold, D. A. W., and Sozen, M. A., "Calculated Inelastic Structural Response to Uniaxial and Biaxial Earthquake Motions," Proceedings, Fifth World Conference on Earthquake Engineering, Rome, 1973, Paper No. 223.

6. Mahin, S. A., Bertero, V. V., Chopra, A. K., and Collins, R. G., "Response of the Olive View Hospital Main Building during the San Fernando Earthquake," Report No. EERC 76-22, Earthquake Engineering Research Center, University of California, Berkeley, October 1976.

7. Selna, L. G., Morrill, K. B., and Ersoy, O. K., "Shear Collapse, Elastic and Inelastic Biaxial Studies of the Olive View Hospital Psychiatric Day Clinic," Proceedings, U.S.-Japan Seminar on Earthquake Engineering, Berkeley, 1973.

8. Takizawa, H., and Aoyama, H., "Biaxial Effects in Modeling Earthquake Response of R/C Structures," Earthquake Engineering and Structural Dynamics, Vol. 4, 1976, pp. 523-552.

9. Takizawa, H., "Biaxial and Gravity Effects in Modeling Strong-Motion Response of R/C Structures," Proceedings, Sixth World Conference on Earthquake Engineering, New Delhi, 1977, Paper No. 3-9, pp. 49-54.

10. Takiguchi, K., Kokusho, S., and Ohada, K., "Experiments on Reinforced Concrete Columns Subjected to Biaxial Bending Moments," Transactions of A.I.J., No. 229, March 1975, pp. 25-33.

11. Takiguchi, K., Kokusho, S., and Ohada, K., "Experiments on Reinforced Concrete Columns Subjected to Biaxial Bending Moments--II," Transactions of A.I.J., No. 247, September 1976, pp. 37-43.

12. Takiguchi, K., Kokusho, S., and Ohada, K., "Analysis of Reinforced Concrete Sections Subjected to Biaxial Bending Moments," Transactions of A.I.J., No. 250, December 1976, pp. 1-8.

13. Okada, T., Seki, M., and Asai, S., "Response of Reinforced Concrete Columns to Bi-directional Horizontal Force and Constant Axial Force," Bulletin of Earthquake Research Center, University of Tokyo, No. 10, 1976, pp. 30-36.

14. ACI-ASCE Committee 426, "The Shear Strength of Reinforced Concrete Members," Journal of the Structural Division, ASCE, Vol. 99, No. ST6, Proc. Paper 9791, June 1973, pp. 1091-1187.

15. Mattock, A. H., "Connections in Precast Concrete Buildings Subjected to Earthquake," Proceedings, U.S.-Japan Seminar on Earthquake Engineering, Berkeley, September 1973.

16. Building Research Institute, Ministry of Construction, Japan, "A List of Experimental Results on Deformation Ability of Reinforced Concrete Columns under Large Deflection (No. 3)," (in Japanese), Kenshiku Kenkyu Shiryo, No. 21, February 1978.

17. Yamada, M., and Kawamura, H., "Resonance Capacity Criterion for Evaluation of the Aseismic Capacity of Reinforced Concrete Structures," Reinforced Concrete Structures in Seismic Zones, SP-53, American Concrete Institute, Detroit, 1977, pp. 81-108.

18. ACI Committee 318, Building Code Requirements for Reinforced Concrete (ACI 318-77), American Concrete Institute, Detroit, 1977.

19. Woodward, K. A., and Jirsa, J. O., "Design and Construction of a Floor-Wall Reaction System," CESRL Report No. 77-4, Civil Engineering Structures Research Laboratory, The University of Texas at Austin, Texas, December 1977.

20. Higashi, Y., Ohkubo, M., and Ohtsuka, M., "Influence of Loading Excursions on Restoring Force Characteristics and Failure Modes of Reinforced Concrete Columns," Proceedings, Sixth World Conference on Earthquake Engineering, New Delhi, 1977, pp. 11-135-140.

21. Umemura, H., Hirosawa, M., and Endo, T., "Experimental Research on Ductility of Reinforced Concrete Columns," Proceedings, U.S.-Japan Seminar on Earthquake Engineering, Berkeley, September 1973.

22. Muto, K., Tsugawa, T., Niwa, M., and Shimazu, H., "Simulation Analysis of a Highrise Reinforced Concrete Building in Two Different Earthquakes," Proceedings, Sixth World Conference on Earthquake Engineering, New Delhi, 1977, Paper 3-15, pp. 85-90.

23. Maruyama, K., "Shear Behavior of Reinforced Concrete Members under Bidirectional Reversed Lateral Loading," unpublished Ph.D. dissertation, The University of Texas at Austin, May 1979.

24. Jirsa, J. O., Maruyama, K., and Ramirez, H., "Development of Loading System and Initial Tests--Short Columns under Bidirectional Loading," CESRL Report No. 78-2, Civil Engineering Structures Research Laboratory, The University of Texas at Austin, September 1978.